In presenting the dissertation as a partial fulfillment of the requirements for an advanced degree from the Georgia Institute of Technology, I agree that the Library of the Institute shall make it available for inspection and circulation in accordance with its regulations governing materials of this type. I agree that permission to copy from, or to publish from, this dissertation may be granted by the professor under whose direction it was written, or, in his absence, by the Dean of the Graduate Division when such copying or publication is solely for scholarly purposes and does not involve potential financial gain. It is understood that any copying from, or publication of, this dissertation which involves potential financial gain will not be allowed without written permission.

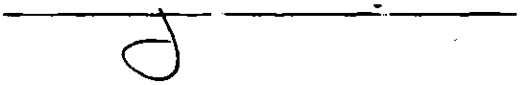

3/17/65
b

THE EFFECT OF LONG RANGE INTERFERENCES ON THE INTRAMOLECULAR LIGHT SCATTERING FUNCTION

A THESIS

Presented to

The Faculty of the Graduate Division

by

Terry Edward Smith

In Partial Fulfillment

of the Requirements for the Degree

Doctor of Philosophy

in the School of Chemistry

Georgia Institute of Technology

June, 1967

THE EFFECT OF LONG RANGE INTERFERENCES

ON THE

INTRAMOLECULAR LIGHT SCATTERING FUNCTION

Approved:

Chairman

Date approved by Chairman: 4-21-67

ACKNOWLEDGMENT

Many people in many different ways have helped to make this thesis a reality; a few, however, have made special efforts and thus their help is acknowledged in a special way. I am particularly grateful to Dr. Dewey K. Carpenter, my thesis advisor, who suggested the topic of research and generously gave of his time in many helpful discussions throughout the course of the investigation. I am also indebted to the other members of the reading committee, Dr. George A. Miller and Dr. Robert A. Pierotti, who made many constructive suggestions during the preparation of the thesis, and to Mrs. Betty Sims, who typed the final manuscript. Generous financial assistance was given by the National Aeronautics and Space Administration, who provided a fellowship for the first three years of my stay in graduate school, and by Dr. William M. Spicer, who, as Director of the School of Chemistry, provided departmental employment for the period not covered by the NASA fellowship.

Gratitude for help in the accomplishment of this major undertaking, however, does not end with those who were directly involved, but rather must go back, often many years, to those who made it possible. To these, especially to two wonderful parents who sacrificed beyond measure, I am particularly thankful.

Finally, and foremost, I am thankful to my wife, Linda, not only for her forbearance through an often lonely experience, but also for the encouragement which she afforded.

TABLE OF CONTENTS

Page

ACKNOWLEDGMENTS. ii

LIST OF TABLES v

LIST OF FIGURES. vi

NOMENCLATURE x

SUMMARY. xii

Chapter

I. INTRODUCTION. 1

Light Scattering by Small Particles
Light Scattering by Large Particles
Purpose of the Research

II. INSTRUMENTS AND MATERIALS 14

Light Scattering Photometer
Differential Refractometer
Viscometers
Polymer Samples
Solvents

III. PROCEDURE 33

Light Scattering
Refractive Increments
Intrinsic Viscosities

IV. RESULTS AND DISCUSSION. 67

Molecular Weights and Second Virial Coefficients
Angular Results
Experimental Error

V. CONCLUSIONS 116

APPENDIX 118

Page

BIBLIOGRAPHY 150

VITA 155

LIST OF TABLES

Table		Page
1.	Refractive Increments	56
2.	Viscosity Results	66
3.	Molecular Weights and Second Virial Coefficients.	73
4.	Radii of Gyration Determined by Initial Tangent Method. . .	76
5.	Polymer Dimensions and Related Quantities	107

LIST OF ILLUSTRATIONS

Figure		Page
1.	Refractive Increment Data for PS-I in Carbon Tetrachloride at Three Wave Lengths.	54
2.	Relative Viscosities for PS-III in Benzene at Different Rates of Shear	61
3.	Viscosity Data for PS-I in Benzene at 30.0°C.	63
4.	Viscosity Data for PS-I in Carbon Tetrachloride at 30.0°C.	63
5.	Viscosity Data for PS-III in Benzene at 30.0°C.	64
6.	Viscosity Data for PS-III in Cyclohexane at 34.5°C.	64
7.	Viscosity Data for PDMS Fractions in Carbon Tetrachloride at 30.0°C	65
8.	Zimm Plot$_o$ for PS-III in Cyclohexane at 34.49°C. λ = 4358 Å.	68
9.	Zimm Plot for PS-III in Benzene at 30.0°C. λ = 4358 Å. . .	70
10.	P^{-1} Data for PDMS-III in Benzene at 30.0°C. Demonstrates Overlapping of Data for Three Wave Lengths.	75
11.	Comparison of the Isihara and Debye Scattering Functions. .	78
12.	P^{-1} Data for PS-I in Cyclohexane at 34.94°C	82
13.	P^{-1} Data for PS-II in Cyclohexane at 34.76°C.	83
14.	Comparison of the Debye and Ptitsyn Scattering Functions. .	87
15.	Log-log Plot of [η] versus M for PDMS in Carbon Tetrachloride	90
16.	Log-log Plot of [η] versus M for PS in Benzene.	90
17.	P^{-1} Data for PDMS-III in Carbon Tetrachloride at 30.0°C . .	92
18.	P^{-1} Data for PDMS-IV in Carbon Tetrachloride at 30.0°C and in Bromocyclohexane at 29.12°C.	93

Figure		Page
19.	P^{-1} Data for PDMS-I in Carbon Tetrachloride at 30.0°C . . .	94
20.	P^{-1} Data for PDMS-II in Carbon Tetrachloride at 30.0°C. . .	95
21.	P^{-1} Data for PS-I in Benzene at 35.0°C.	97
22.	P^{-1} Data for PS-I in Carbon Tetrachloride at 30.0°C	98
23.	P^{-1} Data for PS-I in Carbon Tetrachloride at 30.0°C. Attempt to Fit with Ptitsyn Function.	100
24.	P^{-1} Data for PS-II in Carbon Tetrachloride at 30.0°C. . . .	101
25.	P^{-1} Data for PS-III in Benzene at 30.0°C and in Cyclohexane at 34.49°C	103
26.	Log-log Plot of R^2/M versus M for PDMS in Carbon Tetrachloride.	109
27.	Log-log Plot of R^2/M versus M for PS in Benzene	109
28.	Scattering Data for PS-I in Benzene at 35.0°C. λ = 5460 Å	119
29.	Scattering Data for PS-I in Benzene at 35.0°C. λ = 4358 Å	120
30.	Scattering Data for PS-I in Benzene at 35.0°C. λ = 3650 Å	121
31.	Scattering Data for PS-I in Carbon Tetrachloride at 30.0°C. λ = 5460 A.	122
32.	Scattering Data for PS-I in Carbon Tetrachloride at 30.0°C. λ = 4358 Å	123
33.	Scattering Data for PS-I in Carbon Tetrachloride at 30.0°C. λ = 3650 Å.	124
34.	Scattering Data for PS-I in Cyclohexane at 34.94°C. λ = 5460 Å	125
35.	Scattering Data for PS-I in Cyclohexane at 34.94°C. λ = 4358 Å	126
36.	Scattering Data for PS-I in Cyclohexane at 34.94°C. λ = 3650 Å	127

Figure		Page
37.	Scattering Data for PS-II in Carbon Tetrachloride at 30.0°C. λ = 5460 Å	128
38.	Scattering Data for PS-II in Carbon Tetrachloride at 30.0°C. λ = 4358 Å	129
39.	Scattering Data for PS-II in Carbon Tetrachloride at 30.0°C. λ = 3650 Å	130
40.	Scattering Data for PS-II in Cyclohexane at 34.76°C. λ = 5460 Å	131
41.	Scattering Data for PS-II in Cyclohexane at 34.76°C. λ = 4358 Å	132
42.	Scattering Data for PS-II in Cyclohexane at 34.76°C. λ = 3650 Å	133
43.	Scattering Data for PS-III in Benzene at 30.0°C. λ = 3650 Å	134
44.	Scattering Data for PS-III in Cyclohexane at 34.49°C. λ = 3650 Å	135
45.	Scattering Data for PDMS-I in Carbon Tetrachloride at 30.0°C. λ = 4358 Å	136
46.	Scattering Data for PDMS-I in Carbon Tetrachloride at 30.0°C. λ = 3650 Å	137
47.	Scattering Data for PDMS-II in Carbon Tetrachloride at 30.0°C. λ = 4358 Å	138
48.	Scattering Data for PDMS-II in Carbon Tetrachloride at 30.0°C. λ = 3650 Å	139
49.	Scattering Data for PDMS-III in Carbon Tetrachloride at 30.0°C. λ = 5460 Å	140
50.	Scattering Data for PDMS-III in Carbon Tetrachloride at 30.0°C. λ = 4358 Å	141
51.	Scattering Data for PDMS-III in Carbon Tetrachloride at 30.0°C. λ = 3650 Å	142

Figure Page

52. Scattering Data for PDMS-III in Benzene at 30.0°C. λ = 5460 Å. 143

53. Scattering Data for PDMS-III in Benzene at 30.0°C. λ = 4358 Å. 144

54. Scattering Data for PDMS-III in Benzene at 30.0°C. λ = 3650 Å. 145

55. Scattering Data for PDMS-IV in Carbon Tetrachloride at 30.0°C. λ = 4358 Å. 146

56. Scattering Data for PDMS-IV in Carbon Tetrachloride at 30.0°C. λ = 3650 Å. 147

57. Scattering Data for PDMS-IV in Bromocyclohexane at 29.12°C. λ = 4358 Å 148

58. Scattering Data for PDMS-IV in Bromocyclohexane at 29.12°C. λ = 3650 Å 149

NOMENCLATURE

a	Mark-Houwink exponent
A_2	second virial coefficient
b	effective bond length
c	concentration of the solute, usually in grams per cubic centimeter
C_n	refractive index correction factor
d	density
Δd	total deflection for the solution
dn/dc	refractive increment
f	Fresnel correction factor
$i(\theta)$	scattered intensity per unit volume at θ
K	optical constant; Mark-Houwink constant
M	molecular weight
$\overline{M_n}$	number-average molecular weight
$\overline{M_v}$, M_v	viscosity-average molecular weight
$\overline{M_w}$, M_w	weight-average molecular weight
$\overline{M_z}$	z-average molecular weight
n	refractive index
N	total number of scattering points or chain segments
N_A	Avagadro's number
$P(\theta)$, P	intramolecular light scattering function
PDMS	polydimethylsiloxane
PS	polystyrene

r	distance from the scattering volume to the observer
$\overline{r^2}$	mean square end-to-end distance
r_{ij}	distance between segments i and j
R	gas constant; root mean square radius of gyration
$R(\theta)$	absolute reduced scattering intensity
$R'(\theta)$	relative reduced scattering intensity
t	viscosity flow time, in seconds
T	absolute temperature
V	volume of a particle; variable in treating light scattering data
x	variable in Equation (16)
α	molecular expansion factor
Γ_2	A_2M
ε	segment-solvent interaction parameter
$[\eta]$	intrinsic viscosity
η_{rel}	relative viscosity
η_{sp}	specific viscosity
θ	angle
Θ	Flory theta temperature
λ	wave length in a vacuum
λ'	wave length in the medium
μ	$(4\pi/\lambda')\sin(\theta/2)$
Φ	variable in Equation (18); Flory viscosity constant

SUMMARY

A light scattering investigation of the shape of the intramolecular scattering function was made for dilute solutions of several samples of polystyrene and polydimethylsiloxane, ranging in molecular weight from several hundred thousand to several million. All of the samples except one, which had a weight to number average molecular weight ratio of two, possessed very sharp molecular weight distributions; hence the polydispersity problems so often associated with previous investigations were mostly eliminated. By using theta solvents as well as good solvents, it was possible to investigate the predictions of both Isihara and Ptitsyn. Isihara has criticized the well-known Debye equation for Gaussian coils from the standpoint of the inapplicability of Gaussian statistics for small intramolecular distances, even at the theta temperature. On the other hand, Ptitsyn, along with other workers, pointed out that the Debye equation is not valid for good solvent systems, where excluded volume effects are present. Both workers presented generalizations of the Debye scattering function, and it was a purpose of this investigation to critically examine their predictions with reliable experimental data.

For polydimethylsiloxane the theta solvent used was bromocyclohexane and the good solvents were carbon tetrachloride and benzene, which, coincidentally, were also the good solvents for polystyrene. The theta solvent for the latter, however, was cyclohexane.

The Brice-Phoenix photometer that was used for the measurements

was modified, with particular emphasis on temperature control and a well-aligned optical system with sharp beam definition and precise angular resolution. By means of a fabricated constant temperature jacket for the cell, it was possible to regulate the temperature for the theta measurements accurately to ±0.05°C. For good solvent systems, however, it was sufficient to use an air bath which could be regulated to ±0.5°C. The alignment of the photometer was checked with scattering from dilute fluorescein solutions and from benzene.

In view of the fact that the scattered intensity is a function of not only the angle of observation but also of the wave length of the incident light, the angular measurements were made for different wave lengths. This simple, but very helpful innovation permitted the data for the different wave lengths to be overlapped, thus extending considerably the range over which the scattering function previously has been studied.

The absolute intensities were obtained from the relative intensities in the normal manner, making a Fresnel correction for reflection and an n^2 refractive index correction. The scattering standard was benzene.

Measurements at the theta condition were made for three polystyrene samples and one polydimethylsiloxane sample; and the results were plotted as P^{-1} versus $\sin^2(\theta/2)/\lambda'^2$, where P is the scattering function, θ is the angle of observation, and λ' is the wavelength of the light in the medium. In all but one of the four cases, the data were fit within experimental uncertainty by the Debye equation. The one exception, the results for the polydisperse polystyrene sample,

exhibited no detectable curvature in the data, thus permitting a characterization of the polydispersity. Numerical calculations indicated that when visible incident light is used, the Debye and Isihara functions are indistinguishable for systems of practical interest; therefore, it was concluded that the data supported equally well both predictions.

The results for the good solvent systems were plotted in the same way as those for theta systems. In this case, however, comparison was made with the Debye and Ptitsyn functions. In addition to the radius of gyration, a parameter which was required for the evaluation of both functions, the Ptitsyn curves involved a parameter ε, which is assumed to be related to the mean square distance between chain elements i and j by

$$\overline{r_{ij}^2} = |i - j|^{1 + \varepsilon} b^2$$

where b is the effective length of an element. The segment-solvent interaction parameter ε is zero for theta solvents and positive for good solvents. In keeping with the suggestion of other workers, the value of ε which was used in the calculations was determined from the exponent of the Mark-Houwink intrinsic viscosity-molecular weight relationship. Unlike the refinements of the Isihara treatment, numerical calculations indicated that the Ptitsyn equation predicts an appreciable departure from the Debye equation for systems of practical interest. The departures are in the form of downward curvature at large angles for the P^{-1} curve.

For all samples except two, the polystyrene samples having the

highest molecular weights (about 3.5 and 5 x 10^6), the good solvent data were adequately described by the Debye function; moreover, most of the data which were in accordance with the Debye prediction could not be fit within experimental error by the Ptitsyn function using the *a priori* value of ε. Instead, values close to zero were required. This result was especially surprising for those samples which had molecular weights exceeding one million.

Of the two samples that showed departures from the Debye prediction, only one exhibited large deviations that were easy to assess. The other, the polystyrene sample which yielded a straight line for P^{-1}, showed a small amount of downward curvature, thus indicating the presence of the excluded volume effect. For the other sample, however, which had a molecular weight of about five million, the deviation from the Debye curve at large angles was significantly large. In fact, by using a value for ε of 0.11 (compare with the *a priori* value of 0.16), the data were well fit by the Ptitsyn function. Therefore, even though the Ptitsyn function could be forced to fit the data, use of the ε calculated from viscosity measurements overestimated the influence of the excluded volume effect.

No reason is given for the success of the Debye intramolecular scattering function over the surprisingly large range of molecular weight. However, it is pointed out that the reason the Ptitsyn function overestimates the influence of volume effects in all cases is that it fails to account for the dependence of ε on the molecular weight or $|i - j|$. This failure is especially fallacious in a treatment of the scattering function, for the optimum conditions for

observing deviations from the Debye function are the very conditions where ε is most different from the value which is naively calculated from the Mark-Houwink exponent. That is to say, the deviations from the Debye prediction are greatest for large values of $\sin^2(\theta/2)/\lambda'^2$; however, for large angles the greatest contribution to the intensity is made by small intramolecular distances, whereas the *a priori* value of ε is based on large intramolecular distances.

Finally, it is shown that by fitting the scattering data with the Debye function over the entire angular range, the radii of gyration for essentially monodisperse samples can be determined with about half the uncertainty that is involved in the determination by the initial tangent method.

CHAPTER I

INTRODUCTION

For many years following the birth of polymer chemistry about 100 years ago, there was wide misunderstanding concerning the nature of polymers, or colloids, as they were called. It was commonly believed that the very high apparent molecular weights of all colloids resulted from extensive aggregation of molecules, and it was not until the 1920's that the existence of macromolecules was finally recognized.

Although polymer molecules are commonly several orders of magnitude larger than the solute molecules normally encountered and exhibit abnormally large entropy effects, polymer solutions are subject to the same thermodynamic laws as other solutions. Therefore, even though unusually large deviations from ideality are present, it is profitable to make use of some of the results of the general theory of non-ideal solutions and non-ideal gases (1).

In a manner analogous to that used in the treatment of non-ideal gases, it is convenient to express the change in chemical potential for a liquid, in which is dissolved any non-electrolyte, in the form of a virial equation, i.e.,

$$\mu_1 - \mu_1^0 = -RTV_1^0 c\,(1/M + A_2 c + A_3 c^2 + \ldots) \qquad (1)$$

where μ_1 = the chemical potential of the solvent in the solution;

μ_1^0 = the chemical potential of the pure solvent;

R = the gas constant;

T = the absolute temperature;

V_1^0 = the molar volume of the solvent;

M = the molecular weight of the solute;

c = the concentration of the solute in grams per milliter;

A_2 = the second virial coefficient;

A_3 = the third virial coefficient.

It is seen from Equation (1) that any experiment which allows one to measure the change in chemical potential of the solvent as a function of c, such as measurement of the vapor pressure, depression of the freezing point, elevation of the boiling point, and osmotic pressure, leads to the determination of the molecular weight of the solute and the virial coefficients. In practice, however, insufficient sensitivity to the high molecular weights prevalent in polymers precludes the use of all these methods except osmotic pressure measurements; in fact, with molecular weights exceeding a few hundred thousand the same limitation applies to osmotic pressure measurements. Since the molecular weights of polymers of interest often lie in the range from a few hundred thousand to a few million, a method more sensitive than those of a colligative nature is needed.

Before beginning a discussion of light scattering, which is a method that fulfills the need for added sensitivity to very high molecular weights, it is helpful to carry the comparison of polymer solutions to non-ideal gases one step further. For a non-ideal gas

there exists a temperature, called the Boyle temperature, at which attractive forces between the molecules counterbalance the repulsive forces associated with the finite molecular volumes, thus causing the second virial coefficient to vanish. In a similar manner, for polymer solutions there exists a temperature, called the Flory theta temperature (2), at which the attractive forces between polymer segments offset repulsive forces associated with the intramolecular excluded volume. In both cases the systems are pseudo-ideal: in the case of gases, PV is equal to RT over wide ranges of pressure; and in the case of polymer solutions, the excess chemical potential of the solvent is proportional to c over an extended range of concentration.

Light Scattering by Small Particles

Whenever a medium is subjected to light having a frequency differing from any absorption frequency of the particles composing the medium, the oscillating electric field in the incident radiation induces dipole moments in the particles, which, in turn, act as secondary emitters, thus giving rise to the phenomenon of light scattering. Furthermore, except for a very minor contribution from Raman emission, the scattered light has the same frequency as the incident light.

The calculation of the scattering by a system has been approached by two complementary methods. The first was pioneered by Rayleigh (3) and later adapted to the study of high polymer solutions by Debye (4). In this approach the scattering from individual scattering centers is first calculated, and then all such contributions are summed, being

careful to consider phase differences if correlation between scattering centers is present over distances comparable with the wave length of the light. In order to sum individual contributions, the scattering elements must not interact; therefore, the results of this approach have been applied most successfully to systems which approach ideality.

Using the model of a dilute ideal gas and assuming that the particles are optically isotropic, small compared to the wave length of the light, and have a refractive index not greatly different from the refractive index of the medium, one obtains for the scattering per unit volume, using unpolarized incident light (5),

$$\frac{i(\theta)}{I(0)} = \frac{2\pi^2(1 + \cos^2\theta)Mc(dn/dc)^2}{N_A\lambda^4 r^2} \qquad (2)$$

where θ = angle between the direction of observation and that of the incident beam;

$i(\theta)$ = the scattered intensity per unit volume at θ;

$I(0)$ = the intensity of the incident beam;

M = the molecular weight;

c = the concentration;

N_A = Avagadro's number;

λ = the wave length of the light;

r = the distance from the scattering volume to the observer.

It is interesting to note the following features of Equation (2). (1) Since all the quantities can be measured experimentally, light scattering affords an independent method for the determination of

Avagadro's number; and, indeed, this benefit caused much of the early interest in the field. (2) The inverse fourth power dependence of the scattered light on the wave length explained for the first time many well-known facts such as the blue appearance of the sky and large bodies of water. (3) The presence of M in the equation shows immediate applicability to molecular weight determinations; moreover, consideration of the analogous expression for the scattering per particle shows that the intensity is proportional to the square of the molecular weight, thus showing the promise of sensitivity to very high molecular weights. (4) For small particles the scattering is symmetrical about 90 degrees.

Equation (2) can also be applied to ideal solutions when an additional factor of n_o^2 is added to the numerator of the right hand side, n_o being the refractive index of the solvent. On the other hand, two cases of greater interest are pure liquids and non-ideal solutions, and neither of these can be described adequately by the Rayleigh treatment. Fortunately both of these examples can be explained in terms of the Einstein-Debye fluctuation theory.

When the Rayleigh theory is extended to pure liquids, the predicted scattered intensity is found to be about 50 times too large (6). This disappointing failure can be better understood by noting that pure liquids lie between a dilute gas, in which random motion is implicit, and a crystalline solid, in which individual particles are so regularly arranged that with visible light virtually no scattering is observed. Extending the Rayleigh theory by accounting for phase differences proved prohibitively difficult; however, Einstein (7),

by developing an idea originally set forth by Smoluchowski (8), was able to circumvent the problems by considering the liquid as a continuous medium with ever present statistical fluctuations in density, which lead to corresponding fluctuations in the refractive index. By assuming the volume elements in which these fluctuations occur are small compared to the cube of the wave length and yet large enough to contain many molecules, he derived an expression relating the scattered intensity to the isothermal compressibility, density, temperature, and the density dependence of the refractive index, as well as the wave length and angle of observation. The same result was derived much later using a molecular theory of light scattering (9).

By considering fluctuations in concentration as well as density, Einstein (7), and later Debye (10), also treated the case of a non-ideal solution. By assuming that the density fluctuations for the solution and pure solvent are identical, the problem of determining the scattering of a solution in excess of that of the solvent, called the excess scattering, reduces to the determination of the mean square concentration fluctuation, which, in turn, is related to the change of the chemical potential of the solvent with respect to concentration. The result of this approach is

$$\frac{i(\theta)}{I(0)} = \frac{2\pi^2 n^2 (dn/dc)^2 (1 + \cos^2\theta) c}{N_A \lambda^4 r^2 (1/M + 2A_2 c + 3A_3 c^2 + \ldots)} \qquad (3)$$

where all quantities have the same meaning as before. Since n for dilute solutions does not differ greatly from n_o, Equation (3) reduces to

$$Kc/R(\theta) = 1/M + 2A_2c + 3A_3c^2 + \ldots \quad (4)$$

where $K = 2\pi^2 n_o^2 (dn/dc)^2 / N_A \lambda^4)$ is the optical constant and $R(\theta) = r^2 i(\theta)/(I(0)(1 + \cos^2\theta))$ is the reduced scattering intensity. Note that $R(\theta)$ differs from Rayleigh's ratio, $r^2 i(\theta)/I(0)$, by a factor of $1 + \cos^2\theta$.

Therefore, for a solution in which the dimensions of the solute molecules are small compared to the wave length of the light (less than about $\lambda/20$), a plot of $Kc/R(\theta)$ versus c has a slope equal to twice the second virial coefficient and an intercept equal to the reciprocal of the molecular weight. If, as is always the case with high polymers, not all solute species have the same molecular weight, the value obtained is the weight average molecular weight, $\bar{M}_w$, given by

$$\bar{M}_w = \frac{\Sigma\, n_i M_i^2}{\Sigma\, n_i M_i} = \frac{\Sigma\, c_i M_i}{\Sigma\, c_i} \quad (5)$$

where n_i = the number of moles of species i;

M_i = molecular weight of species i;

c_i = concentration of species i in g/cc.

Equation (5) may be compared with the following equation which gives the number average molecular weight, $\bar{M}_n$,

$$\bar{M}_n = \frac{\Sigma\, n_i M_i}{\Sigma\, n_i} = \frac{\Sigma\, c_i}{\Sigma\, (c_i/M_i)} \quad (6)$$

The latter average molecular weight may be obtained from osmotic pressure measurements; and a comparison of this value with that obtained from light scattering is a measure of the polydispersity of the sample.

Light Scattering by Large Particles

Whenever visible light is used, most polymers of interest have at least one dimension which exceeds the small particle upper limit of approximately $\lambda/20$, thus leading to an added complication in the determination of the molecular weight and second virial coefficient. In order to determine M from Equation (4) not only must the excess scattering be extrapolated to zero concentration but also to zero angle. This is readily seen by considering a large particle and a pair of scattering points within the particle which are separated by a distance comparable to the wave length. If the observation is made at $\theta = 0$, that is, looking toward the light source, two parallel light waves which interact with both points travel the same distance from the source to the observer. Therefore, two waves having a phase difference at the source will have the same phase difference when they reach the observer. When, however, the observation is made for non-zero angles, the path length differs for the two waves, and this difference increases with the angle of observation, thus giving rise to destructive interference, the magnitude of which varies with angle. Consequently, for large particles the excess scattering at a given angle θ is smaller than that for a small particle of the same molecular weight, unless, of course, $\theta = 0$, in which case the two values are equal.

At this point it is convenient to introduce a function, $P(\theta)$, called the intramolecular light scattering function, which is defined as the ratio of the average scattered intensity at θ with interference to the average scattered intensity without interference (5). Thus the reduced scattering intensity observed at any angle is proportional to $P(\theta)$, which, in turn, approaches unity as θ approaches zero. Accordingly, for large particles Equation (4) becomes

$$Kc/R(\theta) = 1/MP(\theta) + 2A_2c + 3A_3c^2 + \ldots \qquad (7)$$

Most treatments which result in theoretical expressions for $P(\theta)$ for different molecular models begin with the following equation, which is taken from the theory of the X-ray scattering of gases (11):

$$P(\theta) = \frac{1}{N^2} \sum_i \sum_j \frac{\sin \mu r_{ij}}{\mu r_{ij}} \qquad (8)$$

Here r_{ij} is the distance between the ith and the jth scattering point, N is the total number of such points, and $\mu = (4\pi/\lambda')\sin(\theta/2)$, where λ' is the wave length in the medium. In its application to polymer solutions, Equation (8) relates to an isolated molecule which has definite shape, but which has been allowed to assume with equal probabilities all possible orientations. Furthermore, it is assumed that the size of the molecule and the difference in refractive index between the molecule and its environment are small enough that the primary electric field of the electromagnetic radiation is not appreciably distorted by its reaction with the molecule. If, as is often the case with very

large particles (dimensions much greater than λ) the primary field is appreciably distorted, it is no longer valid to begin with Equation (8); rather, the very complex general problem, which has been solved for the special case of a homogeneous sphere by Mie (12), must be considered. Although the error is difficult to quantitatively evaluate, it is generally felt that for the systems of interest in this study, namely, coiling molecules of moderately high molecular weight, consideration of the primary field distortion is not necessary (10).

Before proceeding with the actual evaluation of $P(\theta)$ for a coiling molecule it is interesting to examine the generalized form of Equation (8), in the limit of small values of θ (5). If the quantity $\sin \mu r_{ij}/\mu r_{ij}$ is expanded in terms of a power series, it is found that

$$P(\theta) = 1 - \mu^2 R^2/3 + \ldots \tag{9}$$

or, following substitution for μ and inversion,

$$1/P(\theta) = 1 + \frac{16\pi^2}{3\lambda'^2} R^2 \sin^2(\theta/2) + \ldots \tag{10}$$

where R, called the radius of gyration, is the root mean square distance of the mass elements in a macromolecular coil from its center of gravity, or more generally,

$$R^2 = (1/V) \int r_g^2 \, dv \tag{11}$$

where V is the volume of the particle, r_g is the distance from any point to the center of gravity, and dv is a volume element. For flexible molecules the r_g values are continuously changing and thus the radius of gyration is actually an average quantity.

It is seen from Equation (10) that the angular dependence of the scattering, which was formerly described as an added complication in the practice of light scattering, actually provides an unambiguous measure of the size of solute particles in solution. The initial slope of the curve drawn through the angular intensity data which have been extrapolated to zero concentration is proportional to the square of the radius of gyration.

Although $P(\theta)$ expressions for many different molecular models have been derived, including spheres (13), rods (14), and flexible coils, because of the nature of the polymers used in this study, only flexible coils will be discussed.

Flexible Coils: Theoretical Considerations

Most synthetic polymers form amorphous solids, and in solution they seem to demonstrate little preference for one molecular configuration over another. If the polymers are linear or, in other words, if they have few or no long side branches, the picture of a coil which is continuously changing shape seems to be consistent with experimental results. From a theoretical point of view, it appears beyond the limit of human capabilities to mathematically account for each of the incomprehensibly large number of possible configurations for chains comparable in length to those normally encountered, even over relatively short

periods of time; consequently, the problem is approached from a statistical standpoint and quantities describing the dimensions of the coil are time average quantities, which are obtained by averaging over all possible configurations.

Therefore, for flexible coils Equation (8) becomes

$$P(\theta) = \frac{1}{N^2} \sum_i \sum_j \left[\overline{\frac{\sin \mu r_{ij}}{\mu r_{ij}}} \right]$$

where the bar indicates an average over all distances r_{ij}. At this point it is desirable to picture the polymer molecule as a series of N-1 segments of zero volume with all the mass distributed at points of zero volume located at the intersection of the segments and at the ends of the chain. It is also convenient to assume that the N scattering points coincide with the mass points. Thus if fixed bond angles and restricted internal rotation are neglected and if the molecule is assumed to have negligible volume, the length of a chain segment corresponds to the bond length between the atoms in the backbone of the polymer.

To determine the value of the averaged quantity in Equation (12), one must know the probability for obtaining a given value of r_{ij}, the distance between the ith and the jth emitters. A relatively simple and often realistic expression for this probability may be derived by the method of random flights (15). The assumptions are that the average extension of the chain is much less than the contour length and that the total number of segments is much greater than

unity; and the result of the calculation is the well-known Gaussian distribution function. Thus the probability for finding an intersegmental distance between r_{ij} and $r_{ij} + dr_{ij}$, without regard to direction, is given by

$$W(r_{ij})dr_{ij} = 4\pi r_{ij}^2 (3/2\pi \overline{r_{ij}^2})^{3/2} \exp(-3r_{ij}^2/2\overline{r_{ij}^2})dr_{ij} \qquad (13)$$

$W(r_{ij})$ is called the Gaussian radial distribution function, and $\overline{r_{ij}^2}$ for Gaussian statistics depends only on the number of segments between the ith and jth emitters:

$$\overline{r_{ij}^2} = |i - j| \, b^2 \qquad (14)$$

where b is the length of a segment.

Using Equation (13) the bracketed quantity in Equation (12) can be evaluated; and the expression for $P(\theta)$ becomes

$$P(\theta) = \sum_i \sum_j \exp(-\mu^2 \overline{r_{ij}^2}/6) \qquad (15)$$

Debye (16) performed the indicated summations, the result being

$$P(\theta) = (2/x^2)(e^{-x} + x - 1) \qquad (16)$$

where x is given by

$$x = (16\pi^2/\lambda'^2)R^2 \sin^2(\theta/2) \qquad (17)$$

Note that the Debye function, Equation (16), can be described with one adjustable parameter, R^2, which is an experimentally measurable quantity (17).

The validity of Equation (16), the Debye function, may immediately be questioned because of the unrealistic assumptions about internal rotation and bond angles. Kuhn (18), however, showed that a real polymer chain with fixed bond angles and restricted internal rotation may be thought of in terms of an equivalent Gaussian chain and still retain the same average dimensions. Instead of allowing each bond to be a statistical segment, a fixed number of bonds are replaced by an equivalent segment, the number of bonds chosen to be large enough so that there is no correlation between the directions of the first and the last bond and small enough to give a large number of segments in the equivalent chain. Following the replacement of each segment length with the root mean square segment length, the result is a chain which is equivalent to the real chain but is freely jointed and has a large number of segments, each with the same length.

Isihara (19) has pointed out that Equation (13) is not valid for very small values of intramolecular distances and thus that the Debye function should not be used for low values of N and high angles. His treatment of the flexible chain, which is more rigorous than that of Debye, results in the following expression, which reduces to the Debye equation at low angles:

$$P(\theta) = N^{-1} + 2(1 - \Phi/N)[\Phi - 1 + (1 - \Phi/N)]^{N}\Phi^{-2} \qquad (18)$$

where

$$\Phi = N[1 - \sin(4\pi b\sin(\theta/2)/\lambda')/(4\pi b\sin(\theta/2)/\lambda')] \qquad (19)$$

Thus the scattered intensity depends not only on x but also on N.

Several workers (20-23) have questioned the validity of the Debye equation when applied to good solvent systems, that is, when A_2 is positive and T is greater than the theta temperature. This objection centers about the assumption in the Gaussian chain treatment that the chain segments have zero volume, which, then, allows two or more segments of a chain to occupy the same place in space at the same time. The supposition is reasonable in a poor solvent (under theta conditions), where the excluded volume effect vanishes; however, in a good solvent the polymer segments definitely "feel" the presence of one another, and in order to reduce segment-segment contacts the coil expands, thus disturbing the distribution of intramolecular distances. Moreover, it has been shown from the theory of Markov chains that the presence of long range correlation in the form of excluded volume precludes the validity of Gaussian statistics (24). That the Gaussian assumption is no longer valid in good solvents is also pointed out in theoretical treatments of polymer solutions which demonstrate that in a good solvent the dimensions no longer are proportional to the first power of the molecular weight but to a power greater than unity (25,26). This result led Ptitsyn (21), Benoit (22), and Hyde (23) to assume that

$$\overline{r_{ij}^2} = |i - j|^{1 + \varepsilon} b^2 \qquad (20)$$

where ε is a parameter which is zero in a theta solvent and greater than zero in a good solvent. For the sake of tractability, however, they retained Equation (13). Following substitution into Equation (15) and replacement of the summation by integration, $P(\theta)$ becomes

$$P(\theta) = 2 \int_0^1 (1 - y)\exp[- \frac{16\pi^2}{\lambda'^2} R^2 \sin^2(\theta/2)(1 + 5\varepsilon/6 + \varepsilon^2/6)y^{1+\varepsilon}]dy \qquad (21)$$

which reduces to Equation (16) when $\varepsilon = 0$.

Equation (21) is obviously just an approximation since it is assumed that volume effects merely influence the mean square distances between segments (or emitters) and not the statistical distribution of these distances. Therefore, a more appropriate thing to do would be to use a better distribution function. Evidence of this kind of work has been given for a distribution function which was deduced from Monte Carlo computer calculations, but the details are not known (27).

Flexible Coils: Experimental Evidence

In this section discussion will be limited, for the most part, to experiments which attempt to test the validity of Equations (16), (18), and (21). Before examining such investigations, however, it seems worthwhile to very briefly note experimental evidences of a different nature which testify to the existence of the excluded volume effect and the inappropriateness of the Gaussian approximation in good solvents.

Many papers have appeared recently which report directly calculated influences of excluded volume by means of Monte Carlo computer methods for various kinds of lattices (24,28,29,30). Suffice it to say, the presence of volume effects does cause non-Gaussian behavior, and in some cases actual distribution functions for intramolecular distances were obtained (24,31). Remaining evidence centers about the functional dependence of R^2/M on M; and this dependence has been demonstrated directly by light scattering and indirectly by viscosity measurements (32,33,34).

At first it is rather surprising that there are very few explicit experimental verifications of Equation (16) in the literature; however, it should be realized that the Debye equation applies only to a monodisperse polymer, and until recently the only way to prepare samples with even relatively narrow molecular weight distributions was a very laborious fractionation procedure. Thus, before the availability of "monodisperse" polymer samples through anionic polymerization techniques (35), most angular data had to be corrected for polydispersity (36,37).

Eskin (38) made measurements on two narrow fractions of polystyrene which was originally polymerized at room temperature over a period of two years. The investigation was carried out in cyclohexane at 34.4°C, the theta temperature, using 5460 Å incident light. For both fractions the data are fit reasonably well by the Debye function, the result expected for a theta solvent. However, when angular measurements were made for the same two fractions in toluene, a good solvent, different results were obtained. The data for the lower

molecular weight fraction, $M = 4.5 \times 10^6$, could be fit within experimental error (about 5 per cent) by the Debye function; on the other hand, the $1/P(\theta)$ data for the second fraction, $M = 20 \times 10^6$, exhibit downward curvature at large angles, characteristic of the Ptitsyn function, Equation (21). It should be pointed out that the data are fit very well at all but the highest angles by the Debye function, and his justification for saying the Ptitsyn function better fits the data than does the Debye function is somewhat questionable. Nevertheless, the data do qualitatively agree with the Ptitsyn prediction. Similar measurements (34) were also reported for seven fractions of poly-2,5-dichlorostyrene in dioxane, a good solvent. In this investigation, however, the lack of significant polydispersity effects was judged from ultracentrafuge measurements on one of the fractions. The angular data are given only for the two samples having the highest molecular weights (19.6×10^6 and 16.7×10^6), and the data for both of these exhibit the same general characteristic as do the data for the high molecular weight fraction ($M = 20 \times 10^6$) of polystyrene in toluene, namely, downward curvature at only the highest angles.

Loucheux, Weill, and Benoit (39) investigated the angular dependence of the scattering for a polystyrene fraction ($M = 9 \times 10^6$) in benzene, a good solvent, and in cyclohexane, a theta solvent, using 5460 Å incident light. In this study, however, the polymer sample possessed a rather broad molecular weight distribution ($\overline{M_w}/\overline{M_n} = 1.8$) and thus a polydispersity correction was necessary. Because of this complication their evidence favoring the use of the Ptitsyn function in good solvents is of an indirect rather than a

direct nature. Using the result for a polydisperse polymer that the establishment of the $1/P(\theta)$ asymptote along with the initial tangent permits the characterization of the extent of polydispersity by light scattering measurements alone (37), the authors determined $\overline{M_n}$, $\overline{M_w}$, and the next higher moment of the distribution function, $\overline{M_z}$, from the measurements in cyclohexane. When the earlier theoretical treatment (37) was extended to account for volume effects, the scattering data for the benzene system yielded values for the various average molecular weights which agreed well with those in cyclohexane, whereas treatment without allowance for volume effects indicated a much too broad molecular weight distribution. Since it is often quite difficult to precisely locate the $1/P(\theta)$ asymptote (40) and since this method makes paramount the importance of the data obtained at high angles, which in this study were admittedly imprecise, the high angle data were verified by overlapping the results obtained at two wave lengths, the second being 4358 Å. Even though the data overlapped smoothly, indicating that all the points obtained at 5460 Å were reliable, the fact that this verification was done with the data obtained for one of the solutions and not with the zero concentration data leaves something to be desired.

Hyde, *et al.* (23), made independent measurements on essentially the same sample as that used by Loucheux, Weill, and Benoit, the principal difference being that the French workers performed additional fractionation and thus probably had a somewhat sharper fraction (41). In this study Hyde, *et al.*, investigated the scattering in benzene and 2-butanone, the latter liquid being a poorer solvent than

benzene but not a theta solvent. Once again, the conclusion favoring the Ptitsyn function in good solvents was founded on the failure of the theory for Gaussian coils to correctly predict the broadness of the molecular weight distribution. This time, however, since measurements were not made in a theta solvent, the extent of polydispersity was not measured, but rather estimated. Although 5460 Å incident light was used in both of these independent studies, it is interesting to note that the shapes of the reciprocal scattering function curves are quite different, especially at high angles.

Using six fractions with molecular weights ranging up to 1.1×10^6, which exhibited negligible polydispersity, Prud'homme and Sicotte (42) investigated the scattering of dilute solutions of polystyrene in toluene with 5460 Å light. Even though their estimated precision for the scattered intensities was on the order of 1 per cent, within experimental error their results are fit equally well with the Debye and Ptitsyn functions. They blamed their inability to differentiate between the two expressions on the small range of the variable x which they covered in their experiments.

Debye, Chu, and Kaufmann (43) reported results for an anionically polymerized polystyrene with a very sharp molecular weight distribution ($\overline{M_w}/\overline{M_n} = 1.02$) in benzene. Since their measurements were made with 4358 Å incident light and since the molecular weight of the sample was relatively high ($M = 1.5 \times 10^6$), the values of x obtained were high enough to make a distinction between Equations (16) and (21). Although the authors did not mention Equation (21), they did report that within experimental error (5 per cent) their results

were fit well by Equation (16), concluding that for polystyrene in benzene the Gaussian approximation is valid.

Finally, it should be noted that although the results of Isihara (19) have been available for some time and although Isihara himself proposed to make numerical calculations, there appear to be neither experimental verification nor numerical calculations for Equation (18) in the literature.

Purpose of the Research

Although light scattering has long been recognized as an important tool in the characterization of polymers and thus has received much attention from experimental and theoretical workers, there remain several fundamental areas of practical interest which are poorly understood. One such area is that of the form of the intramolecular light scattering function for flexible macromolecules. The validity of the Debye equation has been questioned not only for the case of good solvents but also for theta solvents, and theoretical generalizations have appeared. However, the experimental evidence verifying these theoretical treatments is inconclusive and, in the case of theta solvents, lacking.

It has been the purpose of this investigation to systematically study the angular dependence of the light scattered by different polymer-solvent systems and by this study to better know the experimental regions of applicability of the various theoretical results. In order to be more critical than previous studies, the following objectives have been pursued: (1) measurements for two linear polymers

differing in chain flexibility; (2) the use of several very sharp fractions of moderately high molecular weight; (3) measurements in both good and theta solvents; (4) the extension of the range of the variable x and the verification of the high angle data by the use of more than one wave length for each experiment.

The two linear polymers chosen for the study were polystyrene, $H[CH_2CH(C_5H_6)]_xH$, and polydimethylsiloxane, $CH_3[Si(CH_3)_2O]_xSi(CH_3)_3$. In addition to being readily available and very easy to handle experimentally, polystyrene is one of the polymers most often used in light scattering investigations and thus offers obvious advantages with respect to availability of characterization information and comparison of results. Polydimethylsiloxane, though not as well characterized as polystyrene, exhibits greater chain flexibility, a property very important in the consideration of segment distributions.

All the samples except one, polystyrene-II, possessed very sharp molecular weight distributions, and hence the polydispersity problems associated with some of the former investigations were mostly eliminated. By using theta solvents as well as good solvents, the polydispersity effect was examined and evaluated without any excluded volume complications. For polydimethylsiloxane the theta solvent used was bromocyclohexane and the good solvents were carbon tetrachloride and benzene, which, coincidentally, were also the good solvents for polystyrene. The theta solvent for polystyrene, however, was cyclohexane.

Finally, as it has recently been pointed out (40), the fact that $P(\theta)$ is a function of wave length as well as angle can have

considerable experimental significance. Although this double functional dependence is quite obvious upon inspection of Equation (10), experimental workers have evidently failed to appreciate its significance. All the investigations noted in the previous section fully utilized only one wave length, and often that wave length was 5460 Å. When 3650 Å radiation is also used and the data are overlapped, the range of abscissa values is approximately twice that using the green wave length alone. In view of the fact that departures from the Debye equation are expected at high abscissa values, this extension has great importance. In all the experiments of this study, measurements were made for both 4358 Å and 3650 Å incident light, and for several systems 5460 Å radiation was also used.

CHAPTER II

INSTRUMENTS AND MATERIALS

Although the instruments and materials used in this study in many respects were essentially the same as those used in conventional light scattering investigations, several additional provisions and considerations were necessary, especially with regard to the light scattering photometer and the polymer samples.

Light Scattering Photometer

All light scattering measurements were made with a modified Brice-Phoenix Universal Light Scattering Photometer, 1000 series. Although this kind of instrument has been in wide use for several years and although descriptions are available (44), it seems profitable to give a general description before proceeding with a listing of the modifications.

The Brice-Phoenix photometer is especially designed to measure the intensities of the scattered light at different angles of observation and to relate these small scattered intensities to the very large intensities of the incident beam. The light source is an AH-3 mercury vapor lamp, and the intensities are measured with a very sensitive galvanometer (the present galvanometer had a sensitivity of .0007 micro amps per mm. deflection) which receives an amplified signal from a 1P21 photomultiplier tube. In order to minimize stray light, the light scattering compartment is painted black and the light

which is not scattered or reflected at the interfaces is absorbed in a light trap tube.

Before entering the light scattering cell, the light from the lamp passes through a monochromatic filter, an achromatic lens, optional neutral filters, a plano-cylindrical lens, and two slits, respectively. The light which is scattered in the direction of the photomultiplier housing passes through two more slits before striking the photomultiplier tube. When the housing is in the 0° position, that is to say, looking at the light source, a working standard, which greatly reduces the intensity of the light, is automatically inserted between the two slits that define the incident beam.

Although several kinds of scattering cells are available, the one used in this study was a cylindrical pyrex cell with flat entrance and exit windows (Phoenix number C-101), similar to the one described by Witnauer and Scherr (45).

Modifications

In spite of the great versatility of the commercially available instrument, several modifications were found advisable. Most of the changes were of a minor character but nonetheless improved the angular data obtainable.

Electronic Circuitry. Two minor changes were made in the electronic circuitry: (1) in order to reduce to a minimum the instability in the galvanometer circuit, the mercury battery used for regulating the dark current was removed, thus permitting a mechanical zeroing of the dark current; (2) a "very fine" voltage adjust was introduced by placing a 100K variable resistor in series with the

normally present "fine" adjustment (5 meg.).

Temperature Control. Because of the gradual increase in temperature of the scattering compartment with time and because of the precise control demanded by measurements at the theta temperature, two kinds of temperature control were employed.

The first, utilizing an air bath, was accomplished by circulating either heated or cooled air through the scattering compartment, which was insulated with foamed polystyrene. A blower forced air through an electrical heater which was controlled by a Variac, around a cooling coil of copper tubing, and through a one-inch hole in the back of the photometer. In order to provide an exit for the air, a blackened tube was fitted to the end of the light trap, bent in such a way so as to eliminate reflected and stray light. Since abnormally high temperatures lead to instability and possible damage of the photomultiplier tube, the photomultiplier housing was cooled with two copper coils, through which tap water was circulated. The temperature inside the box was monitored with a bridge-type circuit employing a thermistor and an ammeter.

Further control was accomplished by the fabrication of a constant temperature jacket which fitted snugly about the cell. The jacket consisted of a brass pipe, about which was tightly coiled and soldered one-fourth inch copper tubing, which, in turn, was insulated with polystyrene foam and black tape. A section of the pipe about two inches in height and subtending an angle of about 200° was removed to permit the unobstructed passage of light through the cell. An insulated brass lid, which was placed on top of the glass

cell cover, was also fabricated.

Temperature control was achieved by circulating water from a constant temperature bath through insulated rubber tubing and through the jacket. The temperatures of the water before entering and after leaving the jacket were monitored by two calibrated 100 degree thermometers, and the stability of the bath temperature was determined with a Beckmann differential thermometer.

Optical Considerations. Because of the stringent demands on the angular data necessitated by this study, great care was taken to insure sharp beam definition and precise angular resolution.

The principal modification in this area was the replacement of the two beam defining slits with two made from double edge razor blades. The slit immediately in front of the cell was 2.0 mm by 5.0 mm, considerably narrower than that supplied with the instrument. The slits were blackened with a benzene flame to reduce stray light.

Further changes were made which increased the angular range of the measurements. The standard limit stop for the photomultiplier housing was replaced by another stop which permitted an upper angular limit of 140°; the lower limit was extended to 25° by removal of part of the shield from the working standard.

Finally, everything inside the box was given a flat black finish, either with a latex paint or with a benzene flame. Included was the entire outside surface of the light scattering cell, except for the entrance and exit windows and a section on one side about two inches in height.

Alignment

Following the introduction of the new slits, the lamp housing and the cell table were adjusted until the light beam passed centrally through the two slits, across the cell table, and through the light trap tube. A further restriction was that the light pass through both slits on the photomultiplier housing when the working standard was removed and the housing was placed in the zero degree position.

Furthermore, it was necessary to align the scattering cell. This was done by geometrically centering the cell on the cell table with the entrance window perpendicular to the incident beam, as judged by the reflection of light onto the defining slit. The cell was then glued to a square piece of glass which fitted snugly into slots on the cell table. Although the cell was visually aligned, it was important to check the optical alignment. This was first done by measuring the angular dependence of the intensity of the fluoresced light emitted by a dilute solution of fluorescein in methanol. In order to examine only the fluoresced light, a green Wratten gelatin film light filter, series 62, was placed in the nosepiece of the photomultiplier housing. After making a sin θ volume correction, the intensities were found to be constant to ± 1 per cent for angles between 30° and 135° for both 4358 Å and 3650 Å unpolarized incident light. A further check on the optical alignment was made by determining the angular scattering of benzene and by confirming the following relationships (46):

$$G(\theta)/G(90) = [1 + \cos^2\theta\ (1 - \rho)/(1 + \rho)]/\sin\theta \qquad (22)$$

where $G(\theta)$ is the galvanometer reading at an angle θ and ρ is the depolarization of benzene. Using the data obtained with 4358 Å and 3650 Å unpolarized incident light and the experimentally determined values of ρ for each of these wave lengths, $G(\theta)/G(90)$ agreed with the right-hand side of Equation (22) to within 1 per cent for angles between 25° and 140°. Similar results were obtained with 5460 Å light for angles between 35° and 140°.

Differential Refractometer

All measurements of the refractive increments, dn/dc, were made with an unmodified Brice-Phoenix Differential Refractometer (47), which, as the name suggests, is designed to measure directly small differences in refractive index between two liquids, such as between the solvent and its dilute polymer solutions. The limiting sensitivity of the instrument is about three in the sixth decimal place of the refractive index.

Basically the instrument consists of a mercury lamp with monochromatic filters, an adjustable slit, the differential cell, a projection lens, and a micrometer microscope, all accurately aligned on an optical bench. The square optical cell is divided into two parts by a thin glass plate set at an angle such that the incident beam passes through both sections of the cell and is deflected, the magnitude of the deflection being dependent on the difference in refractive index of the liquids in the two compartments. Accessory features include a semi-transparent mirror, which permits the use of another light source, and the freedom of the cell and its holder

to be turned through 180°, which approximately doubles the deflections obtained.

Viscometers

Three different viscometers were used to determine the intrinsic viscosities; however, all three were of the Ubbelohde type and available commercially. The principle advantage of this kind of viscometer over the conventional U-tube variety is that the effective pressure head is independent of the total volume of liquid in the viscometer. This advantage also facilitates dilutions in the viscometer, a feature especially helpful when determining flow times for a series of solutions which differ only in concentration.

One of the instruments, called a rate of shear viscometer, had an additional feature providing for the measurement of flow times at different rates of shear. This was accomplished by having four pairs of fiducial marks, instead of the normal one pair, at progressively lower levels with respect to the liquid reservoir.

In all cases the viscometers were mounted vertically (visually) in a constant temperature water bath, and they could be removed and replaced in a reproducible manner.

Polymer Samples

One sample used in this study was purchased from the National Bureau of Standards, and all others were graciously donated by workers in other laboratories; therefore, most preliminary data characterizing the samples were obtained through private communications.

The four polydimethylsiloxane (PDMS) fractions were supplied

by Mr. Robert Buch of the Dow Corning Corporation. Other PDMS fractions having lower molecular weights were characterized by light scattering, membrane osmometry, and intrinsic viscosity measurement, and the results of these characterizations led to an estimated value of $\overline{M_w}/\overline{M_n}$ for the four fractions used in this study of 1.10 or less (48).

PS-705, the polystyrene sample obtained from the National Bureau of Standards, was anionically polymerized and characterized by osmometry, light scattering, sedimentation equilibrium, viscosity, and fractionation measurements. Accordingly, $\overline{M_w}$ (L.S.) = 179,300 and $\overline{M_w}/\overline{M_n}$ (from fractionation data) = 1.07 (49).

PS-I, another anionically polymerized polystyrene sample, was supplied by Dr. F. Wenger of the Mellon Institute. Although the molecular weight distribution was already quite narrow (for a similar sample, $\overline{M_w}/\overline{M_n}$ = 1.02) (50), further fractionation was undertaken. The sample was dissolved in enough freshly distilled 2-butanone to make a 0.5 per cent solution. About 10 per cent of the sample was precipitated with methanol and removed. Then enough methanol was added to precipitate about 90 per cent of the polymer remaining in solution, and this fraction, called PS-I, was used in this study. Following the removal of the polymer-rich phase, the polymer was precipitated in a Waring blender filled with methanol, dried, dissolved in benzene, reprecipitated in the Waring blender, and finally dried under vacuum at 60°C.

A sedimentation velocity analysis of PS-II, a high molecular weight sample obtained from Dr. H. W. McCormick of the Dow Chemical

Company, yielded $\overline{M}_w = 3.22 \times 10^6$ and $\overline{M}_w/\overline{M}_n = 1.29$. The broad molecular weight distribution attributed to this sample, which was anionically polymerized, was rationalized by the observation that for unknown reasons the polymerization developed in a very abnormal manner (51).

Finally, PS-III, the polystyrene fraction with the highest molecular weight, was received from Dr. G. Berry of the Mellon Institute. Its weight average molecular weight was assessed to be 4.40×10^6 (52).

All the samples except PS-I, which was obtained by a fractionation, were used without further treatment.

Solvents

All four of the solvents used in this study were originally reagent grade or better, and in all cases except that of the bromocyclohexane the solvents were redistilled immediately before use.

Reagent grade benzene was dried with freshly prepared sodium wire, fractionally distilled at atmospheric pressure through a packed column, and stored over sodium wire. The carbon tetrachloride, reagent grade, was dried with $CaCl_2$, fractionally distilled at atmospheric pressure, and stored over P_2O_5. Two kinds of cyclohexane were used: reagent grade solvent was dried with $CaCl_2$, fractionally distilled at atmospheric pressure, dried over sodium wire, passed through a column of alumina, and finally stored over sodium wire; spectroscopic grade solvent was dried with Drierite, fractionally distilled at atmospheric pressure, and stored over Drierite. Finally, the bromocyclohexane, Eastman white label, was fractionally distilled at 5 cm. of mercury and used without further purification.

CHAPTER III

PROCEDURE

The time required to develop the good experimental technique needed for this investigation was considerable, and even after the period of development, occasional minor improvements in technique and data treatment were discovered and used. Therefore, the procedure given here, though not the acme of perfection, is the collection of methods found to give the best results.

Light Scattering

The above comments on procedure are particularly applicable to the light scattering investigation; in fact, at times the collection of reliable data to some extent took on the semblance of an art.

Preparation of Solutions

In keeping with the theoretical treatments discussed in Chapter I, which are applicable to very dilute solutions, the concentrations of the polymer solutions used in this study usually lay between 0.2×10^{-3} and 1.4×10^{-3} grams of polymer per cubic centimeter of solution. For molecular weights exceeding one million, this lower limit of concentration corresponds approximately to a 10^{-7} molar solution.

For all systems except that of PS-I in benzene, several solutions (usually four) were prepared by weighing the polymer directly into each of the 50 ml. volumetric flasks, the amount of polymer

chosen in such a way to effect approximately equal spacing with respect to concentration. Each of the flasks was then half filled with freshly-distilled solvent and allowed to sit until the polymer was dissolved. Since some systems required two days or more for the completion of the dissolution process, it was found especially helpful to gently shake the flasks overnight in a mechanical shaker, the time required then being reduced to a few hours. During the shaking process, the tops of the flasks were covered with aluminum foil, and for theta systems the flasks were maintained at a temperature about 10 to 20° above the theta temperature with an infrared heat lamp.

After the polymer was dissolved, the solutions were set aside until needed for measurements, at which time they were diluted to volume. In order to prevent polymer precipitation in the theta solvent systems, the solutions were kept warm and the dilutions were made in a constant temperature bath, whereas other dilutions were performed at room temperature.

For PS-I in benzene, the principal difference in the solution preparation was that a mother solution was prepared by direct weighing and more dilute solutions were prepared by aliquots.

Removal of Dust

Since the presence of dust has an overwhelming effect on the scattered light intensities from both pure solvents and solutions, it is imperative that it be removed before the measurements are commenced. The two methods of removal commonly used, filtration and high speed centrifugation, usually are very effective; however, under certain circumstances neither method is completely satisfactory.

Because of early success with the filtration method, it was chosen for this study.

In all cases except PDMS-I in carbon tetrachloride, for which it was necessary to use an ultrafine filter, the solvents and solutions were filtered through Corning sintered glass filters of either fine or very fine porosity, using about 15 psi of dry nitrogen. The filter discs were purchased in the form of Buchner funnels and fabricated into pressure funnels with ground glass inner joints on the top.

Before proceeding with the filtration, it was necessary to remove the ubiquitous dust from the cell. The otherwise clean cell was placed upside down in a fabricated cell cleaner, which basically was a distillation apparatus with the cell serving as the condensor. When the liquid in the pot (usually the same as the solvent used in the measurements) was heated, vapor condensed in the air cooled cell, to a large extent removing the dust. The condensed vapor then flowed into a reservoir and periodically siphoned back into the pot. After about 30 minutes in the cell cleaner, the cell was removed and quickly covered with a clean glass plate.

For each experiment both the pure solvent and the series of solutions were filtered; in both cases similar provisions were made. All the solution or about 50 ml. of solvent was poured into the clean filter and the ground glass connection was put in place. About three or four ml. was then forced through the disc and discarded.

In order to rinse away any loose dust from the bottom of the filter, most of the remaining liquid was filtered into a clean flask and then poured back into the filter funnel. Finally, the solution

(or solvent) was forced directly into the clean cell, which, in order to minimize dust contamination from the atmosphere, was shielded by an inverted glass funnel attached directly to the filter funnel apparatus.

When working with theta systems, in addition to the above considerations, the filter was preheated and kept warm with an infrared heat lamp.

In order to ascertain the effectiveness of the filtration procedure, the cell was placed in the photometer and the scattering of the unfiltered mercury light by the solution was visually observed at very low angles with a mirror. This "mirror test" was a surprisingly sensitive test for the presence of dust; in fact, a positive result did not necessarily preclude suitability for intensity measurements. By experience it was learned approximately how much dust could be tolerated without seriously affecting the resulting data.

More often than not, one filtration did not prove satisfactory, and the solution was swirled vigorously and poured back into the filter apparatus. Unless the clarification was particularly ineffective, in which case the cell was cleaned again, the solution was filtered directly into the cell and given the mirror test. Usually no more than three such attempts were necessary; however, in some cases at least twice that number of efforts were made, all to no avail. When this happened, the filter was cleaned with solvent, dried, cleaned with hot chromic acid, rinsed with distilled water, and dried. When this treatment failed, a filter of finer porosity was used.

After the solution was sufficiently well clarified, the filter was rinsed with solvent to prevent clogging with dried polymer. Also, the unpainted exterior of the cell, especially the windows, was cleaned

to remove large dust particles and greasy films. Again, effectiveness of the procedure could be ascertained by visual observation when using the very intense mercury light source.

In view of the great difficulty often experienced in removing dust from some systems, it seems worthwhile at this point to note briefly an interesting occurrence which was observed late in the experimental part of this investigation. When filtering a solution of polystyrene in cyclohexane, it was noted that a static charge developed about the filter disc. Since cyclohexane is a solvent that is particularly easy to free from dust, it seemed worthwhile to filter some of the more incorrigible solvents using a charged filter disc. The innovation of the artificially charged filter did not appreciably improve the clarification of water. However, when acetone was forced through several filters of different porosity which were charged with a Tesla coil, in all cases the liquid contained considerably less dust than that filtered without the charged discs. Because, however, of the belatedness of the observation, the innovation was not used in any of the experiments of this investigation.

Collection of Data

In order to give the electronic circuitry ample time to stabilize, the high voltage supply was switched on about two or three hours before proceeding with the actual measurements. Similarly, because of considerable initial instability which presumably resulted from a gradual temperature increase when the bulb was turned on, the spot light galvanometer was plugged in at the same time as the high voltage supply. Then about one-half hour before beginning measurements, the

mercury lamp was allowed to warm up. Ordinarily these provisions resulted in relatively stable galvanometer readings and thus greatly facilitated the measurements; however, when it was necessary to work at voltages very near the upper limit of the high voltage supply, as was often the case with pure solvents, an instability was introduced which could not be removed, even by extending the period of stabilization.

Since the primary beam was always much more intense than the scattered light, the relative intensities of the two could not be measured directly but had to be related by indirect means. Along with the automatic insertion in the beam of the working standard for the zero degree reading, this relation was accomplished by using the four calibrated neutral filters to further reduce the intensity of the incident beam. A similar problem arose with the angular measurements. Because of the wide range of angles, the large dissymmetries associated with very high molecular weight polymers made it difficult to precisely relate the readings for the lowest angles (highest readings) and those angles around 90° (lowest readings). Early in the investigation, this difficulty was circumvented by putting a neutral filter in the beam for the very low angles and removing it for the rest of the angular range. Later, however, it proved better to record the data for the low angles, say 25° through 50°, and then increase the voltage such that the 50° reading would be approximately full scale. Data for the remaining angles were then recorded at the high voltage setting and related to the others by means of the two readings at the overlap angle, which in this case was 50°.

After the solvent (or solution) was sufficiently dust-free, the cell was carefully placed in the photometer and allowed to remain there for about one-half hour before beginning the collection of data. If the system to be studied was a theta system, the constant temperature jacket was carefully placed around the cell; otherwise, the jacket was not used. The one-half hour waiting period accomplished two things: (1) it allowed the cell and its contents to come into thermal equilibrium with the environment; (2) it allowed some residual dust to settle out, away from the scattering volume.

After the pause, the voltage was adjusted to give the lowest angle, 25°, nearly a full-scale deflection and, after the shutter was closed, the galvanometer was mechanically zeroed with the screw adjustment. Then, by means of the very fine voltage adjust, the reading for the overlap angle (usually 50° for solutions and 40° for solvents) was carefully set on one of the lines of the galvanometer scale, thus facilitating the checking and reproduction of that value. While recording the readings for all angles at 5 degree increments between 25° and the overlap angle, the zero current and the overlap angle readings were periodically checked, and if any difference from the original values was noted, readjustments were made and the measurements were continued. As soon as all the measurements in this angular range were made, they were checked, and then the voltage was increased to give a full scale reading for the overlap angle. After zeroing the galvanometer, this high value for the overlap angle was also set on some galvanometer line and was used as a reference for all angles in 5 degree increments up to and including 140°. Again, if any

differences were noted, the voltage was changed or the galvanometer was re-zeroed, and the measurements were continued. After all the values were recorded and checked, the value at 0° was recorded along with the numbers of the filters required to give the largest on-scale reading. Then the voltage was decreased slightly and another pair of readings for 0° and the overlap angle were recorded. Because of the importance of this relationship, the process was repeated two more times, thus giving four pairs of values for 0° and the overlap angle, each pair being obtained at different voltage settings.

Actually, because of good reproducibility, the zero degree reading was made at -1°, but the photomultiplier was still viewing the unscattered beam. Another confession should also be noted: in Brice-Phoenix terminology, the angular measurements actually were made at negative angles, with the zero degree reading being made at + 1°. However, to reduce confusion, we shall continue to speak of the zero degree reading and the positive scattering angles.

The mechanics of data collection which were described above were repeated for each of the different wave lengths of incident light; and then, following such measurements on the solvent, they were repeated for each of the solutions, beginning with the most dilute. For the special case of PS-I in cyclohexane, for which measurements were made at temperatures above and below the theta temperature, data were recorded for different wave lengths, different temperatures (beginning with the highest), and different solutions, respectively.

Concentration Analysis

As soon as the measurements for one of the solutions were completed, the cell was removed from the photometer, swirled vigorously, and emptied into a clean, glass-stoppered flask. For theta systems, the flask was partially submerged in a constant temperature bath; in other cases, it was allowed to come to room temperature. After a few minutes, a 25 ml. portion of the solution was pipetted into a previously dried and weighed aluminum pan, and the rest of the solution was sealed in a glass vial for future viscosity measurements. The pan was then placed in a hot air bath, and after it and all the pans from the other solutions were dry, they were placed in a vacuum dessicator and heated under vacuum at about 80°C for approximately three days. Earlier measurements had indicated that about two days was sufficient to give a weight constant to 0.0001 grams.

Since it was found that warm bromocyclohexane reacts vigorously with aluminum, a preliminary attempt was made to analyze solutions with very light glass receptacles. This proved unsuccessful, for after a relatively short time the warm bromocyclohexane turned yellow, and upon evaporation it left a tar-like residue. Finally, for the system PDMS-IV in bromocyclohexane, it was decided to carefully prepare the solutions and use the initial concentrations. This was done by dissolving the polymer in benzene, filtering the solution to remove lint, and then freeze drying. The polymer was then very carefully weighed into the calibrated volumetric flasks and dissolved.

Ordinarily the concentration analysis was not performed at the temperature of the measurements, and the concentrations were converted

to the correct temperature by using the temperature dependences of the solvent densities. The needed density data for benzene (53), cyclohexane (54), carbon tetrachloride (55), and bromocyclohexane (56) were found in the literature.

In most cases the initial and final concentrations agreed within 3 per cent; however, it was the final values, rather than averages, that were used in the data analyses.

Calibration

In order to obtain absolute results from the relative scattering measurements, it was necessary to calibrate the photometer both internally and externally.

In view of reported discrepancies between the measured transmittances of the neutral filters taken singly and in pairs (57), it was decided to experimentally measure the needed values. Since the values for the combinations having the lowest and highest transmittances differed by about three orders of magnitude, it was necessary to make the determinations in a step-wise manner. With the phototube in the zero angle position, galvanometer readings were recorded for the case of no filter (full-scale deflection) and then for a series of filter combinations, singly or otherwise, in the range of high transmittance, followed by at least four repeated measurements at slightly different voltage settings. Then the voltage was increased such that the reading for one of the former high transmittance combinations was at full scale, and the above process was repeated for an overlapping series in a range of lower transmittance. By continuing this procedure for all the needed filter combinations at all three

wave lengths, it was concluded that within experimental uncertainty the above-mentioned discrepancy for the filter transmittances did not exist for this photometer. Therefore, measured values for the four individual filters, which were consistently lower than the factory supplied values, were simply multiplied together to obtain the values for the appropriate combinations.

The absolute calibration of the photometer, which had to be considered in order to obtain molecular weights and virial coefficients from the relative intensity measurements, is a complex problem. Although it can be accomplished on the basis of the geometry of the instrument, it is far more common to use some established light scattering standard, such as internationally circulated polymer samples, colloidal dispersions, or pure liquids (58).

Benzene, which was chosen as a standard in this study has several advantages: (1) it is easy to obtain in a relatively pure form; (2) although it is not a strong scatterer, it does scatter more than most pure solvents; (3) many other investigators have utilized it in this same capacity and thus its absolute scattering is reasonably well known. The Rayleigh's ratio values at 90° for 5460 Å, 4358 Å, and 3650 Å light that were used in the calculations were 17.2×10^{-6}, 48.7×10^{-6}, and 112.0×10^{-6} cm^{-1}, respectively, all for 30°C. The first two values were obtained by averaging the results given by Tomimatsu and Palmer (57) for benzene at 26°C and by making the temperature correction suggested by Ehl, *et al.* (59), whereas the value for the violet light was established from the values for 5460 Å and 4358 Å along with the wave length dependence given by Cantow (60).

To convert the relative measurements, it was then necessary to actually measure the 90° scattering of benzene at 30°C. This was done several times and the average values, in Equation (27) called $R'_b(90)$, were 0.001714 (5460 Å), 0.00585 (4358 Å), and 0.1434 (3650 Å).

In order to check the absolute calibration, the weight average molecular weight of PS-705, the sample obtained from the National Bureau of Standards, was determined in benzene at 30°C for all three wave lengths. The results, 1.81×10^5, 1.77×10^5, and 1.69×10^5 for the green, blue, and violet wave lengths, respectively (average is 1.76×10^5), agreed well with the value 1.79×10^5, which was supplied with the sample.

The simple calibration results discussed up to this point were applied without difficulty to those systems in which benzene was the solvent: the relative intensities were multiplied by the ratio of the absolute scattering of benzene to the measured value. However, when the refractive index of the system was significantly different from that of the standard, benzene, a complicating geometrical factor, called the refractive index correction, had to be considered. Since the light striking the photomultiplier tube is first refracted at the liquid-glass and glass-air interfaces and since the total extent of refraction depends on the refractive index of the liquid, the scattering volume of liquid viewed by the photomultiplier tube varies as the refractive index of the liquid changes. Hermans and Levinson (61) concluded that if the phototube does not see past the edges of the primary beam, the refraction effect intro-

duces a factor of n^{-2} in the measured intensity; thus the intensity should be corrected by multiplying by n^2.

A geometrical analysis of the photometer optical system, however, indicated that the phototube did see beyond the primary beam in the vertical direction; therefore, the results of Hermans and Levinson did not strictly apply, and the correction should be something less than n^2. Nevertheless, in view of the difficulty of the more general problem and because the error introduced was probably within experimental uncertainty, the n^2 correction was made. Thus the intensities from non-benzene systems were corrected by multiplying by C_n, given by n^2/n_b^2, where n_b is the refractive index of benzene.

Before beginning a more specific discussion of the treatment of experimental data, another intensity correction, called the reflection correction, needs to be discussed. When light passes perpendicularly through an interface between two transparent media of different indices of refraction, a certain fraction of the light is reflected in the opposite direction. This fraction, f, is given by the Fresnel relationship:

$$f = [(n_1 - n_2)/(n_1 + n_2)]^2 \qquad (23)$$

where the subscripts refer to the different media. The principal effect on the light scattering measurements is that when the primary beam exits from the cell, part of the light is reflected at both the liquid-glass and the glass-air interfaces, the greater reflection occurring at the latter. Since the reflected beam causes a small

reverse scattering envelope to be superimposed on that of the primary scattering, the overall effect for a solution of large particles is to reduce the observed angular dissymmetry. Recently Kratohvil (62) has treated the problem for several cases, including the one applicable to this study. For a cylindrical cell with a black painted back face, the corrected intensity, $i(\theta)$, is given by

$$i(\theta) = \frac{1}{1 - 2f}[i'(\theta) - fi'(180 - \theta)] \qquad (24)$$

where the primed quantities refer to the measured intensities, and f is the Fresnel factor for the glass-air interface. Thus, in order to make the reflection correction for the measured intensities, measurements had to be performed at supplementary angles, and the refractive index of the glass at different wave lengths had to be known.

The angular restriction presented no problems for 40° through 140°; however, for the three lowest angles no supplementary measurements were made, and it was necessary to make an approximation. By experience it was learned that the angular dependence of the scattered intensities was not nearly as pronounced for high angles as it was for low angles. Therefore, the corrections for the low angles, which were determined by the high angle intensities, showed little angular dependence; and, to a good approximation $i'(140)$ could be substituted for $i'(145)$, $i'(150)$, and $i'(155)$.

No data giving the wave length dependence of the refractive index of pyrex could be found in the literature; however, by using

the known value at the sodium D line, 1.474, and a wave length dependence estimated from data for other glasses, values were obtained for all three wave lengths. These values, followed by the corresponding Fresnel factors for the glass-air interface, are 1.476, 0.0370 (5460 Å); 1.484, 0.0380 (4358 Å); and 1.495, 0.0394 (3650 Å). By a similar method for estimating the refractive indices, Kratohvil (62) found 1.476 and 1.482 for the green and blue wave lengths, respectively.

The reflection correction, which could be quite small or relatively large, depending on the angle and the dissymmetry, was made on all the intensities, including the 90° scattering of benzene.

Treatment of Data

Light scattering data are conventionally displayed by plotting the left-hand side of Equation (7) against c, $\sin^2(\theta/2)$, or $kc + \sin^2(\theta/2)$, where k is an arbitrary constant. In any case, the experimentally determined quantities, galvanometer readings, filter transmittances, and concentrations, need to be converted to $Kc/R(\theta)$.

The optical constant, K, given by $2\pi^2 n_o^2 (dn/dc)^2/N_A\lambda^4)$, has no connection with the light scattering measurements per se; that is to say, for each system K can be determined by independent measurements. The refractive indices for benzene (53,63), carbon tetrachloride (54, 64), and cyclohexane (55,63) were all obtained from the literature. For bromocyclohexane (56), however, it was necessary to estimate most of the values; this was accomplished by assuming that dn/dt is independent of wave length and that n varies as $1/\lambda^2$. The determination of the refractive increments, dn/dc, will be discussed later.

The calculation of the absolute scattering intensities was considerably more involved, and the very early calculations, which were done on a desk calculator, were very time consuming and tedious. Later, however, the computations were made using a Burrough's 220 digital computer, and the results compared well with those obtained with the desk calculator. Finally, a change was made to the Burrough's 5500 system, with which the largest portion of the calculations were made. In all cases the basic procedure was the same.

First the galvanometer readings and filter transmittances were used to calculate the relative reduced intensities. For example, the value for the solution, designated $R''_{sn}(\theta)$, is given by

$$R''_{sn}(\theta) = T_f V \frac{G(\theta)}{G(0)} \frac{\sin \theta}{1 - \cos^2\theta} \tag{25}$$

where T_f is the transmittance of the neutral filters; V is unity for the high angles (greater than the overlap angle), and for the low angles it is the ratio of the high reading to the low reading for the overlap angle; $G(\theta)$ and $G(0)$ are galvanometer readings; the numerator of the trigonometric function is a volume correction, while the form of the denominator is appropriate for the use of unpolarized incident light.

Then a correction was made for the reflection of the primary beam. Using Equation (24), the corrected value of the reduced scattering intensity of the solution, denoted by a single prime, is given by

$$R'_{sn}(\theta) = \frac{1}{1 - 2f}[R''_{sn}(\theta) - fR''_{sn}(180 - \theta)] \tag{26}$$

An entirely analogous expression can be given for the corrected reduced intensity of the solvent, $R'_{sv}(\theta)$. For the special case of the 90° scattering of benzene, the analogue becomes

$$R'_b(90) = [(1 - f)/(1 - 2f)]R''_b(90) \tag{27}$$

where the subscript b refers to benzene.

The quantity of interest, however, is the excess scattering, that is, the scattering of the solution in excess of that of the solvent:

$$R'(\theta) = [1/(1 - 2f)][R'_{sn}(\theta) - R'_{sv}(\theta)] \tag{28}$$

Finally, the expression for the absolute excess reduced intensity becomes

$$R(\theta) = R'(\theta)C_n R_b(90)/R'_b(90) \tag{29}$$

where C_n is the refractive index correction factor and $R_b(90)$ is Rayleigh's ratio for benzene.

For the sake of facilitating the programming, however, the actual procedure followed digressed to a small extent from that given above. Since, as it can be seen by substituting for the

quantities in Equation (29), the factor 1/(1 - 2f) cancels and thus is unimportant in the present study, it was never introduced in the calculations. The other digression is that the correction for reflection followed, not preceded, the calculation of the excess scattering. That the order is irrelevant, however, can be seen by making appropriate substitutions in Equation (28) and rearranging the terms.

Refractive Increments

In view of the secondary importance of refractive increments in a study of light scattering, this section contains not only the procedures used for obtaining the experimental and calculated values but also the results themselves.

Experimental Values

As it was pointed out in the description of the experimental apparatus, the differential refractometer that was used in this study measured differences in the refractive index between two liquids by the deflection method. In an early description of the instrument, Brice and Halwer (65) showed that Δn is directly proportional to the deflection of the slit image and that the proportionality constant can be established either by geometrical means or by performing measurements on suitable liquids of known refractive index. Because of the relative ease of the second technique and the availability of data for the difference in refractive index between water and aqueous solutions of sucrose at 28°C, the second method was chosen (66).

Solutions of sucrose having concentrations of 2.000, 4.000, 5.000, and 6.000 per cent sucrose by weight were carefully prepared.

When the deflections were measured for these solutions against water using a sodium vapor lamp (this was necessary because all the data were given for the sodium D line), the resulting average value of the proportionality constant was 9.91×10^{-4}; thus for 5890 Å Δn was given by 9.91×10^{-4} Δd, where Δd was the excess deflection of the solution. By using the magnifications for 5890 Å, 5460 Å, and 4358 Å, which were given in the Brice-Phoenix manual, and the approximated value for 4060 Å, the proportionality constants for 5460 Å, 4358 Å, and 4060 Å were calculated to be 9.92×10^{-4}, 9.94×10^{-4}, and 9.94×10^{-4}, respectively. (4060 Å was used because the 3650 Å slit image was hardly visible.) These values were assumed to be independent of temperature.

Although more polymer-solvent systems were investigated by light scattering, only four were used for experimental determinations of dn/dc. Three of those studied were polystyrene in benzene at 30.0°C, in carbon tetrachloride at 30.0°C, and in cyclohexane at 34.5°C; the fourth was polydimethylsiloxane in carbon tetrachloride at 30.0°C. The polymer used for the PDMS-CCl_4 measurement was PDMS-II; however, because of the limited amount of polymer in each of the polystyrene light scattering samples, another sample was used. This anionically polymerized polystyrene, with a reported (51) weight average molecular weight of 187,000, was used for all three polystyrene systems.

The solutions were prepared by dissolving a weighed amount of polymer in a 50 ml. volumetric flask, with the more dilute solutions being prepared by aliquots. The final gravimetric analysis, from which the concentrations used in the calculations were obtained, was

accomplished by pipetting 25 ml. of the most dilute solution into an aluminum pan, which was then dried and heated under vacuum. The concentrations of the more concentrated solutions were calculated using the aliquot relations.

The actual measurements were made in the manner prescribed in the instrument manual. First, solvent was placed in both the "solution" and the "solvent" sides of the cell, and the cell handle was turned toward the lamp, in the 0° position. After the image was focused and the cross-hair was set, the micrometer reading was recorded. Several times, then, the settings were altered, re-established, and recorded, the average value being called $d_{sv}(0)$. Then the handle was turned away from the lamp, and $d_{sv}(180)$ was measured. The deflection for the solvent, d_{sv}, was simply $d_{sv}(0) - d_{sv}(180)$, and it could be either positive or negative. The procedure then was repeated for the other two wave lengths.

Next, the solvent that was in the "solution" side of the cell was carefully removed and replaced by an approximately equal volume (about 1.5 ml.) of the most dilute solution, with care being taken to rinse the compartment several times with the solution. In a manner like that described for the solvent, d_{sn} was measured by taking the difference in the average values of the deflections obtained in the 0° and 180° positions. The total deflection, then, for that solution, Δd, was given by $d_{sn} - d_{sv}$. Again the measurements were repeated for the other two wave lengths.

Finally, after Δd had been determined for all the solutions at

all three wave lengths, plots similar to Figure 1, which gives the results for polystyrene in carbon tetrachloride, were prepared for each system. The slopes of the lines, when multiplied by the previously determined proportionality constants, gave the refractive increments for the three wave lengths used. The value for the fourth wave length, 3650 Å, was determined by extrapolation of the experimental data, assuming that dn/dc varies as $1/\lambda^2$.

For two systems, PDMS in C_6H_6 (67) and PDMS in $C_6H_{11}Br$ (68), the refractive increments were not measured but were obtained directly or indirectly from the literature. In both cases the available values were for the green wave length and the other two values were approximated on the basis of available data for similar systems.

Calculated Values

As a means of checking and screening the experimental values, the refractive increments for all six systems were calculated from a theoretical expression, using the B-5500 computer. If the Lorenz-Lorentz equation for the refractive index of a binary system (69) is differentiated with respect to the concentration of the solute, the following equation, which was used in the calculations, results:

$$\frac{dn}{dc} = \frac{(X^2 + 2)^2}{6X} \left[\frac{n_2^2 - 1}{d_2(n_2^2 + 2)} - \frac{n_1^2 - 1}{d_2(n_1^2 + 2)} \right] \qquad (30)$$

Here X is given by

$$X = [(2Y + 1)/(1 - Y)]^{\frac{1}{2}} \qquad (31)$$

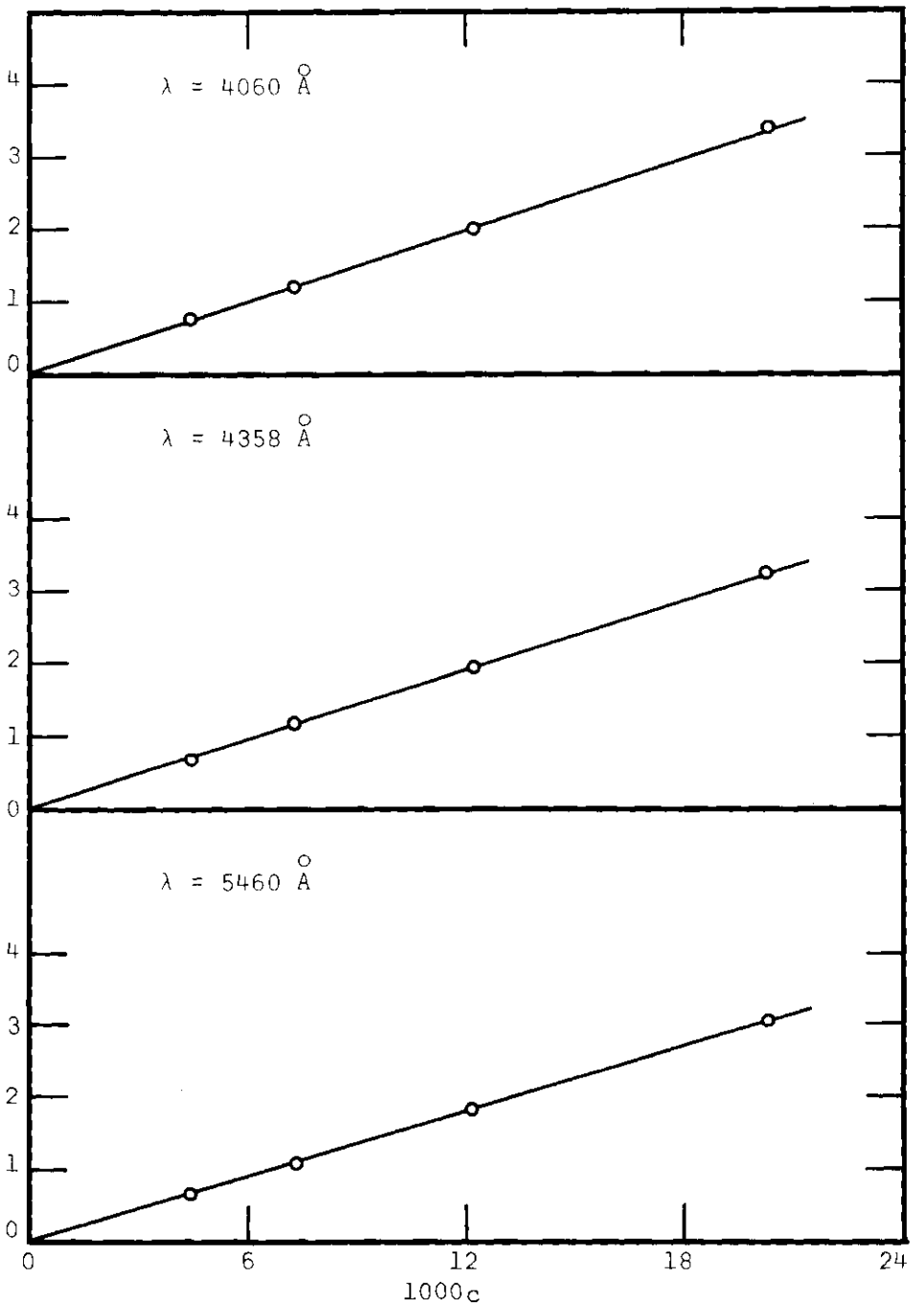

Figure 1. Refractive Increment Data for PS-I in Carbon Tetrachloride at Three Wave Lengths

where

$$Y = (c/d_2)\frac{n_2^2 - 1}{n_2^2 + 2} + (1 - c/d_2)\frac{n_1^2 - 1}{n_1^2 + 2} \qquad (32)$$

The subscripts 1 and 2 refer to the solvent and polymer, respectively; for example, d_2 is the density of the polymer.

Table 1 lists both the experimental and calculated refractive increments for all six of the systems at the three wave lengths used in the light scattering measurements. The refractive indices for polystyrene and polydimethylsiloxane were approximated from literature values (70,71), whereas the densities for the two polymers, 1.05 and 0.98, respectively, were taken directly from a handbook (72). The value for the concentration, c, which was taken somewhat arbitrarily as 10^{-4} g/cc, was found to have little effect on the calculated values of dn/dc over the experimentally utilized range of concentration.

Intrinsic Viscosities

Intrinsic viscosity data, though very useful in the characterization of polymers, are supplementary to the light scattering study; therefore, like the section on refractive increments, this one will contain not only the procedure involved in making the measurements and in calculating the results, but also the results themselves.

In spite of the wealth of information that can be obtained from viscosity data, present purposes are served by obtaining values of the viscosity average molecular weight, $\overline{M}_v$, of the polymer samples using the Mark-Houwink relation:

Table 1. Refractive Increments

System	λ(Å)	dn/dc (exp.)**	n_1	n_2	dn/dc (calc.)**
PS in C_6H_6 at 30°C	5460	0.108	1.499	1.618	0.109
PS in C_6H_6 at 30°C	4358	0.112	1.516	1.637	0.110
PS in C_6H_6 at 30°C	3650	0.117	1.540	1.659	0.108
PS in CCl_4 at 30°C	5460	0.148	1.461	1.618	0.141
PS in CCl_4 at 30°C	4358	0.158	1.469	1.637	0.150
PS in CCl_4 at 30°C	3650	0.168	1.480	1.659	0.160
PS in C_6H_{12} at 34.5°C	5460	0.177	1.420	1.618	0.175
PS in C_6H_{12} at 34.5°C	4358	0.191	1.427	1.637	0.185
PS in C_6H_{12} at 34.5°C	3650	0.205	1.436	1.659	0.196
PDMS in CCl_4 at 30°C	5460	-0.053	1.461	1.406	-0.057
PDMS in CCl_4 at 30°C	4358	-0.055	1.469	1.414	-0.058
PDMS in CCl_4 at 30°C	3650	-0.058	1.480	1.424	-0.058
PDMS in C_6H_6 at 30°C	5460	-0.098*	1.499	1.406	-0.098
PDMS in C_6H_6 at 30°C	4358	-0.108*	1.516	1.414	-0.108
PDMS in C_6H_6 at 30°C	3650	-0.117*	1.540	1.424	-0.123
PDMS in $C_6H_{11}Br$ at 29°C	5460	-0.090*	1.493	1.406	-0.092
PDMS in $C_6H_{11}Br$ at 29°C	4358	-0.091*	1.500	1.414	-0.091
PDMS in $C_6H_{11}Br$ at 29°C	3650	-0.090*	1.508	1.424	-0.089

*Literature value or estimated from literature values.

**Units are ml. g^{-1}.

$$[\eta] = K\overline{M}_v^{\,a} \tag{33}$$

where $[\eta]$ is the intrinsic viscosity, and K and a are constants for a given polymer-solvent-temperature combination, over a relatively wide range of molecular weights.

By definition the intrinsic viscosity is given by

$$[\eta] = \lim_{c \to 0} \frac{\eta - \eta_o}{\eta_o c} \tag{34}$$

where η and η_o are the solution and solvent viscosities, respectively. The term $(\eta - \eta_o)/\eta_o$ is called the specific viscosity and has the symbol η_{sp}; whereas η/η_o is called the relative viscosity, η_{rel}.

The experimentally measured values, solvent and solution flow times, can be related to the above quantities with Poiseuille's law. Accordingly, if the densities of the solutions and the solvent are assumed to be equal, η_{rel} is given by t/t_o, the ratio of the flow times. Therefore, the only remaining obstacle between experimental values and the intrinsic viscosity is a knowledge of the concentration dependence of the viscosity. Huggins (73) proposed

$$\eta_{sp}/c = [\eta] + k_1[\eta]^2 c \tag{35}$$

which predicts that a plot of η_{sp}/c versus c gives a straight line with a slope proportional to the square of the intercept, which is the intrinsic viscosity. Another expression,

$$(\ln \eta_{rel})/c = [\eta] - k_2[\eta]^2 c \qquad (36)$$

predicts similar results when the left-hand side is plotted against concentration.

The discussion up to this point has been rather straightforward, but under certain circumstances corrections must be applied to the experimental data before the above results become applicable. In the present study, two such considerations were necessary, the kinetic energy correction and the correction to zero rate of shear (74).

The necessity for a kinetic energy correction arose when the liquid exited from the viscometer capillary with enough kinetic energy to cause appreciable deviations from Poiseuille's law, which applies to an infinitely slow process. The extent of deviation was determined by measuring the flow times at different temperatures for a liquid of known viscosity and density, water. The thus obtained calibration results were used to determine by the method of least squares the viscometer constants A and B in the following empirical equation:

$$\eta/td = A - B/t^2 \qquad (37)$$

Here t is the flow time of the liquid and d is the density. Rearrangement of Equation (37) results in

$$\eta/Ad = t - B/At \qquad (38)$$

When Equation (38) is combined with an analogous expression for a pure solvent, with the assumption about equal densities, the result is

$$\eta_{rel} = (t - B/At)/(t_o - B/At_o) \qquad (39)$$

Therefore, the effects of large kinetic energies can be empirically accounted for by correcting each of the flow times in the manner prescribed by Equation (39). In only one of the viscosity measurements, PS-II in CCl_4, was it necessary to make the above correction.

The second correction, that to zero rate of shear (velocity gradient), became necessary for the very high molecular weight polymers in good solvents, in which case the large polymer coils were significantly distorted, even by relatively low rates of shear. Since the theoretical aspects of the problem are quite difficult and not well understood, the only correction made was a somewhat unsophisticated visual extrapolation of the data to zero rate of shear.

First, however, it was necessary to evaluate the rates of shear for each of the four bulbs of the rate of shear viscometer. The maximum rate of shear, which occurs at the capillary wall, is given by $4V/\pi a^3 t$, where V, the volume between the fiducial marks, and a, the radius of the capillary, had to be measured experimentally.

To determine the respective volumes, the viscometer was clamped upside down and a stopcock with a capillary tip was attached with rubber tubing to the limb of the instrument containing the bulbs. By using atmospheric pressure, enough mercury was forced into the

viscometer to completely fill all four bulbs; and then, by careful regulation of the stopcock, the mercury was allowed to flow slowly from the buret-type arrangement into glass weighing vessels. The volumes of the bulbs were then calculated from the weights of the delivered portions of mercury and the known density of mercury.

The radius of the capillary was also determined by weighing a certain volume of mercury. This time, however, only a very small amount was introduced into the viscometer, just enough to nearly fill the capillary. After the length of the mercury thread was measured, the mercury was poured into a weighing vessel and weighed, and then the volume was calculated. The radius of the bore was then determined from the volume and length of the mercury thread, using the expression for the volume of a cylinder.

Having, therefore, determined a and V, it was a simple matter to calculate the maximum rates of shear from the observed flow times. Figure 2 shows the relative viscosity data for five solutions of PS-III in benzene, which were obtained at different rates of shear. Also shown are the extrapolations to zero rate of shear.

The viscosity measurements themselves were relatively simple. For all cases except four, PS-II in CCl_4, PS-II in C_6H_{12}, PS-705 in C_6H_6, and PDMS-III in C_6H_6, one solution was prepared and used for the measurements, with dilutions being made directly in the viscometer. The concentrations were calculated using the gravimetrically determined concentration of the most concentrated solution and the dilution ratios. For the four systems listed, the solutions used were those left over from the corresponding light scattering measurements.

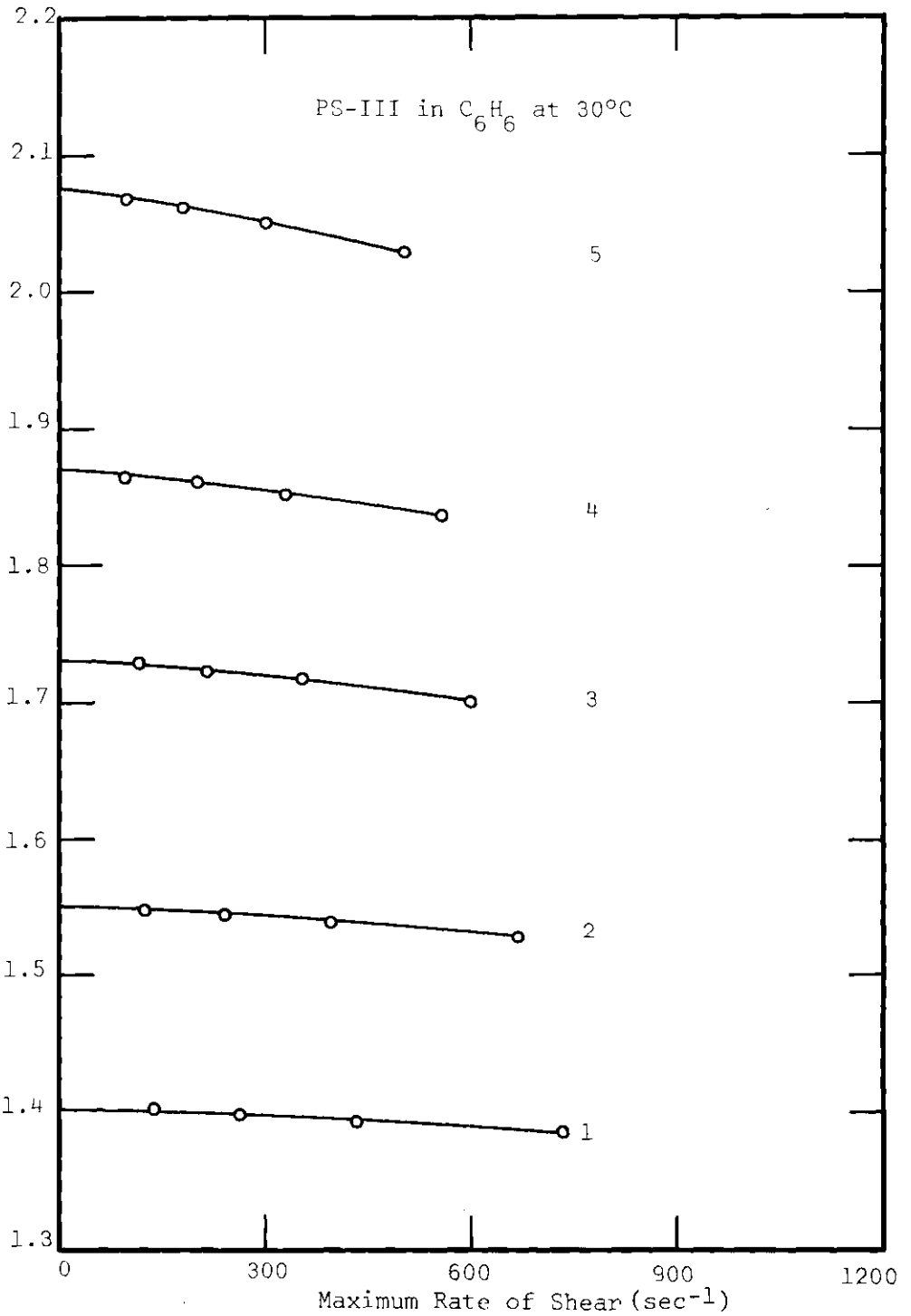

Figure 2. Relative Viscosities for PS-III in Benzene at Different Rates of Shear

The flow times were measured for both the solvent and the solutions with a Meylan stopwatch, which could be read to ±0.05 sec. The timings were usually repeated several times and the average values were used to calculate the relative and specific viscosities. Then the data, which were corrected for kinetic energy and rate of shear if necessary, were graphically displayed according to both Equations (35) and (36), the simultaneous use of the two equations offering the advantage of facilitating the extrapolation to zero concentration. Figures 3-7 show the resulting plots for several of the systems. The open points correspond to Equation (35) and the closed ones correspond to Equation (36).

In order to calculate the molecular weights from the intrinsic viscosities, it was necessary to find experimentally determined values of the Mark-Houwink constants in the literature. Although it was not possible to find values for all the systems, most of the required constants were found in at least one of the extensive tabulations available (75,76). Finally, by means of Equation (33), the molecular weights were calculated. They, along with the utilized values of K and a, and the experimentally determined values of the intrinsic viscosities are recorded in Table 2.

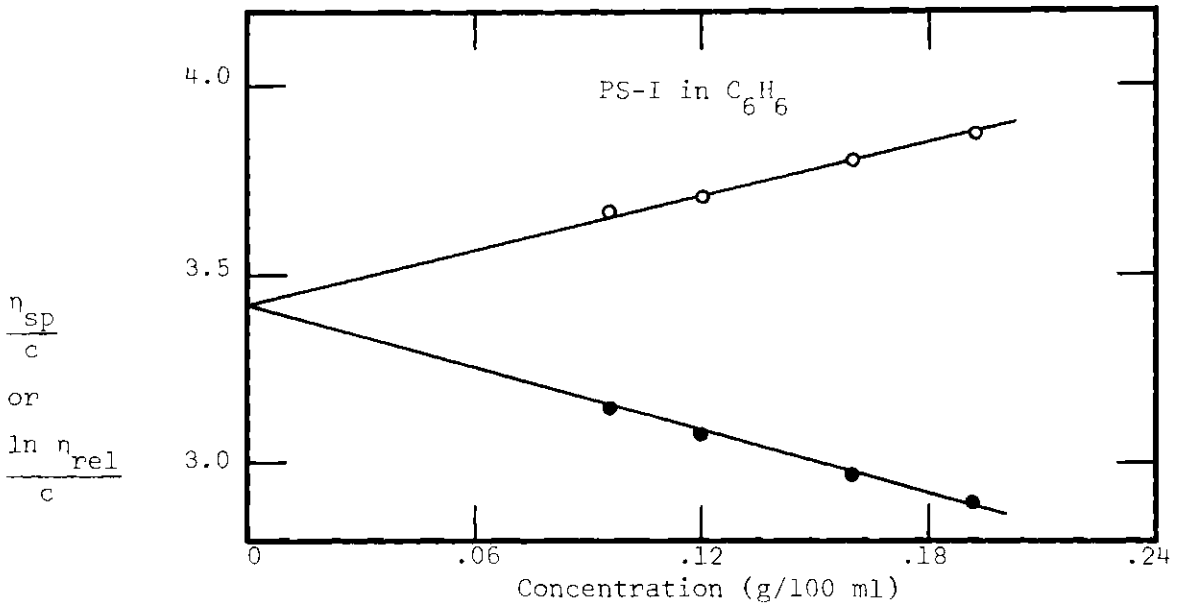

Figure 3. Viscosity Data for PS-I in Benzene at 30.0°C

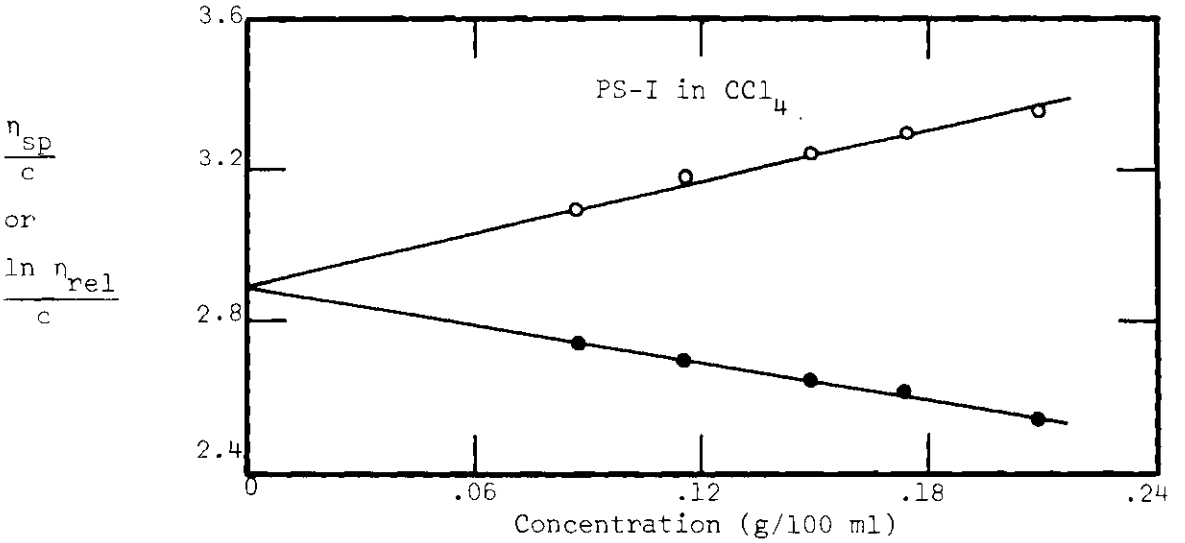

Figure 4. Viscosity Data for PS-I in Carbon Tetrachloride at 30°C

$\frac{\eta_{sp}}{c}$ or $\frac{\ln \eta_{rel}}{c}$

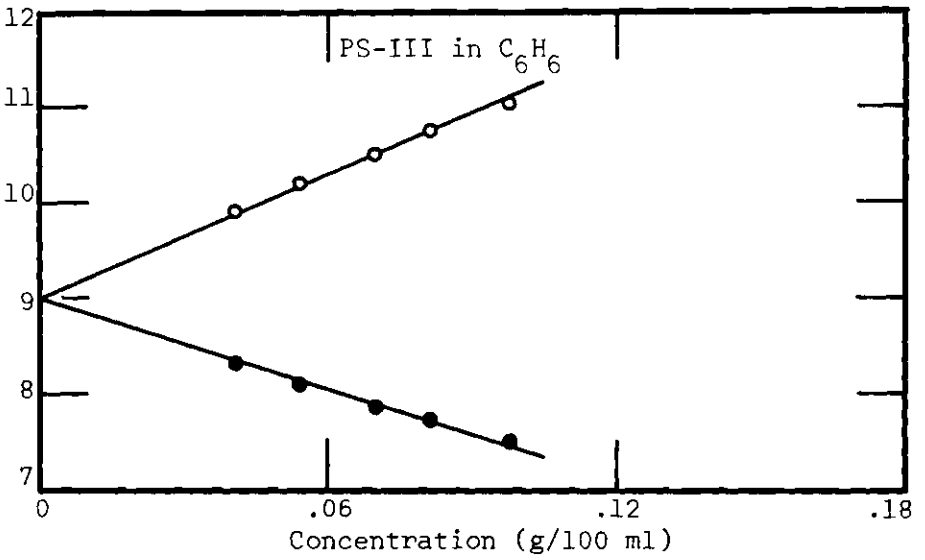

Figure 5. Viscosity Data for PS-III in Benzene at 30.0°C

$\frac{\eta_{sp}}{c}$ or $\frac{\ln \eta_{rel}}{c}$

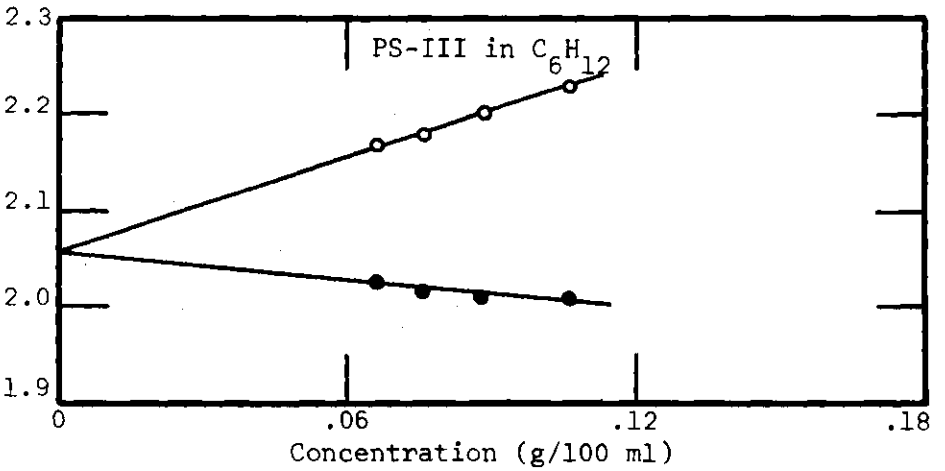

Figure 6. Viscosity Data for PS-III in Cyclohexane at 34.5°C

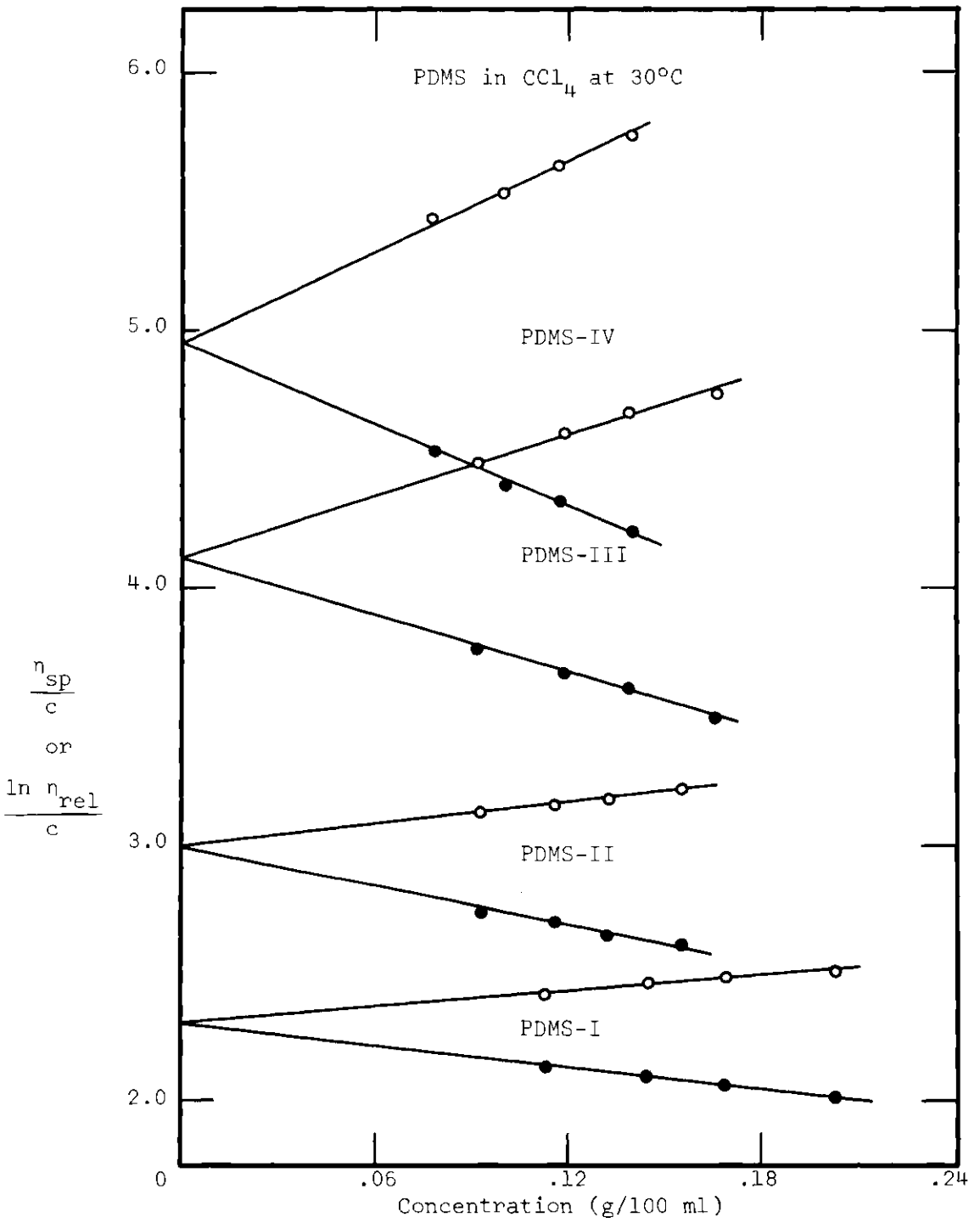

Figure 7. Viscosity Data for PDMS Fractions in Carbon Tetrachloride at 30.0°C

Table 2. Viscosity Results

System	$[\eta]$(dl.g.$^{-1}$)	K x 10^4*	a*	$\overline{M_v}$ x 10^{-6}
PS-I in C_6H_6 at 30.0°C	3.42	0.92	0.74	1.42
PS-I in CCl_4 at 30.0°C	2.89			
PS-I in C_6H_{12} at 34.5°C	1.03	8.0	0.50	1.66
PS-II in CCl_4 at 30.0°C	5.35**			
PS-II in C_6H_{12} at 34.8°C	1.77	8.0	0.50	4.90
PS-III in C_6H_6 at 30.0°C	9.00***	0.92	0.74	5.22
PS-III in C_6H_{12} at 34.5°C	2.06	8.0	0.50	6.63
PS-705 in C_6H_6 at 30.0°C	0.72	0.92	0.74	0.174
PDMS-I in CCl_4 at 30.0°C	2.30	3.56	0.63	1.12
PDMS-II in CCl_4 at 30.0°C	3.00	3.56	0.63	1.70
PDMS-III in CCl_4 at 30.0°C	4.11***	3.56	0.63	2.81
PDMS-III in C_6H_6 at 30.0°C	2.45	1.2	0.68	2.18
PDMS-IV in CCl_4 at 30.0°C	4.95***	3.56	0.63	3.77

*Literature values.

**Kinetic energy correction applied.

***Corrected to zero rate of shear.

CHAPTER IV

RESULTS AND DISCUSSION

One method of systematizing the light scattering results is to divide them according to their dependence on the absolute calibration of the photometer. The results of the first section in this chapter, molecular weights and second virial coefficients, are subject to the absolute calibration; on the other hand, the principal angular results, such as the reciprocal scattering curves and the radii of gyration, were obtained without direct reference to external calibration.

Molecular Weights and Second Virial Coefficients

As it can be seen from Equation (7), the reciprocal of the molecular weight is given by the limit of $Kc/R(\theta)$as c and θ approach zero, and the second virial coefficient, A_2, is just one half the initial slope of the $[Kc/R(\theta)]_{\theta=0}$ versus c curve. Therefore, in order to obtain the molecular weight and A_2 from the experimental $Kc/R(\theta)$ values, the data must be extrapolated to zero angle and zero concentration.

For the purpose of facilitating the determinations, it is quite common to display the data on a Zimm plot (77), which permits both extrapolations to be performed simultaneously. Figure 8 shows a Zimm plot for a theta solvent system, PS-III in C_6H_{12} at 34.49°C, in which the experimental data, represented by the circles, were plotted against $1000c + \sin^2(\theta/2)$. In this case, the data for the four different

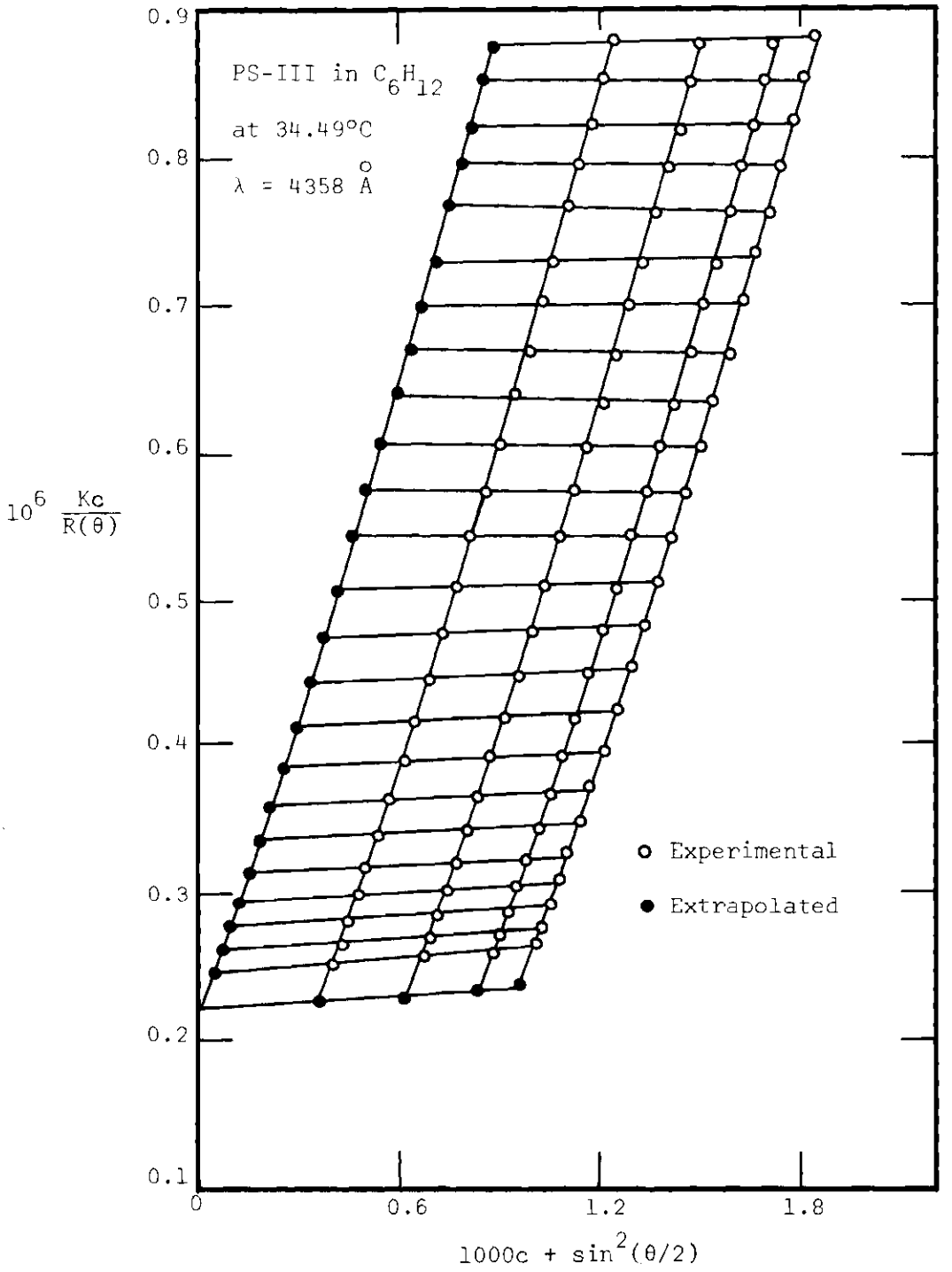

Figure 8. Zimm Plot for PS-III in Cyclohexane at 34.49°C. λ = 4358 A

concentrations and 24 different angles were extrapolated to zero concentration and zero angle, respectively, thus giving rise to the closed points. Finally, the 24 $[Kc/R(\theta)]_{c=0}$ values and the 4 $[Kc/R(\theta)]_{\theta=0}$ values were simultaneously extrapolated to a single intercept, the reciprocal of the molecular weight. Figure 9 displays similar results for PS-III in benzene at 30.0°C, a good solvent system.

At this point in the discussion, attention is drawn to one significant difference between the two Zimm plots: in Figure 8 the extrapolations to zero concentration are all represented by straight lines, whereas in Figure 9 the same extrapolations exhibit upward curvature. This difference is in keeping with the comments of Flory (78), who points out that for the zero angle data, Equation (7) can be rewritten approximately as

$$[Kc/R(\theta)]_{\theta=0} = (1/M)[1 + 2\Gamma_2 c + 3g\Gamma_2^2 c^2] \qquad (40)$$

where $\Gamma_2 = A_2 M$ and g is a slowly varying function of Γ_2, decreasing from about 0.3 for large values of Γ_2 (good solvents) to zero as Γ_2 vanishes. Therefore, for the case of a system which is close to the theta condition, $3g\Gamma_2^2$ is much smaller than $2\Gamma_2$ and thus a plot of $[Kc/R(\theta)]_{\theta=0}$ versus c should give a straight line over a relatively wide range of concentration. On the other hand, for good solvents the third term in the right-hand side of Equation (40) makes a significant contribution, thus causing upward curvature. If, as it is usually valid to do, g is assumed to have the value of 1/3 for good solvents, Equation (40) becomes

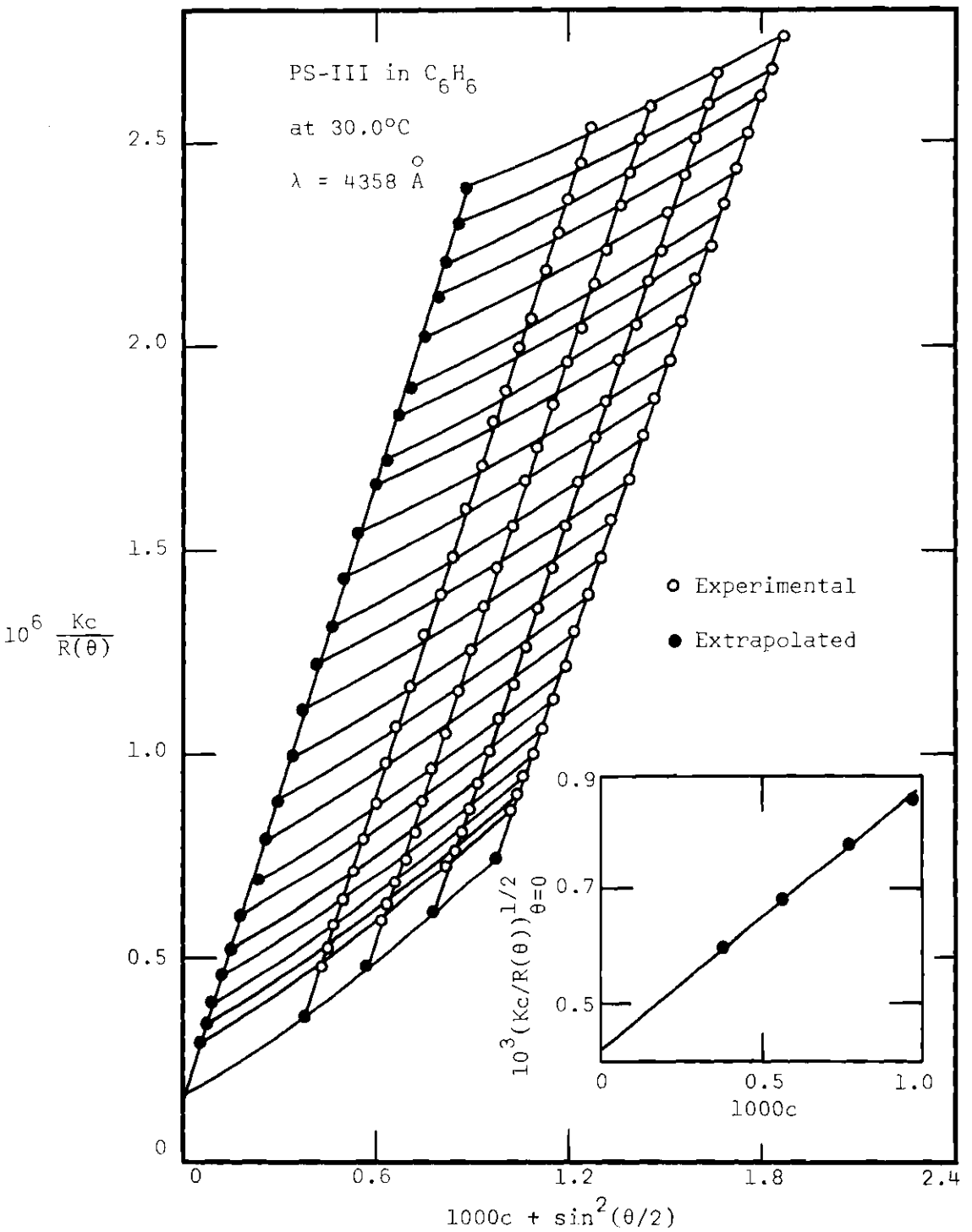

Figure 9. Zimm Plot for PS-III$_o$ in Benzene at 30.0°C
λ = 4358 A

$$[Kc/R(\theta)]_{\theta=0} = (1/M)[1 + \Gamma_2 c]^2 \qquad (41)$$

Consequently, if the data are plotted as $[Kc/R(\theta)]_{\theta=0}^{\frac{1}{2}}$ versus c, as it is done in the insert in Figure 9, the resulting straight line should have an intercept of $(1/M)^{\frac{1}{2}}$ and a slope given by $\Gamma_2/M^{\frac{1}{2}}$.

In view of these considerations, which admittedly apply only to the zero angle data, all the extrapolations to zero concentration were performed in either of two different ways, depending on the kind of system involved: for theta solvents $Kc/R(\theta)$ was plotted against concentration, whereas for good solvents $[Kc/R(\theta)]^{\frac{1}{2}}$ was plotted against concentration. In both cases the data were fit to a straight line by the method of least squares; and, because of the large amount of work involved, all these calculations were done on the B-5500 computer as a part of the original light scattering program.

Since the extrapolations to zero concentration were not performed graphically, it was found convenient to display most of the data not in the customary manner of Zimm but in plots of $Kc/R(\theta)$ against $\sin^2(\theta/2)$. In a few cases (theta systems and some of the very high molecular weight polymer systems) it was necessary to revert to the $1000c + \sin^2(\theta/2)$ abscissa in order to spread out the data; however, even when the reversion was necessary, the only extrapolation to zero concentration that was shown was that for the zero angle data. On the other hand, all of the extrapolations to zero angle were performed graphically using ship curves.

All of the $Kc/R(\theta)$ results except those given in Figures 8 and 9 are displayed in the described manner in the Appendix.

Once the data had been plotted and extrapolated, it was a straightforward procedure to evaluate the molecular weights and the second virial coefficients from the intercepts and slopes. Table 3 contains these two quantities, along with the appropriate refractive indices, refractive increments, and optical constants, for each of the individual experiments.

It should be noted that even though the agreement in the molecular weights for a given polymer sample in different solvents is not especially good, the agreement in the molecular weights obtained at different wave lengths for the same system is well within experimental error. With regard to the virial coefficients, two things should be mentioned: for a given polymer sample A_2 should increase with the goodness of the solvent; and for a given polymer-solvent system, A_2 should decrease slightly with the increasing molecular weight of the polymer (79). The first of these predictions is born out by all the polymer samples that were used with more than one solvent. The second prediction, however, is not so well demonstrated: the polystyrene-benzene and polystyrene-carbon tetrachloride data demonstrate the expected trend, but the polystyrene-cyclohexane and polydimethylsiloxane-carbon tetrachloride data do not.

Angular Results

After the $[Kc/R(\theta)]_{c=0}$ were obtained from the computer output, the next step in the procedure was to determine the P^{-1} values. In accordance with Equation (7), these numbers were obtained by dividing the $[Kc/R(\theta)]_{c=0}$ values by the zero angle intercept. In view of later

Table 3. Molecular Weights and Virial Coefficients

System	λ(Å)	n	dn/dc*	$Kx10^{7}$*	$\overline{M_w}x10^{-6}$	A_2x10^{4}*
PS-I in C_6H_6 at 35.0°C	5460	1.496	.109	0.982	1.28	2.74
	4358	1.513	.113	2.66	1.32	2.82
	3650	1.536	.118	6.12	1.31	2.90
PS-I in CCl_4 at 30.0°C	5460	1.461	.148	1.73	1.38	2.36
	4358	1.469	.158	4.89	1.41	2.43
	3650	1.479	.168	11.38	1.42	2.20
PS-I in C_6H_{12} at 34.94°C	5460	1.420	.179	2.37	1.29	0.12
	4358	1.427	.191	6.71	1.31	0.10
	3650	1.435	.205	16.01	1.32	0.11
PS-II in CCl_4 at 30.0°C	5460	1.461	.148	1.73	4.22	2.10
	4358	1.469	.158	4.89	4.37	2.03
	3650	1.479	.168	11.38	4.45	2.03
PS-II in C_6H_{12} at 34.76°C	5460	1.421	.179	2.37	3.12	0.15
	4358	1.427	.191	6.70	3.22	0.16
	3650	1.436	.205	16.01	3.22	0.20
PS-III in C_6H_6 at 30.0°C	4358	1.516	.112	2.61	5.77	1.91
	3650	1.540	.117	5.99	5.67	2.03
PS-III in C_6H_{12} at 34.49°C	4358	1.427	.191	6.70	4.55	0.08
	3650	1.436	.205	16.01	4.51	0.08
PDMS-I in CCl_4 at 30.0°C	4358	1.469	-.055	0.601	0.605	2.98
	3650	1.479	-.058	1.335	0.572	2.96
PDMS-II in CCl_4 at 30.0°C	4358	1.469	-.055	0.601	0.844	3.07
	3650	1.479	-.058	1.335	0.786	2.87
PDMS-III in CCl_4 at 30.0°C	5460	1.461	-.053	0.218	1.47	2.92
	4358	1.469	-.055	0.601	1.49	3.15
	3650	1.479	-.058	1.335	1.41	2.96
PDMS-III in C_6H_6 at 30.0°C	5460	1.499	-.098	0.796	1.59	1.55
	4358	1.516	-.108	2.43	1.61	1.54
	3650	1.540	-.117	5.99	1.69	1.57
PDMS-IV in CCl_4 at 30.0°C	4358	1.469	-.055	0.601	1.68	2.97
	3650	1.479	-.058	1.335	1.76	2.83
PDMS-IV in $C_6H_{11}BR$ at 29.12°C	4358	1.500	-.091	1.69	2.19	0.06
	3650	1.508	-.090	3.55	2.12	0.01
PS-705 in C_6H_6 at 30.0°C	5460	1.499	.108	0.959	0.181	
	4358	1.516	.112	2.61	0.177	
	3650	1.540	.117	5.99	0.169	

* c.g.s. units.

discussion about overlapping the data for the different wave lengths, it should be pointed out that the scatter in the zero angle and zero concentration data invariably caused a small amount of uncertainty in the determination of the intercept. Furthermore, it is a matter of importance to note that division by the intercept cancels the optical constant and all the factors introduced in the absolute calibration of the photometer; therefore, a simpler plot of $[c/R'(\theta)]_{c=0}$ versus $\sin^2(\theta/2)$ would permit equally well the determination of the P^{-1} values.

Next the P^{-1} data for all the wave lengths were plotted as a function of $\sin^2(\theta/2)/\lambda'^2$, where λ' is the wave length of the light in the medium. Numerical calculations using the Lorenz-Lorentz equation indicate that for the present systems the refractive index of the bulk solution differs insignificantly from that expected in the vicinity of a polymer coil; therefore, for practical purposes, $\lambda' = \lambda/n$. In most cases the data did not overlap as well as might be expected; but small changes in the intercepts, which were always within the extrapolation uncertainty mentioned above, that is, plus or minus approximately 2 per cent, appreciably improved the extent of overlap. The fine adjustment of the intercepts was greatly facilitated by having the $[Kc/R(\theta)]_{c=0}$ values punched out on cards by the light scattering program. These cards then were used as input for another program which determined P^{-1} as a function of $\sin^2(\theta/2)/\lambda'^2$ for different values of the intercepts.

Figure 10 shows for each of the three wave lengths the data for PDMS-III in benzene, which were obtained from the corresponding reciprocal intensity data displayed in the Appendix. Note, as it was pointed out earlier, that the use of 3650 Å light greatly increases the experi-

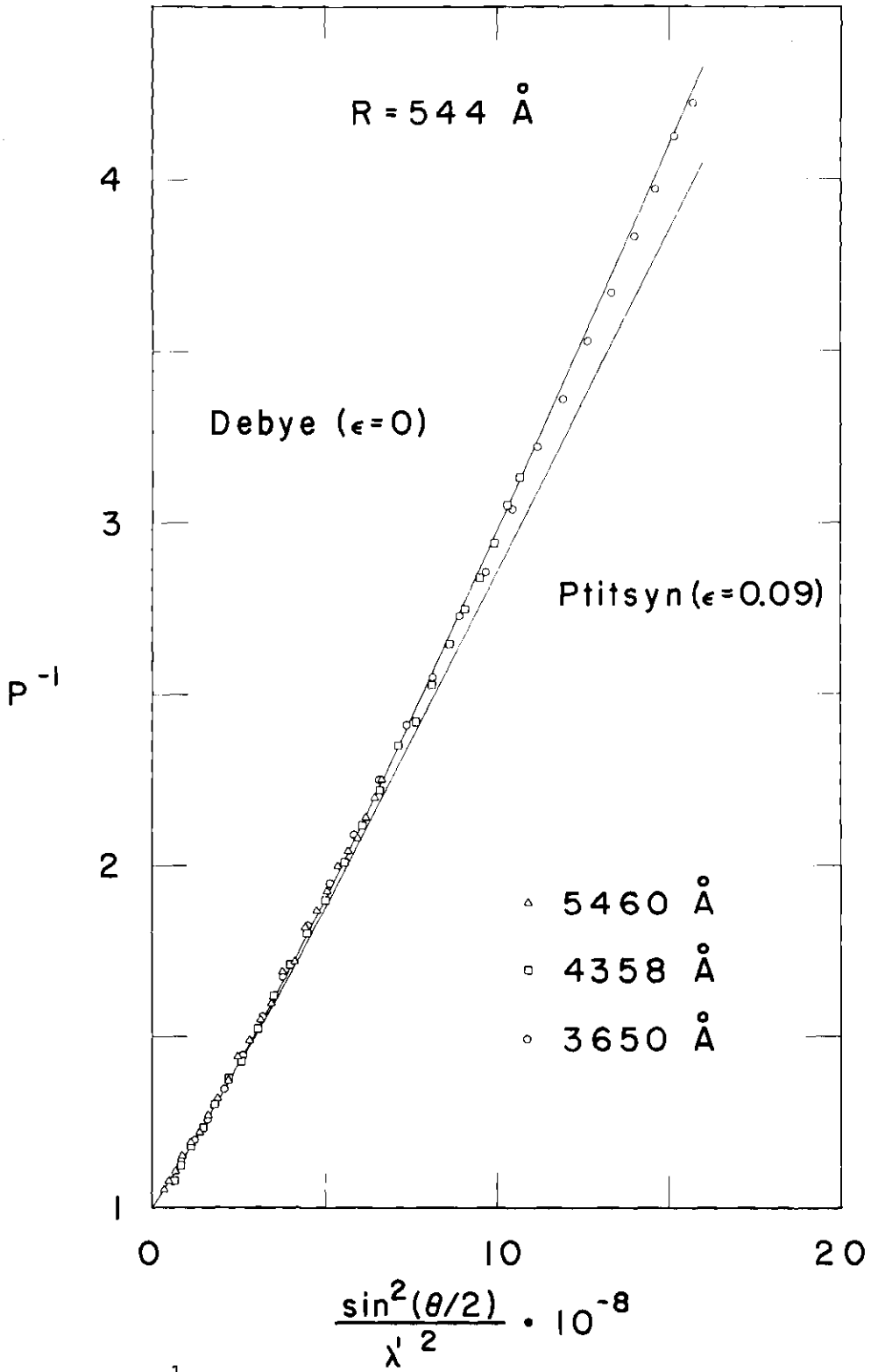

Figure 10. P^{-1} Data for PDMS-III in Benzene at 30.0°C. Demonstrates Overlapping of Data for Three Wave Lengths

mental range with respect to that covered by 5460 Å or 4358 Å, and it also increases the credibility of the high angle data obtained at the other two wave lengths. The curves in the figure are discussed later.

After the P^{-1} data were plotted for all systems, it was then possible, using Equation (10), to determine the radii of gyration from the initial tangents. These values, along with their approximate uncertainties, are listed in Table 4.

Table 4. Radii of Gyration Determined by Initial Tangent Method

System	$\overline{M_w} \times 10^{-6}$	R(Å)
PS-I in C_6H_6	1.30	556 ± 16
PS-I in CCl_4	1.40	547 ± 13
PS-II in CCl_4	4.35	1205 ± 24
PS-III in C_6H_6	5.72	1471 ± 69
PS-I in C_6H_{12}	1.30	344 ± 12
PS-II in C_6H_{12}	3.19	725 ± 10
PS-III in C_6H_{12}	4.53	682 ± 43
PDMS-I in CCl_4	0.588	368 ± 12
PDMS-II in CCl_4	0.815	453 ± 21
PDMS-III in CCl_4	1.46	664 ± 24
PDMS-III in C_6H_6	1.63	551 ± 13
PDMS-IV in CCl_4	1.72	700 ± 33
PDMS-IV in $C_6H_{11}Br$	2.16	453 ± 15

Theta Solvents

As it was pointed out earlier, Isihara (19) has criticized the Debye expression, Equation (16), on the grounds that Equation (13) is no longer valid for small intramolecular distances. His expression, Equation (18), according to his prediction, should be better than Equation (16) for high values of x and low values of N.

Since the Isihara formulation apparently improves Debye's equation, even at the theta condition where volume effects are absent, it is very important to ascertain the magnitude of the error introduced by Equation (16) before considering the Ptitsyn function, Equation (21), which reduces to the Debye function in the absence of volume effects.

Rather than attempt to fit the experimental data obtained at the theta condition with the Isihara function, it was decided to compare Equations (16) and (18) by numerical calculations using the B-5500 computer. In view of the predictions of the Isihara treatment, the calculations were of two kinds: first, the error was determined as $\sin^2(\theta/2)/\lambda'^2$ varied from very small to extremely large values, N remaining constant; then $\sin^2(\theta/2)/\lambda'^2$ was held constant and N was varied.

The results of the first set of calculations are given in Figure 11. The values for R, N, and, consequently, b ($R^2 = Nb^2/6$) correspond to the characteristic data for PS-III in cyclohexane, which system was chosen somewhat arbitrarily. Note, by comparing with Figure 10, that the abscissa range is about three orders of magnitude greater than that covered experimentally. From the insert, which gives the relative error of the Debye equation as a function of the

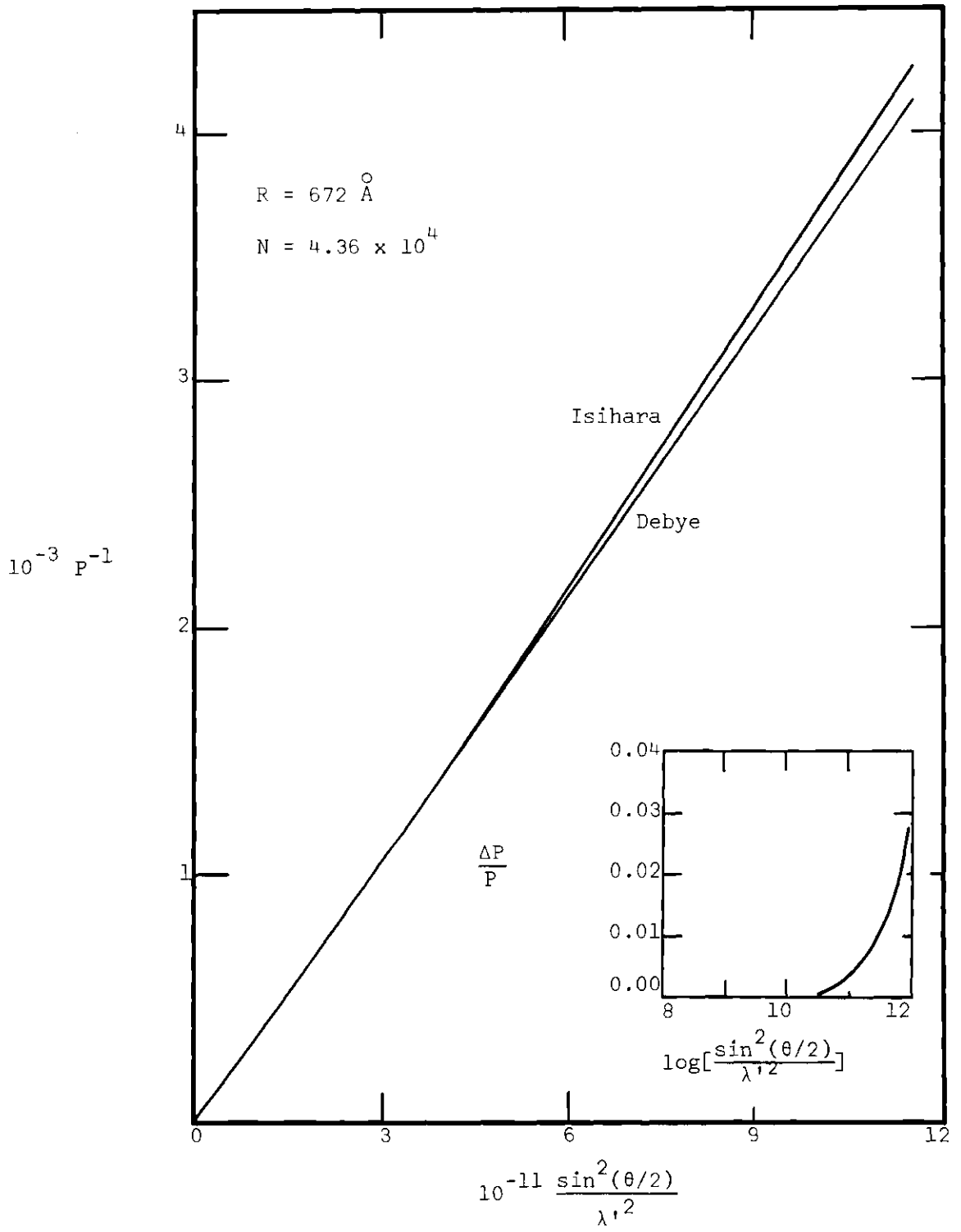

Figure 11. Comparison of the Isihara and Debye Scattering Functions

base 10 logarithm of the normal abscissa, it can be seen that the error is almost nil for values of $\sin^2(\theta/2)/\lambda'^2$ which are experimentally accessible with visible light. Even for the highest angle used, 140°, a 0.1 per cent error would require values of λ, assuming n = 1.5, of about 800 Å.

Next, $\sin^2(\theta/2)/\lambda'^2$ was assigned the constant value 1.5×10^9, on the upper end of the experimentally accessible range; b was given the same value as before; and N was allowed to vary from 10^{10} down to unity.

At this point it should be noted that there exists a subtle difference in the meaning of N in the Debye and Isihara treatments. Although both authors refer to N as the number of segments, each Isihara segment represents one scattering point, whereas N Debye segments represent N + 1 scattering points. Thus, in order to compare the two equations, it was decided to replace the Debye N by N - 1.

The results were in qualitative agreement with the predictions of Isihara. The relative error was zero for N = 1 (as it must be since P = 1 for both cases), passed through a slight maximum at $N = 4 \times 10^3$, and then leveled off for the very high values of N. Even at the maximum, however, the relative error was less than 0.01 per cent.

In light of these calculations and others, in which the effective bond length, b, was allowed to assume different values, it was concluded that the refinements of the Isihara treatment were not necessary in the present study.

Before beginning the experimental measurements, it was necessary to determine the theta temperature for the two polymer-theta solvent

pairs. Although the values for both polystyrene-cyclohexane (80) and polydimethylsiloxane-bromocyclohexane (68) were obtainable from the literature, it was decided to check both values by making light scattering measurements at temperatures above and below the reported values.

Because of the analysis difficulty encountered with the PDMS-$C_6H_{11}Br$ solutions, which was noted earlier, utilization of data obtained for PDMS-II in $C_6H_{11}Br$ was not possible; therefore, the literature value of 29.0°C was accepted as the theta temperature.

Problems of a different nature hampered measurements for PS-I in C_6H_{12} at approximately 33, 34, 35, and 36°C. Drooping of the low angle data, characteristic of dust, necessitated the omission of a few of the low angle points from the reciprocal intensity plots. However, in spite of the relatively large amount of uncertainty introduced in the zero angle values, surprisingly consistent values for the second virial coefficients were obtained. The values for A_2 were averaged over the three wave lengths and plotted against temperature; and the interpolated temperature at which A_2 vanished (by definition, the theta temperature) was 33.9°C. Although the result is close to those given in the literature, it was decided to perform the theta measurements in the generally accepted temperature range of 34.5 to 35.0°C. That attaining the exact theta temperature is not necessary is evidenced by the fact that the P^{-1} curves for PS-I in C_6H_{12} at all four temperatures exhibited essentially the same shape.

Therefore, although any one of the four PS-I in C_6H_{12} measurements would have served equally well for the purpose of testing the Debye function, that for 35°C (or more precisely, 34.94°C) was chosen.

Figure 12 shows the data with the Debye curve for R = 348 Å, which agrees well with the value given in Table 4. Note that except for some very low angle data, which were omitted for reasons mentioned above, the fit is generally to within 1 per cent. This good fit, of course, is the result expected for a theta solvent.

Similar data are presented later for PS-III in C_6H_{12} at 34.49°C and for PDMS-IV in $C_6H_{11}Br$ at 29.12°C. In both cases the fit by the Debye function is very good.

As it was pointed out in the description of the polymer samples, the molecular weight distribution function of PS-II was not nearly as sharp as those for all the other samples. Therefore, the results displayed in Figure 13 are not surprising, insofar as the data cannot be fit by the Debye function, which applies to a monodisperse polymer. Although the agreement could be improved by choosing a value of R less than 725 Å, the upward curvature of the Debye curve precludes its use as a good theoretical approximation to the data, which exhibit no detectable curvature. Thus, R was calculated from the slope of the straight line drawn through the data, using Equation (10); and that value, 725 Å, was employed in the calculation of the Debye curve.

Since this experiment for PS-II was conducted at the theta temperature, volume effects were absent and the results can be interpreted in terms of the polydispersity of the sample. Benoit (37) has shown that for a polydisperse collection of Gaussian coils, irrespective of the actual form of the molecular weight distribution function, $\overline{M_z}/\overline{M_w}$ is given by 3/2 times the ratio of the initial slope of the P^{-1} curve to the slope of its asymptote. Therefore, if it can be assumed

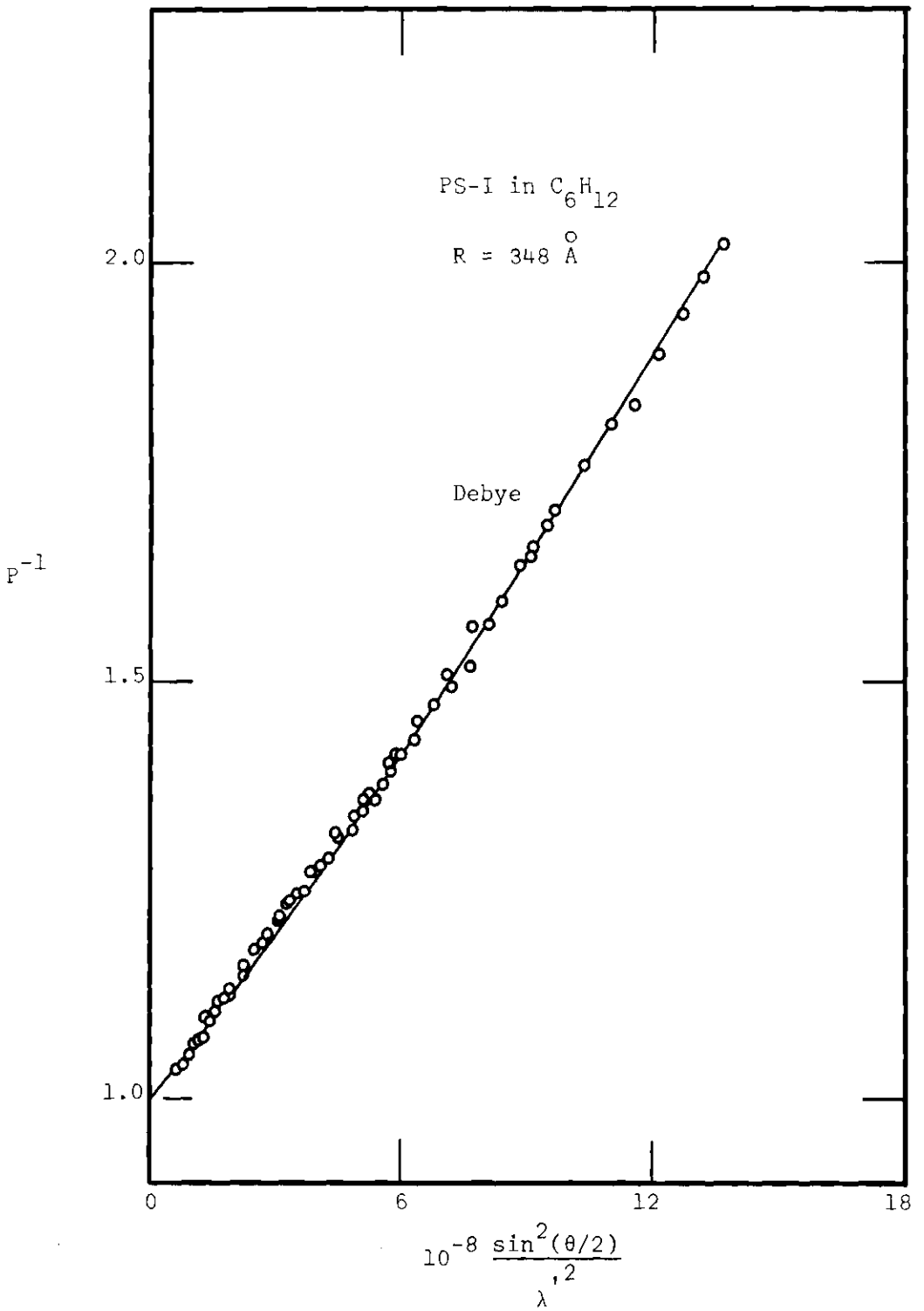

Figure 12. P^{-1} Data for PS-I in Cyclohexane at 34.94°C

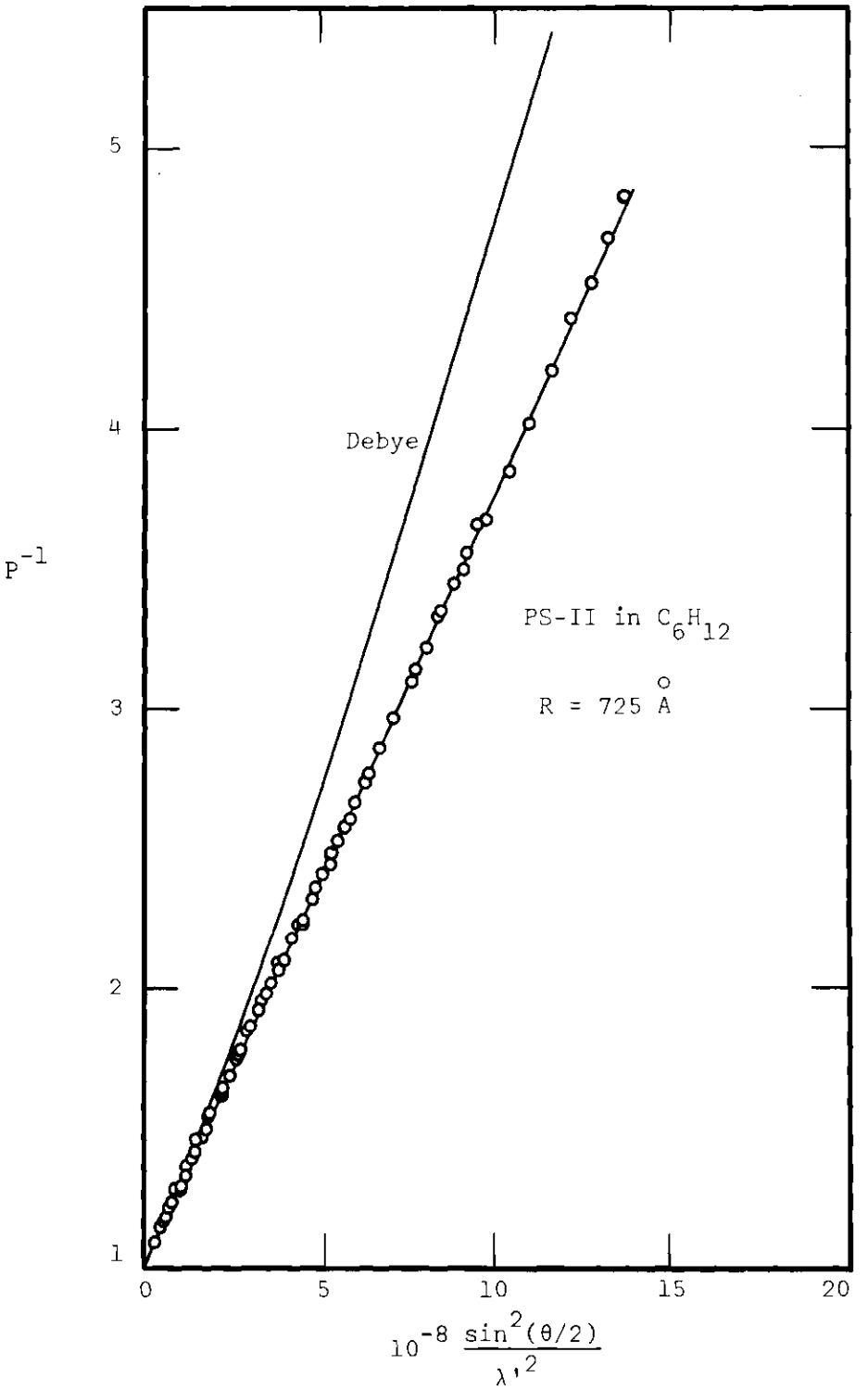

Figure 13. P^{-1} Data for PS-II in Cyclohexane at 34.76°C with Straight Line Drawn Through the Data

that the asymptotic slope of the curve has been reached, the straight line implies $\overline{M_z}/\overline{M_w} = 3/2$. Furthermore, Benoit showed that $\overline{M_w}/\overline{M_n}$ is just twice the zero angle intercept of the asymptote. If it again is assumed that the asymptote has been reached, the results for the present system yield $\overline{M_w}/\overline{M_n} = 2$. Collectively, then, the light scattering results indicate that $\overline{M_z}:\overline{M_w}:\overline{M_n} = 3:2:1$, which is compatible with a Schulz-Zimm distribution (77); thus the distribution is somewhat broader than previously believed.

As a matter of curiosity, three different molecular weight distribution functions, each with $\overline{M_w}/\overline{M_n} = 1.29$ (the value supplied with the sample), were used in combination with the Debye scattering function in the wistful hope that at least one of the calculated curves could be approximated by a straight line and thus, within experimental error, be fitted to the data.

The calculations, which were performed numerically, were based on the expression for the generalized polydisperse scattering function (37):

$$P(\theta) = \int_0^\infty Mf(M)P(M,\theta)dM / \int_0^\infty MF(M)dM \qquad (42)$$

where f(M) is the weight fraction molecular weight distribution function and $P(M,\theta)$ is the scattering function for a monodisperse polymer, which in all three cases was taken as the Debye function. The first two distribution functions, the Schulz-Zimm and the log-normal, are well known (40). The third, however, was obtained from the graph of the distribution function that was determined directly by a sedimentation velocity

analysis (51). Several points were picked at regular intervals off the curve and fit to an eighth order polynomial.

Since the scattering function for the Schulz-Zimm distribution has been obtained in a simple form (77), its evaluation was not as difficult as that for the other two distributions. In both of the other cases, the scattering function was evaluated directly from Equation (42) using a Simpson integration procedure.

As it was suspected, a value of 1.29 for the weight to number average molecular weight ratio was not high enough in any of the calculations to eliminate the pronounced upward curvature.

In conclusion, the measurements in theta solvents served a dual purpose: (1) they established the validity of the Debye equation for theta systems; (2) they allowed departures from the Debye prediction for measurements in the good solvent systems to be attributed to volume and not polydispersity effects, the one exception, of course, being PS-II.

Good Solvents

In order to make comparisons between Equation (16), the Debye equation, and Equation (21), the Ptitsyn equation, it was necessary to make numerical calculations for both. For the most part, the Debye function was evaluated in a very straightforward manner using the B-5500 computer. The numerical results were checked in two different ways: (1) by slide rule calculations and (2) by a computer evaluation of several terms of a series expansion of the function, which is given by

$$P(\theta) = 1 - x/3 + x^2/12 - x^3/60 + x^4/360 - x^5/2520 + x^6/20160 - \ldots \quad (43)$$

Satisfactory agreement was obtained. Since the Ptitsyn function, Equation (21), defies significant simplification, integrations were performed numerically using a Simpson procedure. In this case three different methods were used to check the results. (1) Using Ptitsyn's (21) slightly simplified version of Equation (21), hand calculations were performed with the aid of mathematical tables (81). (2) Values were compared with those tabulated by Hyde, *et al.*, (23). (3) Equation (21) was numerically integrated for the special case of $\varepsilon = 0$ and compared with the previously calculated Debye functions. In all cases the verification was satisfactory.

As it can be seen from Figure 14, the refinements of the Ptitsyn treatment, unlike those of the Isihara treatment, certainly have to be considered for visible light scattering measurements. Pictured are a Debye curve and two Ptitsyn curves, all calculated for R = 600 Å. Although appreciable differences are present for this value of the radius of gyration, they become even more pronounced at higher values.

In order to fit experimental data with the curves, the only parameter, other than R, that has to be known is ε. Loucheux *et al.* (39) have suggested two methods for its evaluation.

The first method requires that viscosity measurements be made as a function of molecular weight. The intrinsic viscosity, then, is related to the mean square end-to-end distance, $\overline{r^2}$, by the Flory Fox equation:

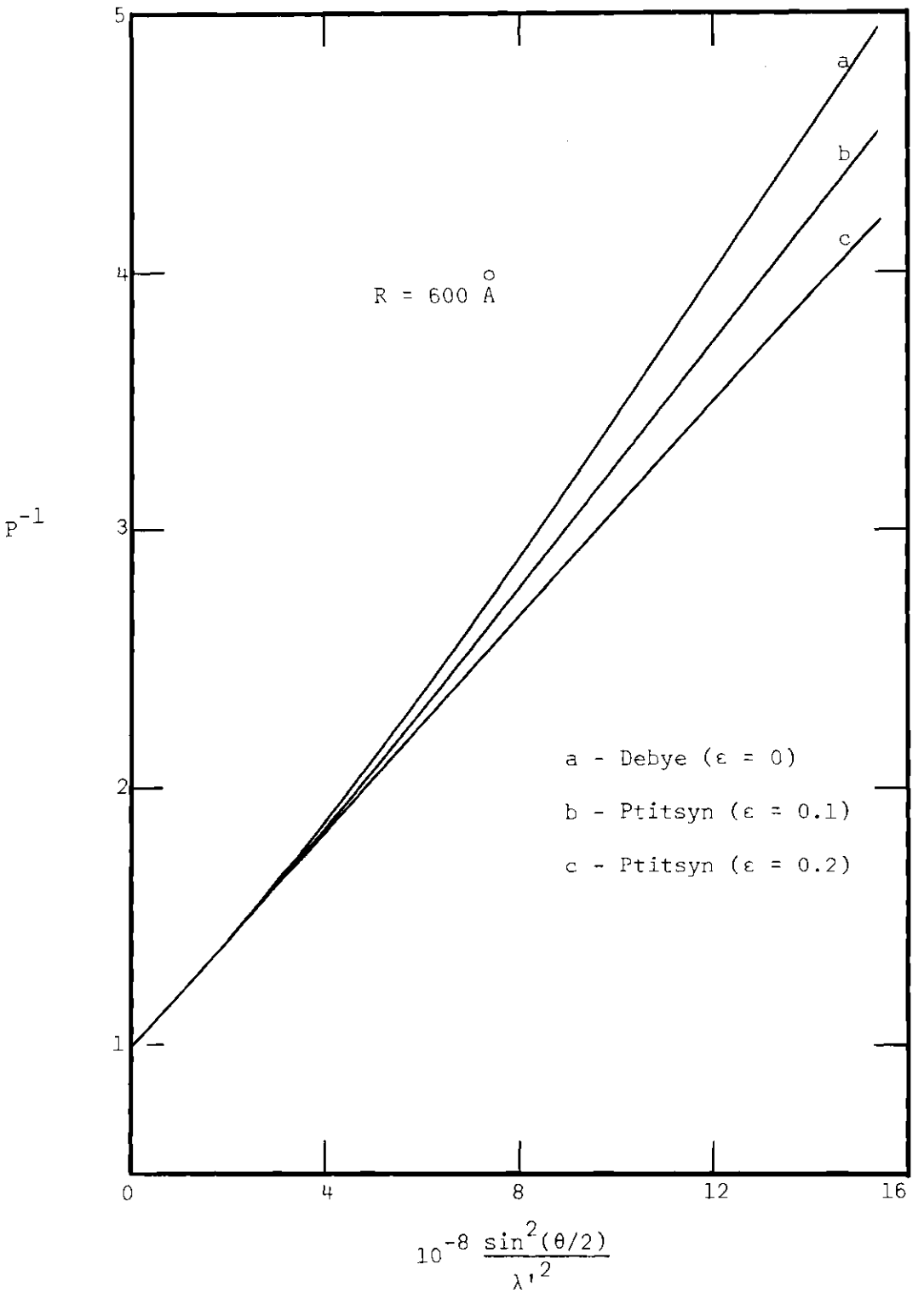

Figure 14. Comparison of the Debye and Ptitsyn Scattering Functions

$$[\eta] = \Phi(\overline{r^2})^{3/2}/M \tag{44}$$

where Φ is a constant. If Equation (44) is combined with Equation (20) for the special case of $|i - j| = N$, there results

$$[\eta] = K'M^{(1 - 3\epsilon)/2} \tag{45}$$

where K' is a constant. Comparison with the Mark-Houwink relation, Equation (33), then immediately leads to

$$\epsilon = (2a - 1)/3 \tag{46}$$

Since Mark-Houwink exponents generally lie between 0.5 (for theta solvents) and 0.8 (for very good solvents), the corresponding values of ϵ are expected to range from 0 to 0.2.

The second method, which evidently is supposed to give the same result as the first method, utilizes the actual light scattering data. Loucheux *et al.* (39) have obtained an asymptotic form of $P(\theta)$, valid at very high values of $\sin^2(\theta/2)/\lambda'^2$ and for a polydisperse system. They suggest that a log-log plot of $P^{-1}(\theta)$ versus $\sin^2(\theta/2)/\lambda'^2$ should give a straight line for high abscissa values. Even though they obtained for their system a value of ϵ compatible with the generally accepted viscosity exponent, others have not been so fortunate (40). Hyde (41) pointed out that the principal problem with this method is that sufficientby high values of $\sin^2(\theta/2)/\lambda'^2$ and the molecular weight

are seldom reached; thus he presented a second approximation for the asymptote, which, however, is valid only for the monodisperse case.

For all cases except one, PS-III in benzene (to be discussed later), the first method was used for the evaluation of the parameter ε. Figures 15 and 16 give the log-log plots of $[\eta]$ against M for the polydimethylsiloxane fractions in carbon tetrachloride and the polystyrene samples in benzene. In both cases, the values of ε that were used in the curve fitting process were calculated from the slope (a) and Equation (46). These values of ε for the PDMS-CCl_4 and PS-C_6H_6 systems, 0.10 and 0.16, respectively, were then used to calculate ε for the other two good solvent systems, PDMS-C_6H_6 and PS-CCl_4. Although a viscosity exponent for PDMS in benzene was found in the literature (see Table 2), consideration of the viscosity results and experimentally determined dimensions indicated that the literature value was too high, and a value slightly lower than that for PDMS in CCl_4 was chosen. This approximation led to $\varepsilon = 0.09$. Similar considerations led to the use of a viscosity exponent for PS-CCl_4 which was slightly lower than that for PS-C_6H_6. This approximation resulted in $\varepsilon = 0.15$.

In view of the large viscosity exponent that was reported in the literature for PDMS in benzene, the first PDMS measurements were made for a benzene system, PDMS-III in benzene. Those results, which are shown in Figure 10, demonstrate very precisely that, even though benzene is a good solvent, the data can be predicted by the Debye function. The only disappointing aspect of the results was the low value of R, which, along with a viscosity measurement, indicated that benzene is not a particularly good solvent for the polymer. As mentioned above, this

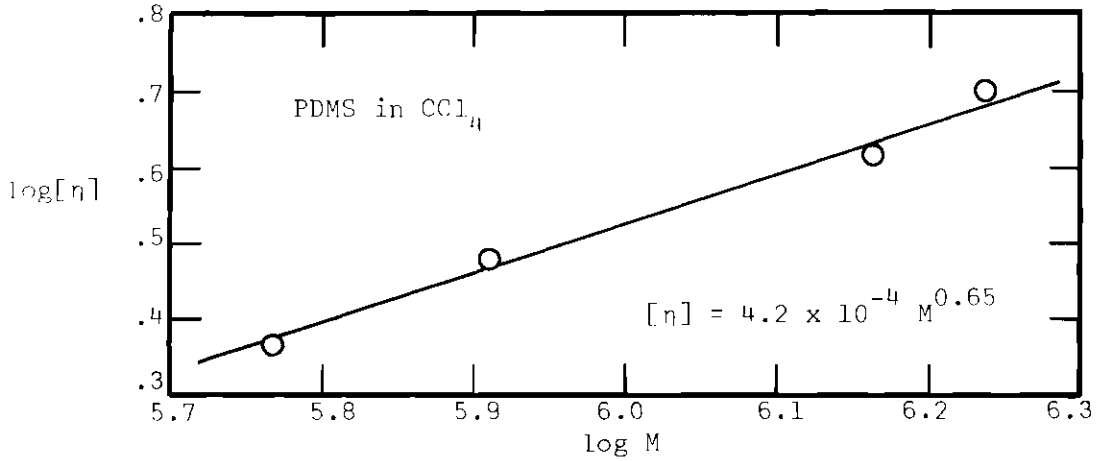

Figure 15. Log-log Plot of [η] versus M for PDMS in Carbon Tetrachloride

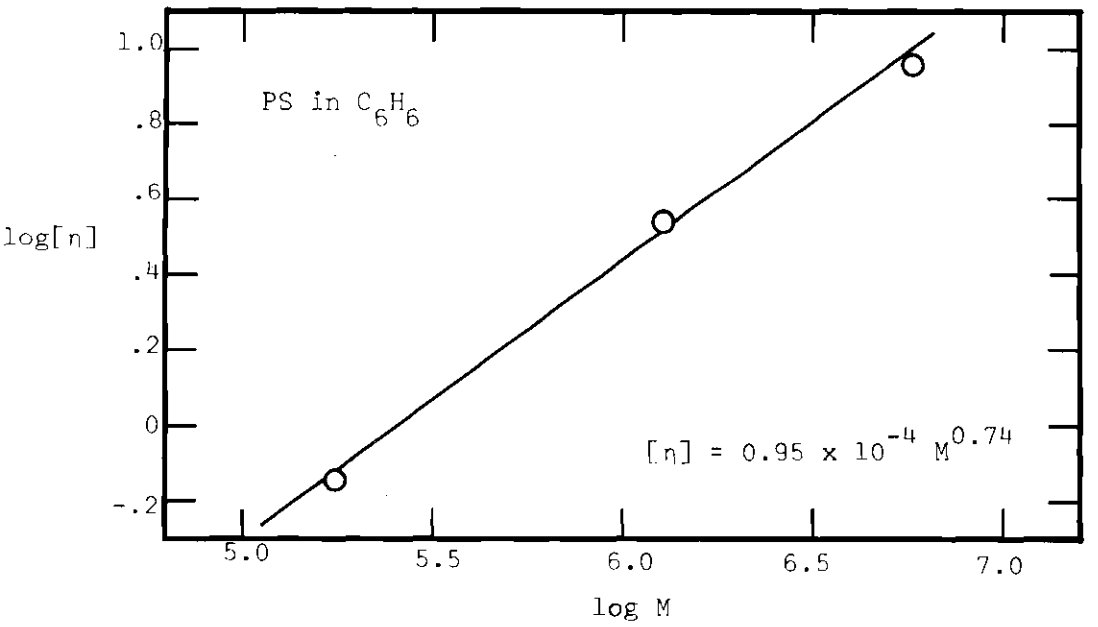

Figure 16. Log-log Plot of [η] versus M for PS in Benzene

discovery is reflected in the low value of ε.

Following a search for a better solvent, which also had to possess a refractive index significantly different from that of the polymer, the next experiment was PDMS-III in CCl_4 at 30.0°C. The results, which are given in Figure 17, are the same as those for the same fraction in benzene; that is, even though the solvent is a good solvent, the data are fit very well by the Debye equation. In this case, it is also evident that the upward curvature precludes a fit by the Ptitsyn function (ε = 0.10).

In an effort to find a system which could not be described by the Debye equation, the highest molecular weight fraction, $\overline{M_w}$ = 1.7 x 10^6, PDMS-IV, was used with carbon tetrachloride at 30.0°C. Figure 18 shows these results and, for comparison, those obtained for the same fraction in the theta solvent. Both sets of data are fit well by the Debye function. As in the previous case, the upward curvature of the good solvent precludes a fit by the Ptitsyn function using the *a priori* value of ε; in other words, if the fit is forced at high angles, the curve passes significantly above the data at moderately low angles. The other case, a forced fit at low angles, is automatically accomplished by using the same radius of gyration in the calculation of both curves. This is discussed more fully for the case of PS-I in CCl_4.

Figures 19 and 20 present the somewhat anticlimactic results for PDMS-I and PDMS-II, the two fractions having the lowest molecular weights. Because of the scatter of the data and the low molecular weights involved, the results, especially those for PDMS-I, serve to show only the appropriateness of the Debye function, and not the

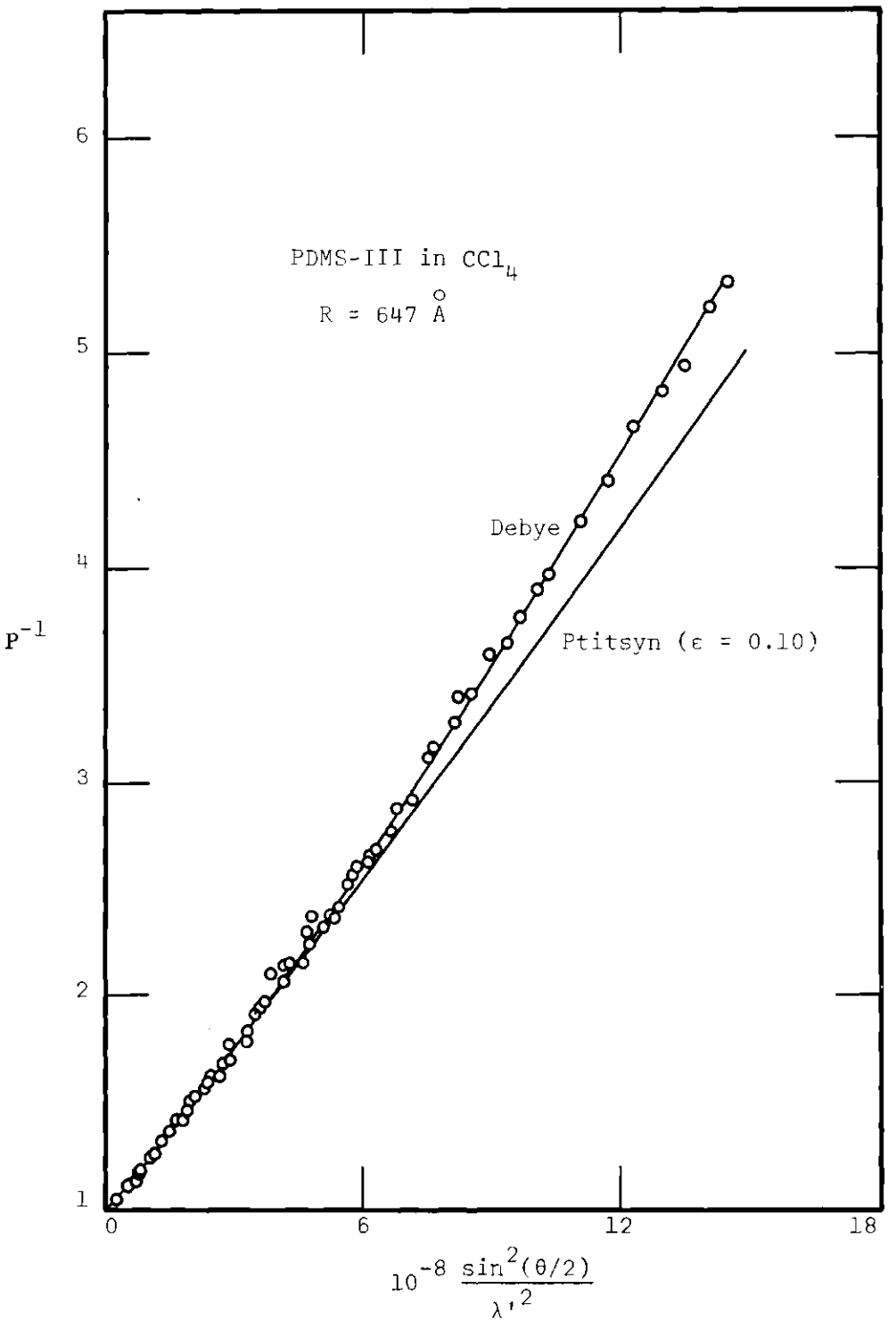

Figure 17. P^{-1} Data for PDMS-III in Carbon Tetrachloride at 30.0°C

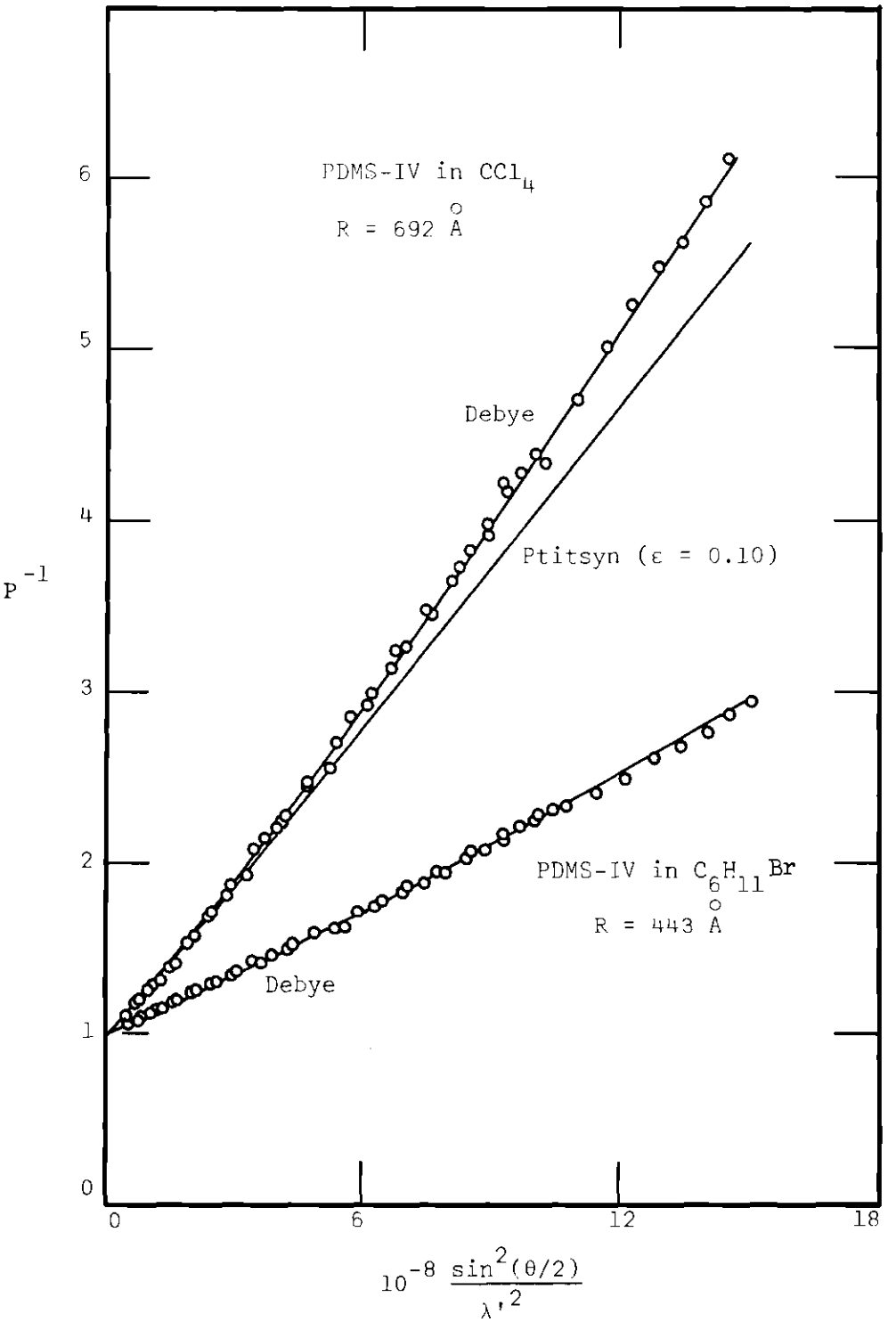

Figure 18. P^{-1} Data for PDMS-IV in Carbon Tetrachloride at 30.0°C and in Bromocyclohexane at 29.12°C

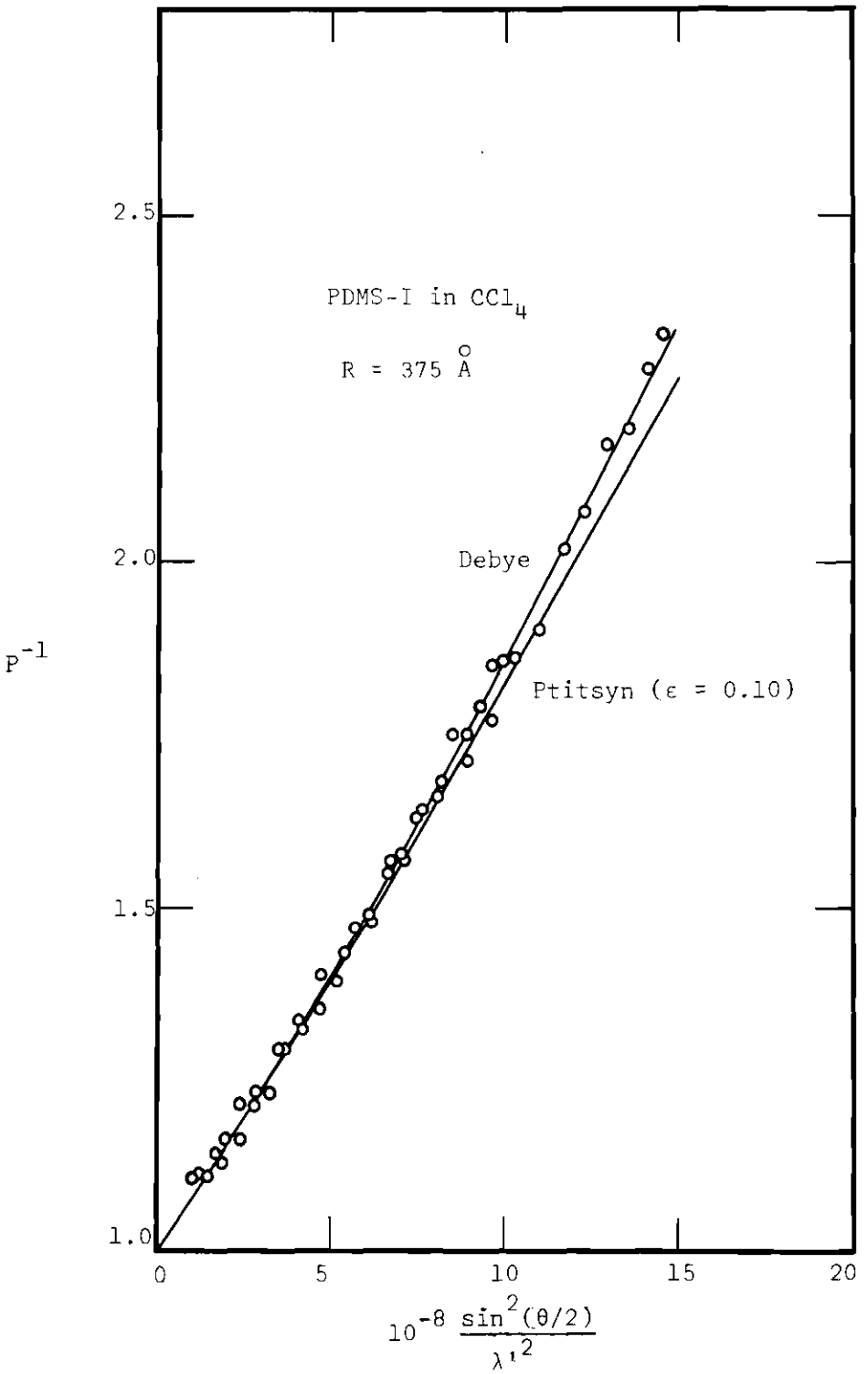

Figure 19. P^{-1} Data for PDMS-I in Carbon Tetrachloride at 30.0°C

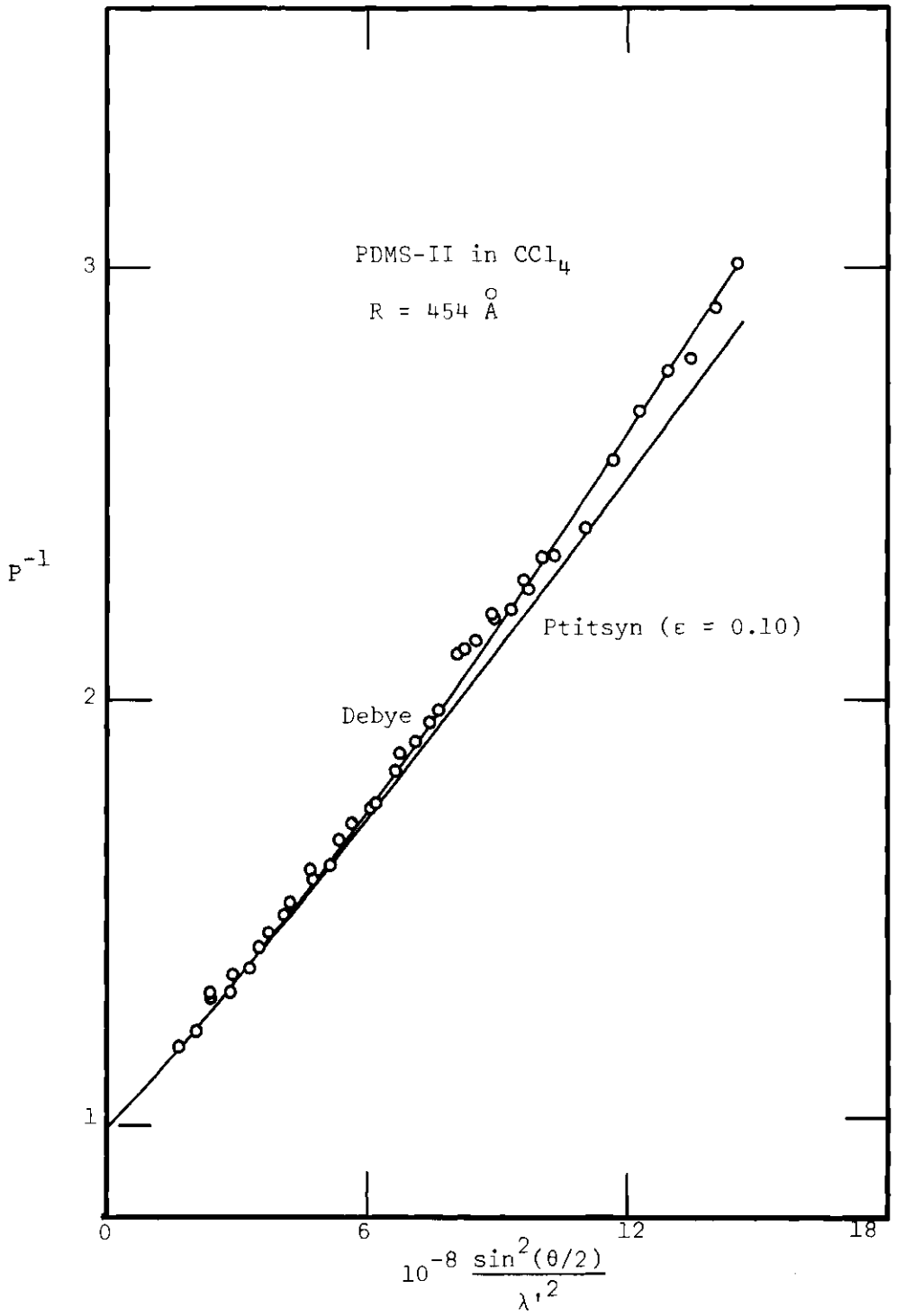

Figure 20. P^{-1} Data for PDMS-II in Carbon Tetrachloride at 30.0°C

inappropriateness of the Ptitsyn function.

Therefore, for each of the polydimethylsiloxane systems the R value was determined by fitting the data over the entire angular range with the Debye function; moreover, in all cases, these values agreed well with those determined by the initial tangent method. Although it was not possible to find a very good light scattering solvent for PDMS, the results of at least two of the measurements in carbon tetrachloride showed a definite preference for $\varepsilon = 0$ over $\varepsilon = 0.10$.

Since the first polystyrene sample to be discussed, PS-I, was essentially the same sample as that used by Debye, Chu, and Kaufmann (43), it had particular significance. As it was pointed out earlier, their results for benzene were adequately described by the Debye equation. They, however, did not report conclusions regarding the Ptitsyn function. Figure 21 shows the P^{-1} data for PS-I in benzene at 35.0°C. Also included is the appropriate Debye curve for the PS-I in cyclohexane results at the same temperature. Even though benzene is a very good solvent and the molecular weight of the fraction is moderately high, the Ptitsyn function with $\varepsilon = 0.16$ is inappropriate and the Debye function fits very well. The realization that the conclusions of Debye, Chu, and Kaufmann were reached by utilizing data extending to an abscissa value of only about 11×10^8 re-emphasizes the importance of using a shorter wave length and also of overlapping the data.

Figure 22 displays the results for the same sample, this time in carbon tetrachloride at 30.0°C. The higher refractive increment of the system, compared to PS in benzene, is evidenced by the decrease in the scatter of the data points. Again the Debye curve fits the data.

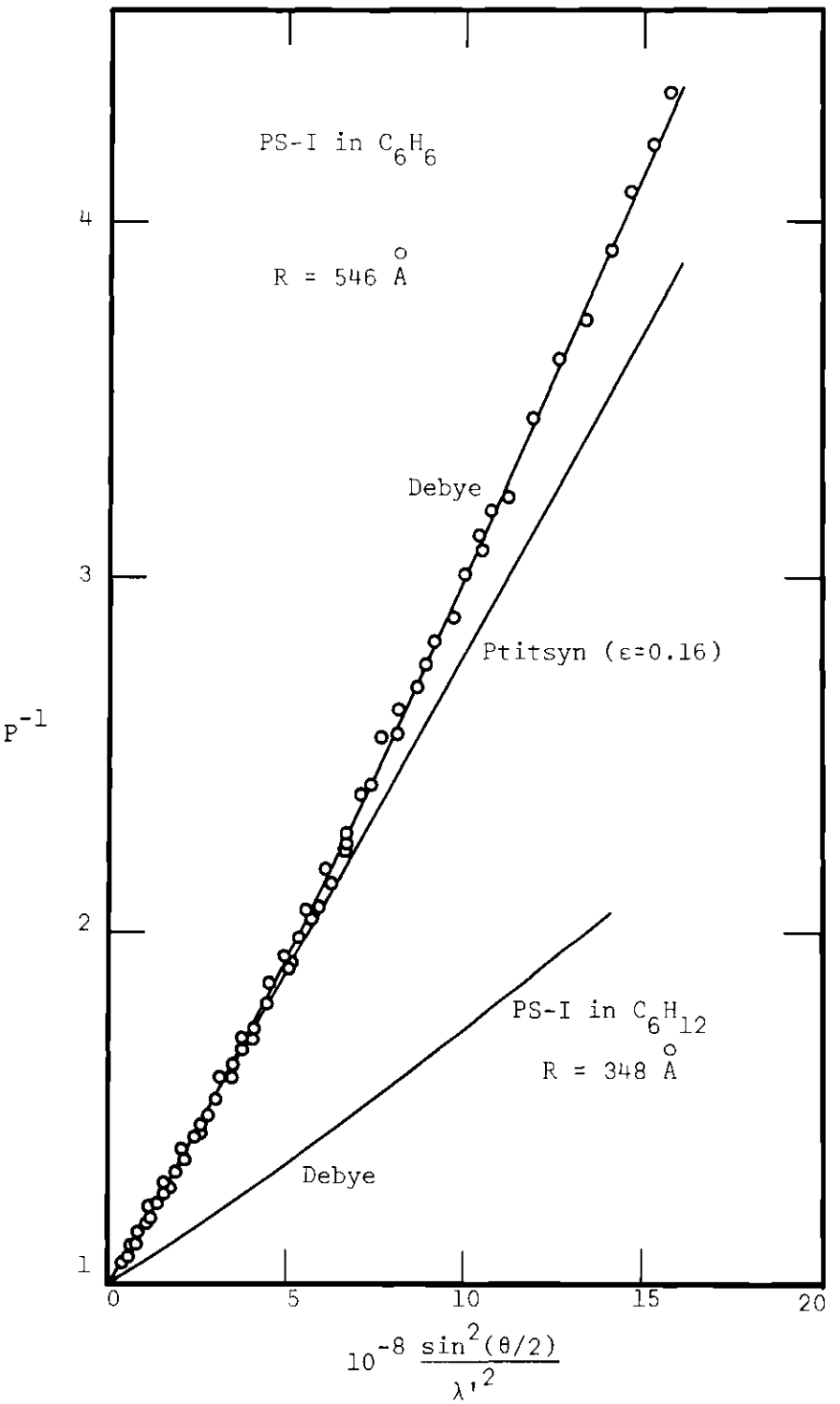

Figure 21. P^{-1} Data for PS-I in Benzene at 35.0°C. Also Debye Curve for PS-I in Cyclohexane at 34.94°C

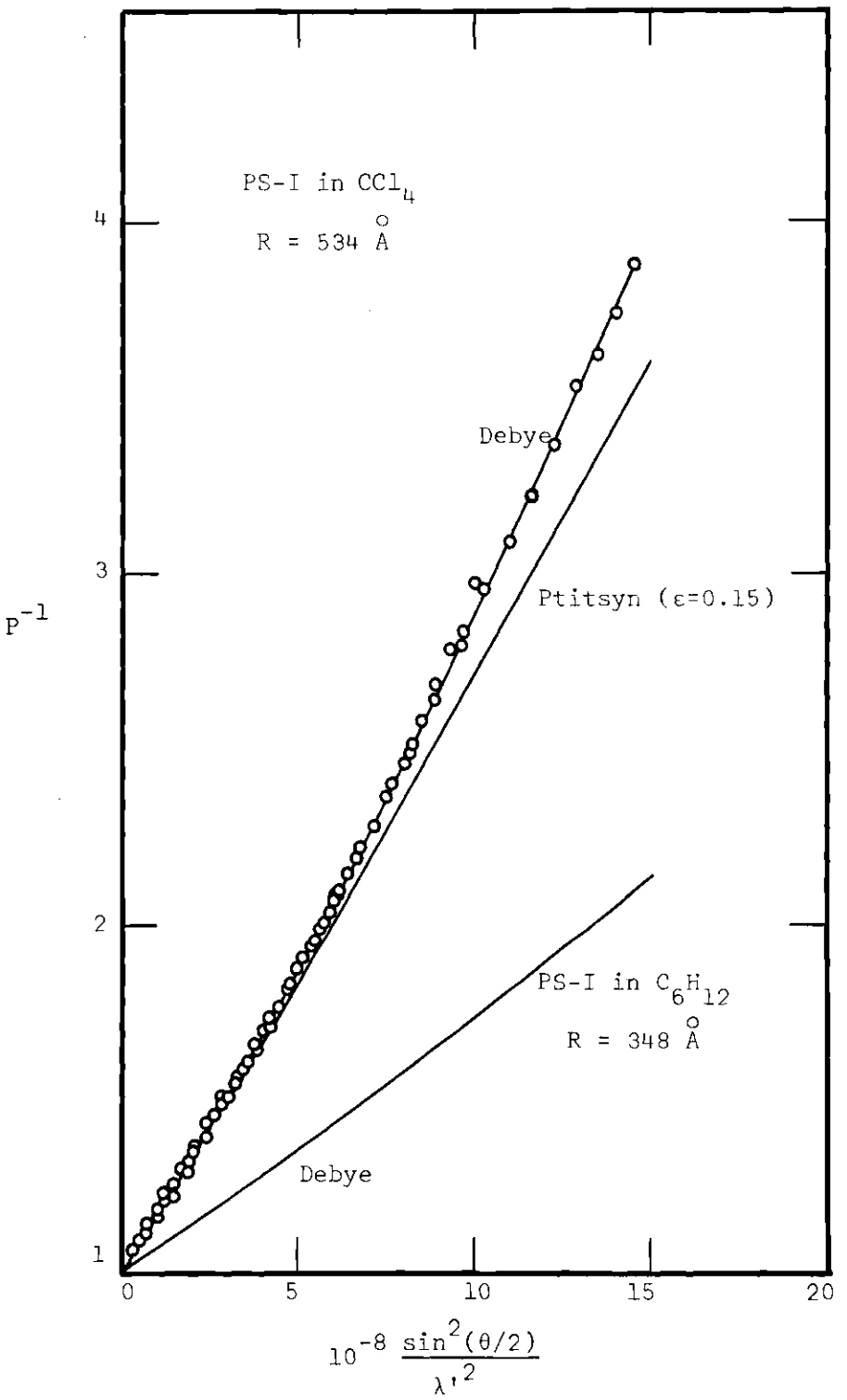

Figure 22. P^{-1} Data for PS-I in Carbon Tetrachloride at 30.0°C. Also Debye Curve for PS-I in Cyclohexane at 34.94°C

Because of the small extent of scatter of these data points, it is worthwhile to ascertain how well the Ptitsyn function predicts the data if a fit is forced at moderately high angles. Figure 23 gives the same PS-I in CCl_4 data as before; however, in this case the theoretical lines are Ptitsyn curves for which the values of ε and R have been varied simultaneously. Note that if ε is some small value (on the order of 0.05), the data can be fit well by the more elaborate theory; but the value of ε determined from viscosity measurements or any value close to it will not permit a fit to the data over the entire angular range.

As it was pointed out in the previous section on theta solvents, PS-II had a relatively broad molecular weight distribution and thus the scattering results for the measurements in the theta solvent could not be fit with the Debye equation. Instead, the data were fit very well by a straight line, thus indicating that $M_z:M_w:M_n=3:2:1$. Consequently, if volume effects do not appreciably affect the results for a good solvent, the same shape for P^{-1} is expected, a straight line, which, of course, exhibits a larger slope than before. Figure 24 presents the data for PS-II in carbon tetrachloride at 30.0°C. For comparison, the straight line corresponding to the theta measurement data is also included. Although the effect is not great, it can be seen that the good solvent data do exhibit downward curvature, away from the straight line which gives the initial slope (and thus the radius of gyration of the polymer) of the data. Because of the difficulties encountered in the attempted numerical integration of Equation (42) when using the Ptitsyn light scattering function and an appropriate molecular weight distribution function, the corresponding Ptitsyn function for this

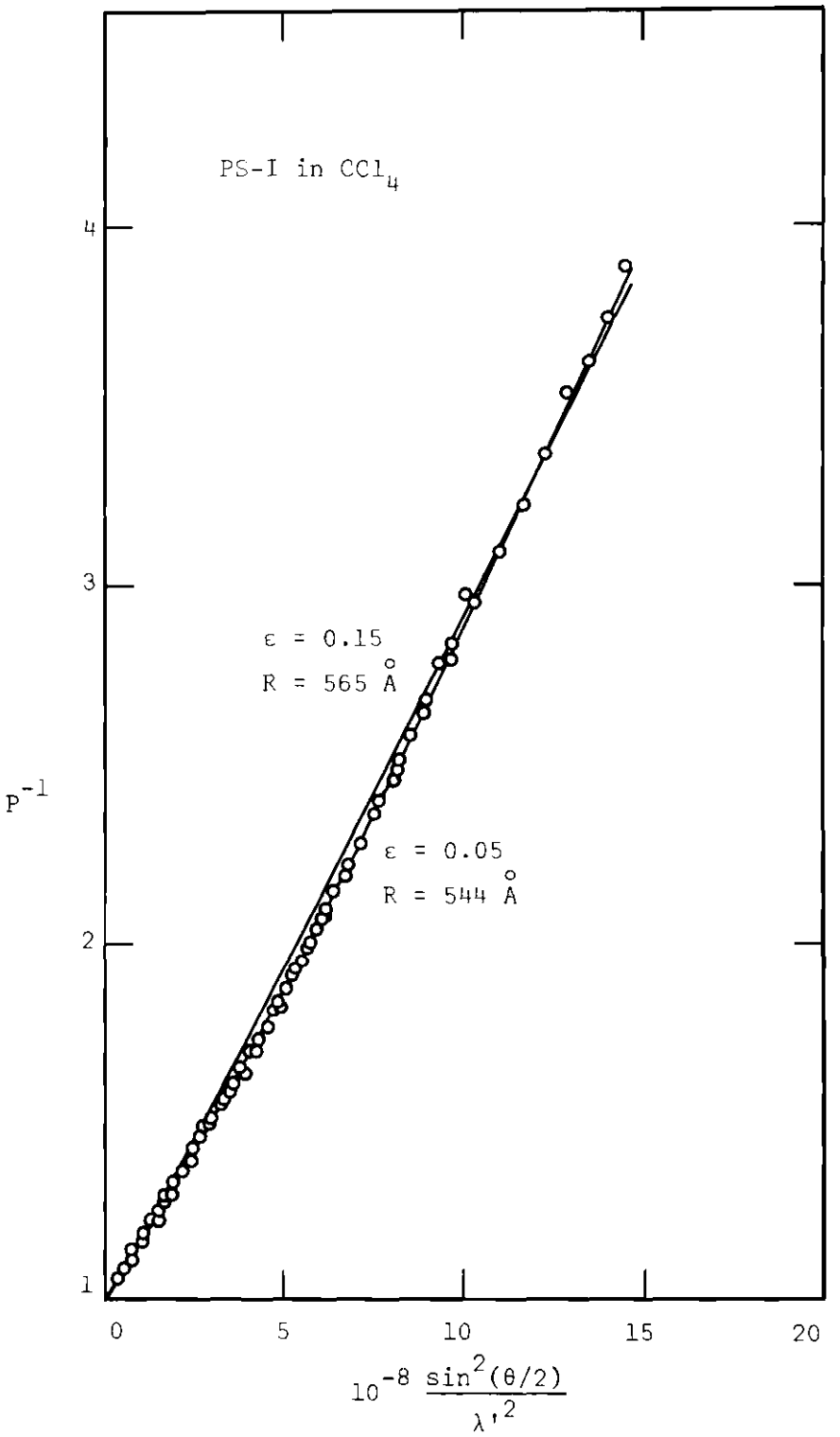

Figure 23. P^{-1} Data for PS-I in Carbon Tetrachloride at 30.0°C. Attempt to Fit with Ptitsyn Function

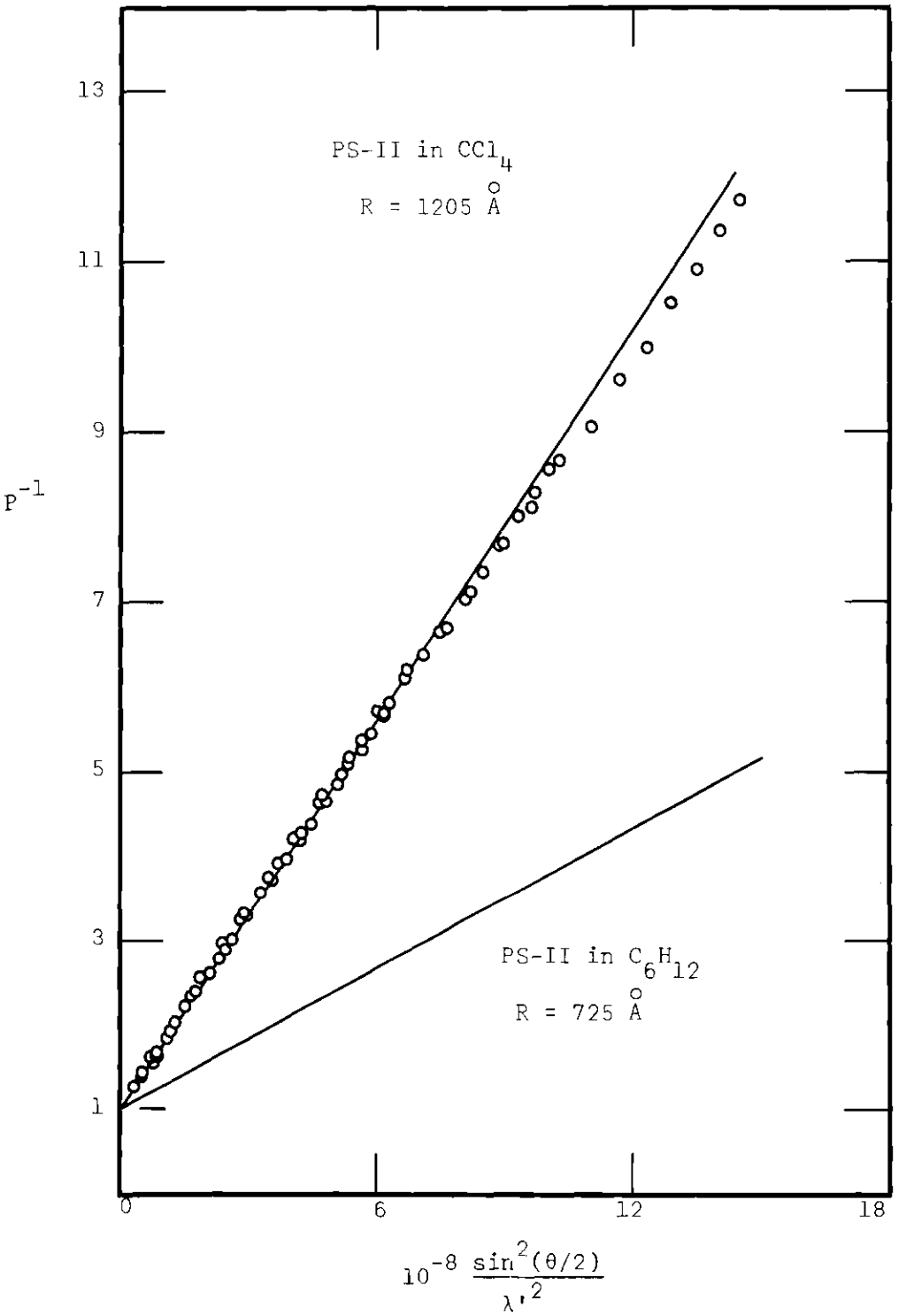

Figure 24. P^{-1} Data for PS-II in Carbon Tetrachloride at 30.0°C, with Straight Line Giving Initial Slope. Also Straight Line for PS-II in Cyclohexane at 34.76°C

polydisperse case was not calculated. However, from previous results it can be seen that using the Ptitsyn function with $\varepsilon = 0.15$ would probably overestimate the downward curvature.

Finally, Figure 25 shows the results for PS-III, the sample having the highest molecular weight, $\overline{M_w} = 5.7 \times 10^6$, in benzene at 30.0°C. Like the previous case, but to a much greater extent, these results depart from the Debye prediction. The downward curvature is so pronounced that, were it not for the included results for PS-III in C_6H_{12} at 34.49°C which indicate that the sample is essentially monodisperse, it would be tempting to attribute the effect to polydispersity. Although the curve drawn through the points is the Ptitsyn curve, it must be pointed out that the value of ε required, 0.11, which was determined by trial and error, is considerably less than the 0.16 calculated from Equation (46).

Qualitatively, then, the expression of Ptitsyn, Benoit, and Hyde correctly predicts the behavior of the angular intensity data for polymers which are dissolved in good solvents. That is, provided that the molecular weight is sufficiently large, the excluded volume effect causes downward curvature in the P^{-1} data at high values of $\sin^2(\theta/2)/\lambda'^2$; moreover, the departure from the Debye prediction increases with the molecular weight of the polymer.

On the other hand, *a priori* values of ε do not lead to quantitative agreement with the observed behavior of the scattering function. For most of the good solvent systems investigated, although large values were predicted, $\varepsilon = 0$ or some other small number quite satisfactorily accounted for the results; and even in the two systems where

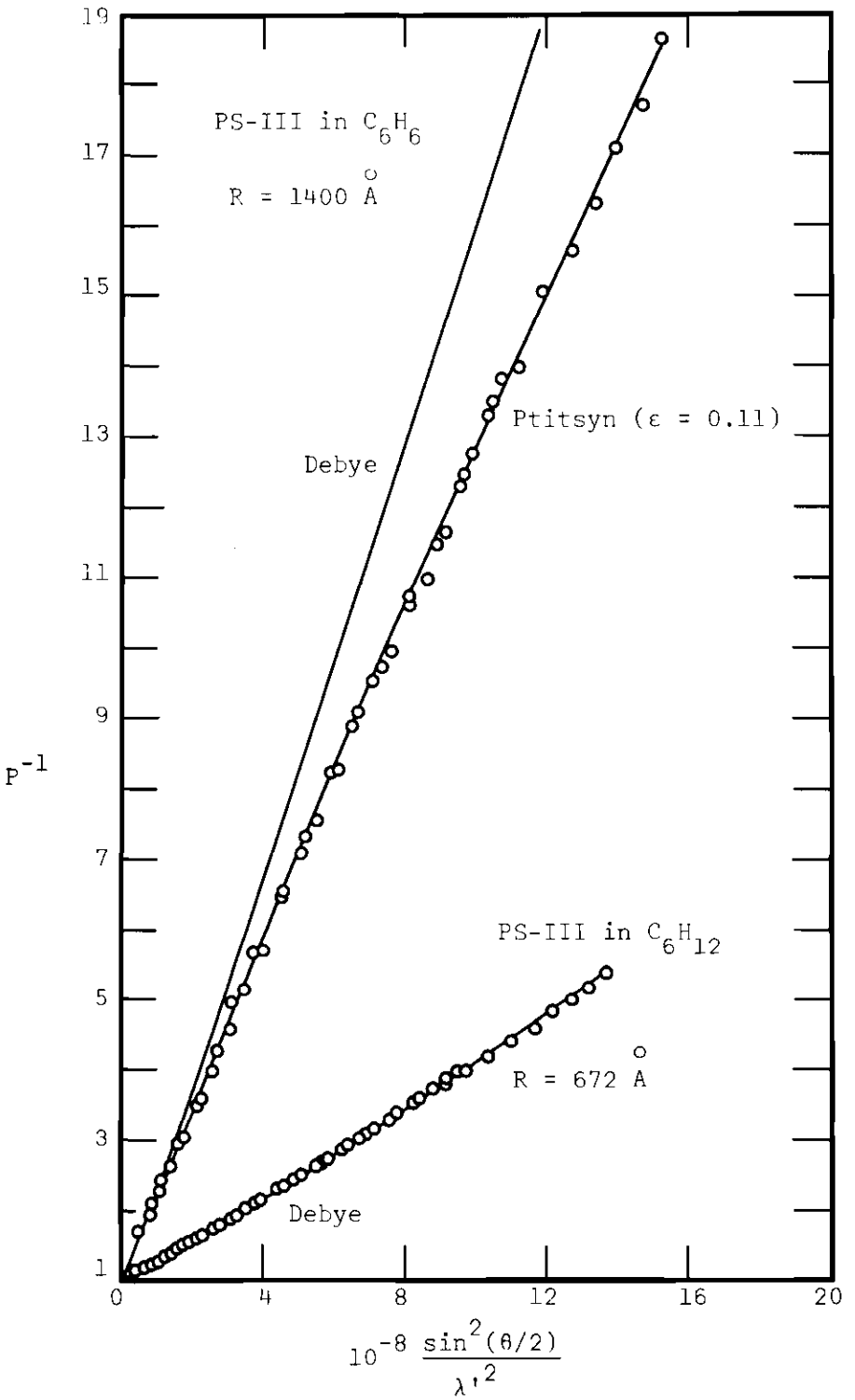

Figure 25. P^{-1} Data for PS-III in Benzene at 30.0°C and in Cyclohexane at 34.49°C

volume effects were clearly manifested, the values of ε required to fit the data were considerably smaller than the *a priori* values. Therefore, if ε was determined not by Equation (46) but rather by a best fit of the actual light scattering data, the Ptitsyn function correctly predicted the results; however, in all cases except PS-II and PS-III in good solvents, the simpler Debye function ($\varepsilon = 0$) was quite satisfactory.

Therefore, it appears that the introduction of Equation (20) into the Ptitsyn treatment has caused problems. As it was pointed out, the assumption is based on experimental evidence for good solvents that the mean square polymer dimensions are proportional to the molecular weight raised to some power greater than unity. What was not mentioned, however, is that over very large ranges of molecular weight the exponent is not a constant. In other words, the Mark-Houwink a, although constant over reasonably wide ranges of molecular weight, does vary when the range is considerably extended. That this variation is not unexpected can be seen from a consideration of the molecular expansion factor, α, which is defined by $(\overline{r^2}/\overline{r_o^2})$, where $\overline{r_o^2}$ is the mean square end-to-end distance of the polymer in a theta solvent. According to Flory (82),

$$\alpha^5 - \alpha^3 = C\Psi_1(1 - \Theta/T)M^{\frac{1}{2}} \qquad (47)$$

where Ψ_1 is an entropy parameter, Θ is the theta temperature, and C is a factor which is independent of M. Note that when $T = \Theta$, $\alpha = 1$, but when T is greater than Θ, α itself is some complicated, slowly

increasing function of the molecular weight. For very large expansions, α^3 is much less than α^5 and thus α is proportional to $M^{0.1}$.

When $\alpha^2\overline{r_o^2}$ is substituted for $\overline{r^2}$ in Equation (44), the Flory-Fox relation becomes

$$[\eta] = \Phi(r_o^2/M)^{3/2}M^{1/2}\alpha^3 \tag{48}$$

where $\overline{r_o^2}/M$ is independent of the molecular weight. If $T = \Theta$, $\alpha^3 = 1$ and Equation (48) gives the Mark-Houwink equation with $a = 1/2$. However, when T is different from Θ, things become considerably more complicated. According to Equation (47), α is not a function simply of M raised to some constant; therefore, when the exponential dependence of α on M is assumed, as is the case with the Mark-Houwink relation, it is not surprising that the exponent is not a constant for all values of M. Equation (47) lends support to the empirical viscosity-molecular weight relationship only at the theta condition, where $[\eta]$ is proportional to $M^{0.5}$, and for very high values of α, in which case α is proportional to $M^{0.1}$ and $[\eta]$ is proportional to $M^{0.8}$.

Returning to a discussion of Equation (20), it is not right, therefore, to assume that very small intramolecular distances can be related to $|i - j|$ in the same way that it is possible to relate the large distances; instead, ε should be an increasing function of $|i - j|$. Failure to account for the molecular weight dependence of ε is particularly fallacious in a treatment of the scattering function, for the optimum conditions for observing deviations from the Debye function (scattering from large angles and small wave lengths, in which

case, as it can be seen by expanding Equation (8), the greatest contribution to the total scattered intensity is made by small intramolecular distances) are the very conditions where ϵ is most different from the *a priori* value, which is naively calculated from the viscosity exponent.

Polymer Dimensions

As it was pointed out earlier in the discussion of the results, most of the values of the radius of gyration were determined by fitting the data over the entire angular range to a theoretical function. Only for PS-II was it necessary to revert to the standard method of evaluating the initial tangent of the P^{-1} curve.

Table 5 lists all the experimentally determined radii of gyration, molecular weights, and intrinsic viscosities, along with two calculated quantities.

In order to facilitate the comparison of polymer dimensions, the two values of R for the PS-II systems were corrected for polydispersity. Since the value of R that is measured for a polydisperse system is actually a z-average quantity (83), the two measured values were corrected by multiplying by $\overline{M_w}/\overline{M_z}$, which was 0.67.

Similar, but more complicated corrections had to be applied to the PS-II values of Φ. For the monodispersed samples Φ was easily calculated from Equation (44), assuming $\overline{r^2} = 6R^2$.

Trementozzi and Newman (84) have shown that for the polydisperse case, Equation (44) becomes

$$[\eta] = (\Phi/q)(\overline{r^2})^{3/2}/M \qquad (49)$$

Table 5. Polymer Dimensions and Related Quantities

System	$M_w \times 10^{-6}$	R(Å)	$R^2/M_w \times 10^{17}$	[η]	$\Phi \times 10^{-21}$
PS-I in C_6H_6	1.30	546	2.29	3.42	1.86
PS-I in CCl_4	1.40	528	2.04	2.89	1.87
PS-II in CCl_4	4.35	984*	2.23	5.35	1.78**
PS-III in C_6H_6	5.72	1400	3.43	9.00	1.28
PS-705 in C_6H_6	0.176	150	1.28	0.72	2.56
PS-I in C_6H_{12}	1.30	348	0.91	1.03	2.18
PS-II in C_6H_{12}	3.19	592*	1.10	1.77	1.98**
PS-III in C_6H_{12}	4.53	672	1.00	2.06	2.09
PDMS-I in CCl_4	0.588	375	2.39	2.30	1.82
PDMS-II in CCl_4	0.815	454	2.53	3.00	1.78
PDMS-III in CCl_4	1.46	647	2.87	4.11	1.51
PDMS-III in C_6H_6	1.63	544	1.82	2.45	1.69
PDMS-IV in CCl_4	1.72	692	2.80	4.95	1.75
PDMS-IV in $C_6H_{11}Br$	2.16	443	0.91		

*Determined from initial tangent; corrected for polydispersity.

**Corrected according to Equation (49) for q = 1.96.

where q depends upon the actual molecular weight distribution function. For a Schulz-Zimm distribution, which is compatible with PS-II,

$$q = [(h + 2)^{3/2}/(h + 1)][\Gamma(h + 1)/\Gamma(h + 1.5)] \qquad (50)$$

where $h = [(M_w/M_n) - 1]^{-1}$ and Γ is the gamma function. For PS-II, $h = 1$ and $q = 1.96$.

Note that, as expected (85), the Φ values generally fall into two groups, theta solvents and good solvents, with the theta solvent values being the greater in magnitude. The only values that appear to be inconsistent with the major portion of the results and with the expected values are those for PS-III in benzene, PS-705 in benzene, and PDMS-III in carbon tetrachloride. For reasons discussed in the next section, the discrepancies for all three of these cases probably resulted from inaccurate values of the radius of gyration.

Figure 26 shows a log-log plot of R^2/M versus M for PDMS in carbon tetrachloride. The value of ε calculated from the slope, according to Equation (20), is about twice that calculated from the viscosity exponent; however, it should be noted that reducing the value of R about 5 per cent for the PDMS-III case, which is compatible with the Φ results, gives a value of ε very close to the previously calculated one.

Figure 27 shows a similar plot for polystyrene in benzene. Two of the three values, PS-705 and PS-III, were mentioned above because of their abnormal Φ values. Once again *a posteriori* adjustments will adequately reduce the slope from a value which is about twice too large.

Experimental Error

To systematically account for all the possible errors in the present light scattering investigation would be almost as difficult as

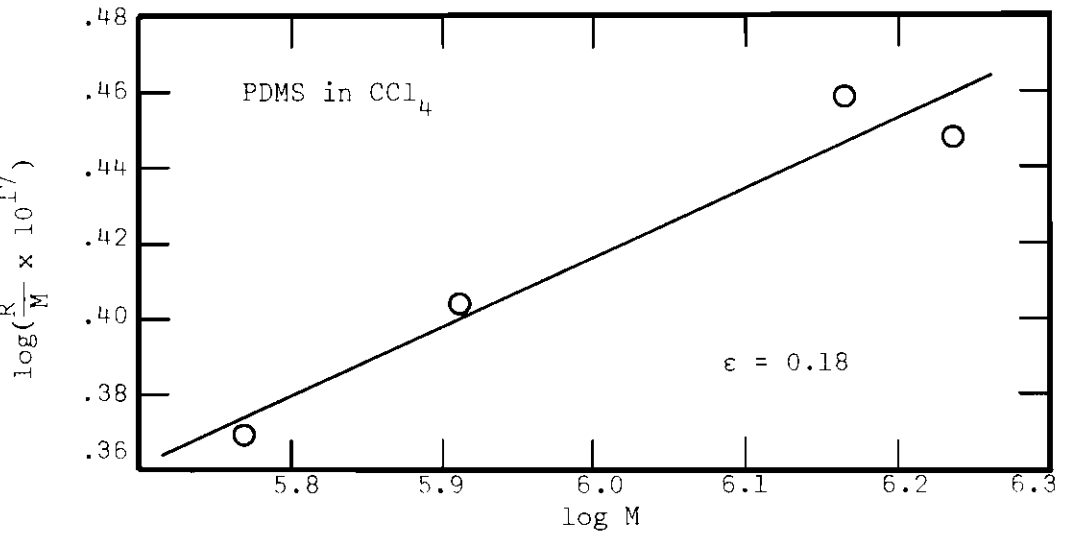

Figure 26. Log-log Plot of R^2/M versus M for PDMS in Carbon Tetrachloride

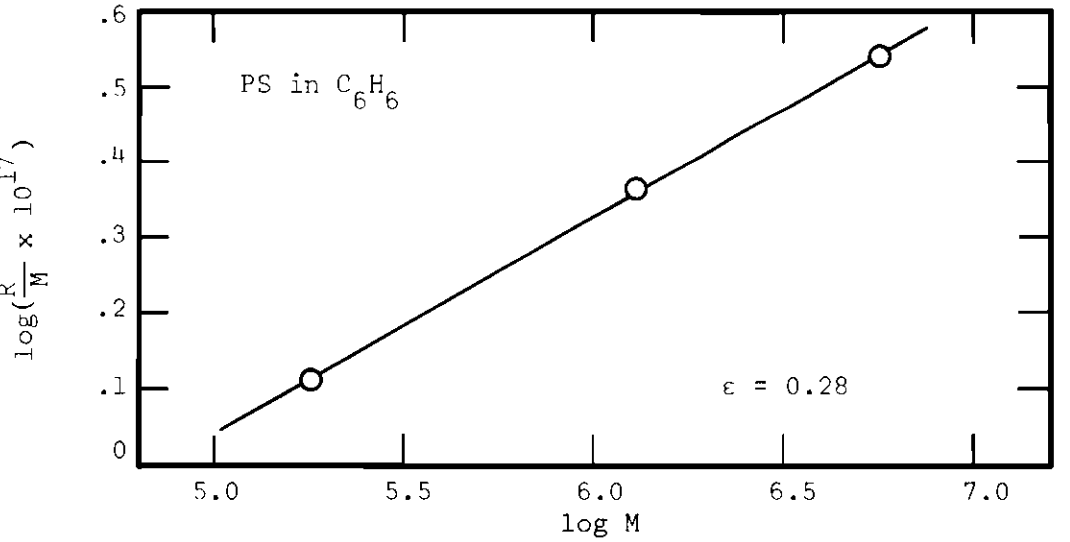

Figure 27. Log-log Plot of R^2/M versus M for PS in Benzene

mathematically accounting for all the possible configurations of the polymers that were studied. Therefore, for the most part the discussion will be limited to an estimation of errors for typical situations.

As it was pointed out early in this chapter, it is convenient to divide the light scattering results according to their dependence on the absolute calibration of the instrument. It is particularly convenient in this section, for the values which do not depend on the absolute calibration are considerably more accurate than those that do.

Calibration-Independent Errors

Perhaps the best place to start in the assessment of random errors is with Equation (25). For the present, attention is called to the three variables which affect the internal consistency of the measurements for a single concentration, that is, $G(\theta)$, V, and θ. The other two quantities, T_f and $G(0)$, are important in relating data for more than one concentration. The simplest of the three variables to discuss is the angle, θ. Because of easy reproducibility of the angular readings, it is felt that failure to turn the photomultiplier housing to the correct angle made negligible contribution to the possible error. There was, however, some uncertainty with regard to the galvanometer readings. If a reading of 6 (out of 10) is taken as a typical reading, normal fluctuations were about $\pm.01$, or about 0.2 per cent uncertainty. Likewise, the measurement of V, which was the ratio of two galvanometer readings, made appreciable contributions to the error; however, because of the fact that V was very carefully determined several times, it is probably accurate to within 0.2 per

cent. Therefore, for those angles which utilized a value of V different from unity, the internal precision of the $c/R'(\theta)$ values for one concentration is on the order of $\pm.4$ per cent; whereas, for the high angles, where V = 1, the internal precision is about $\pm.2$ per cent. Consequently, $\pm.3$ per cent is taken as an average value of the internal precision for solutions. Similar considerations for the solvents, which scattered appreciably less than the solution, leads to a value of $\pm.4$ per cent.

Next, consider the determinations of the excess scattering. Since the ratio of the excess scattered intensity to the total scattered intensity depends upon the refractive increment and concentration of the system in question, it is not surprising to find that in some cases over half of the total scattering was due to the solvent and in other cases the solvent contributed only a few per cent. If it is assumed, as a typical situation, that the scattering of the solvent was 20 per cent of the total, the excess scattering is certain to $\pm.5$ per cent.

Consideration of the reflection correction, which on the average was about 4 per cent of the excess scattering, increases the approximate error negligibly; therefore, the internal consistency of the angular results for one concentration is on the order of 0.5 per cent. This value checks well with the data presented in the Appendix, except in a few cases where dust has appreciable affected the data at low angles.

In order to relate the data for the different concentrations, three more quantities enter the picture, $G(0)$, T_f, and the concentra-

tions. Like the determination of V, much care was given to the measurement of G(0), and thus its uncertainty is estimated to be ±.1 per cent, only half of the possible error for G(θ). Because of the care given to the determination of the filter transmittances and since any error introduced would be systematic rather than random, it is assumed that the uncertainty in T_f is nil. Finally, the concentrations, many of which were determined with a microbalance, probably were accurate to ±.2 per cent. Therefore, an additional 0.3 per cent uncertainty is introduced when the data for more than one concentration are considered, thus making a total uncertainty of about 0.8 per cent.

These conclusions are substantiated by the small extent of scatter in the $[Kc/R(\theta)]_{c=0}$ values, which is usually less than 1 per cent. Further evidence of their validity is given by the average residuals for the least squares extrapolations to zero concentration. In almost all theta systems, the average per cent deviation of the $Kc/R(\theta)$ values from the least squares line (in an absolute sense) was less than 1 per cent; the similar quantity for good solvents (square root plot) was almost always less than 0.5 per cent.

Before determining the quantity of major importance, the radius of gyration, it was first necessary to determine $[c/R'(\theta)]_{c=0}$. In instances where conditions were particularly favorable, moderately high molecular weights and little scatter in the low angle data, it was possible to determine precisely the intercept, perhaps to ±1 or 2 per cent; however, in unfavorable situations the precision was not that good. For example, for a very high molecular weight polymer,

such as PS-III, the intercept is so small that a small absolute uncertainty results in a relatively large percentage uncertainty.

Once the intercept was established, the precision of the value for the radius of gyration depended greatly on the method used for its determination. For systems that were in accordance with the Debye formulation, it was usually possible to determine R to ±.5 per cent, that is, unless the molecular weight was very low. For PS-705 in benzene, for which the data are not shown, the uncertainty was probably more like ±10 per cent. The values of R for the PS-II systems had to be determined from the initial slope; however, since the P^{-1} data exhibited no curvature for the theta system and very little curvature for the other, the uncertainty was probably less than that normally encountered (86).

In summary, then, the $Kc/R(\theta)$ values are probably precise to less than 1 per cent and the extrapolated values to about 1 per cent. Assuming that for a given set of data the uncertainty in determining the intercept is about 1.5 per cent, the total uncertainty in the intercept is about 2.5 per cent. Therefore, for the system in which it was possible to use the Debye equation to fit the data over the entire angular range, the values of R are probably certain to ±3 per cent (compare reference (42)). This should be compared to the lower limit of ±5 per cent which is usually given when the initial tangent method is used (86).

One exception to the above considerations, PDMS-III in CCl_4, should be noted. Reference to Figure 51 in the Appendix will show that the data seem to converge too rapidly at the high angles. It appears

that the slope of the lowest concentration is inconsistently high. The reason is not known, but this does account for the surprisingly high value of R and low value of Φ.

Finally, a few remarks should be made about the accuracy of the reported temperatures. For the good solvent systems, the air bath was monitored continually and kept to within $\pm.5^{o}C$. For the theta systems, using the jacket resulted in an uncertainty at $\pm.05^{o}C$. Neither of these variations was large enough to cause appreciable error in the measured intensities.

Calibration-Dependent Errors

Even though the uncertainty in $[c/R'(\theta)]_{c=0}$ is about 2.5 per cent, it is considerably greater in the value of $[Kc/R(\theta)]_{\substack{c=0 \\ \theta=0}}$ and, therefore, in the molecular weight.

The principal uncertainty in the calculation of the optical constant, K, is in the value of the refractive increment, which for most cases was probably accurate to ± 2 per cent; however, because of the small value of dn/dc for PDMS in CCl_4, the error estimate for that system probably should be somewhat higher. Thus, since K is proportional to the square of dn/dc, the uncertainty in K is about ± 4 per cent.

Two other possible errors were introduced in the actual calibration (see Equation (29)). Rayleigh's ratio for benzene, especially for the two largest wave lengths, is probably accurate to within 1 per cent; and, in keeping with the earlier discussion on the R' values, $R_b'(90)$ is also certain to within 1 per cent. In those systems for which a refractive index correction was necessary, a possible systematic error was

introduced; but, since the true correction is not known, uncertainty is neglected in the analysis. Collecting the possible errors, the molecular weights appear to be certain to ±8 per cent.

The possible error in A_2 is easily seen by its relation to the Γ_2 in Equation (40): $A_2 = \Gamma_2/M$. Since the uncertainty in Γ_2, given the intercept, is on the order of 1 per cent, the A_2 values are probably certain to ±9 per cent.

It is seen from Table 4 that the approximate uncertainties in the determined quantities are sufficiently large to account for any apparent discrepancies in the R^2/M and Φ values. They cannot, however, account for some of the discrepancies between the values of M_w and M_v (see Table 2). Since any constructive comments would necessitate an error analysis of the literature values of the Mark-Houwink parameters, let it simply be said that in some cases the parameters may be wrong. For example, since benzene is a poorer solvent for PDMS than is carbon tetrachloride, its $\underline{a}$ value for PDMS should be lower, not higher than 0.63. Furthermore, some of the parameters were determined under experimental conditions slightly different from those in which they were used.

CHAPTER V

CONCLUSIONS

1. Even in light of the refinements of the Isihara treatment (19), it is still correct to use the Debye scattering function for theta solvents; for, in all cases of practical interest for visible light scattering, the two functions are experimentally indistinguishable.

2. As long as the molecular weight of flexible polymers does not exceed a few million, the value of ε required to fit the data by the Ptitsyn function is essentially zero; therefore, the simpler Debye function may be used. If the sample is polydisperse, the considerations of Benoit (37) may be applied.

3. When the molecular weight exceeds a few million, it is no longer valid to use the Debye approximation; neither, however, is it valid to use the Ptitsyn equation with *a priori* values of ε calculated from the Mark-Houwink exponent. Presumably because of the failure to allow for the molecular weight dependence of ε, the Ptitsyn treatment overestimates the extent of the non-uniform expansion of the coil, and lower values of ε are required to give a good fit. Additional experimental work for very high molecular weight, monodisperse polymers in good solvents will be required to ascertain quantitatively the extent of the overestimation.

4. As it was pointed out by other workers (42), a knowledge of

the scattering function permits the radius of gyration to be determined by a best fit of the data over the entire angular range. Since the values determined by this method are considerably more precise than those determined by the estimation of the initial tangent, the method should be used whenever the Debye function is known to apply.

APPENDIX

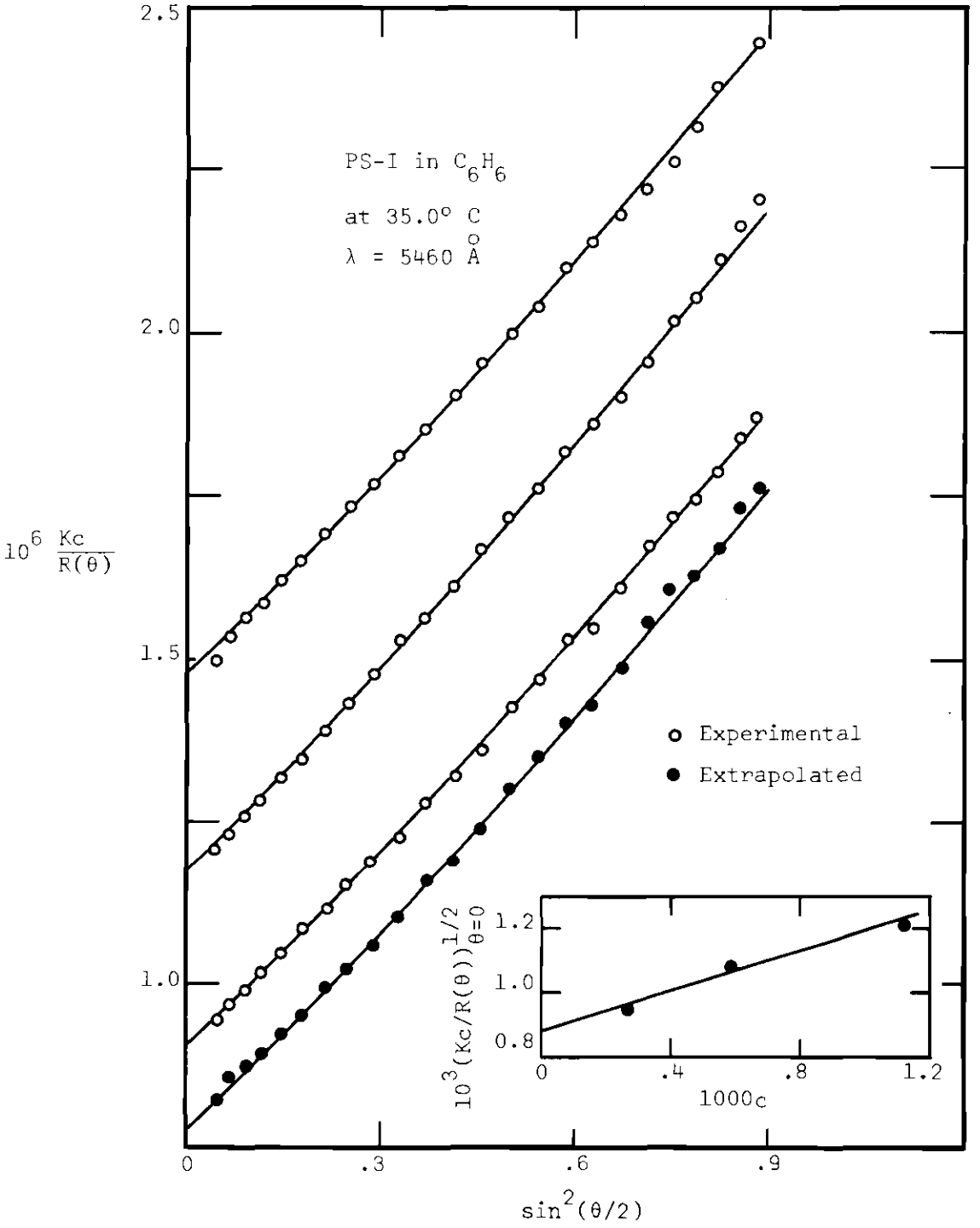

Figure 28. Scattering Data for $PS_{\bar{o}}I$ in Benzene at 35.0°C. λ = 5460Å

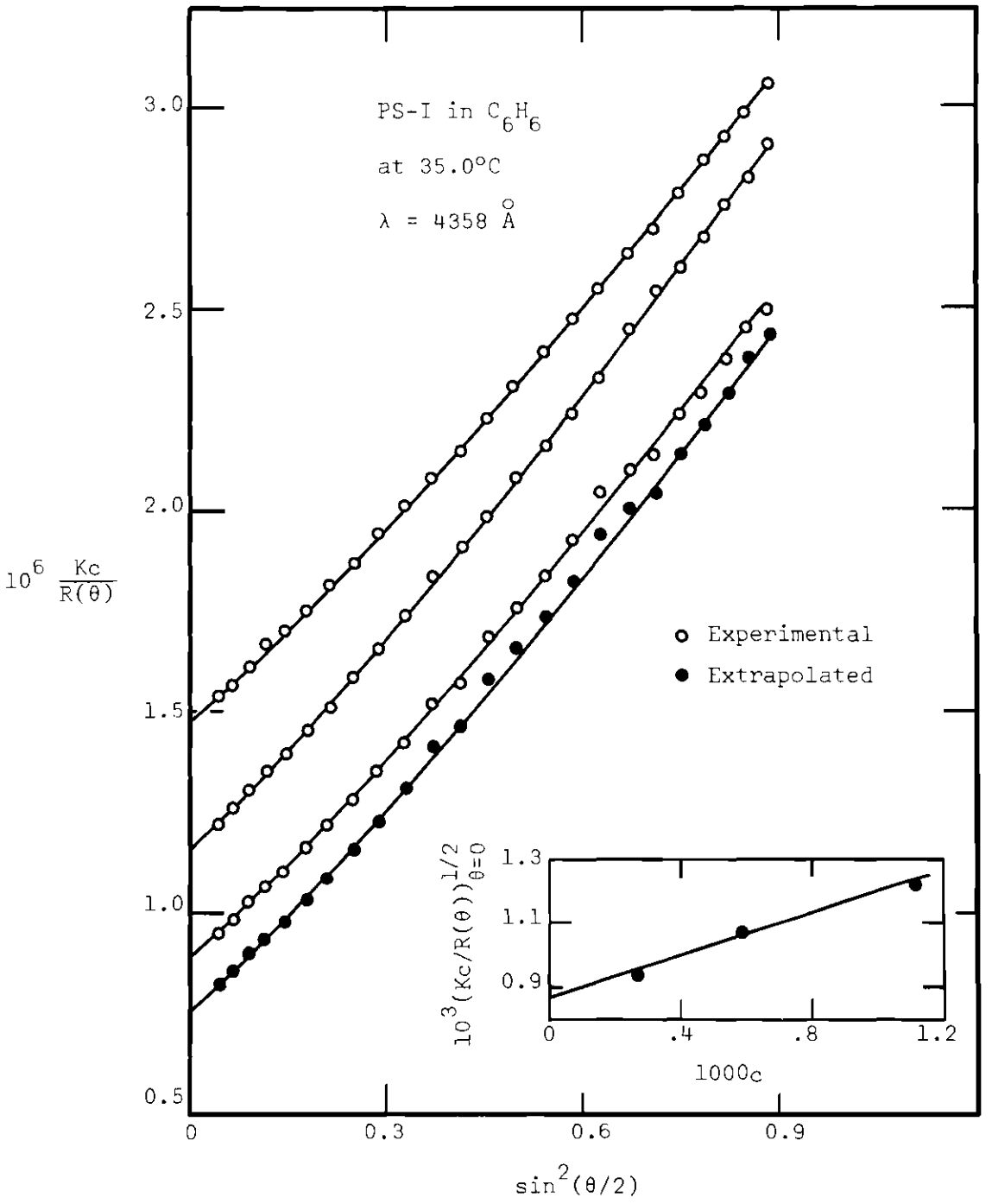

Figure 29. Scattering Data for PS-I in Benzene at 35.0°C. λ = 4358 Å

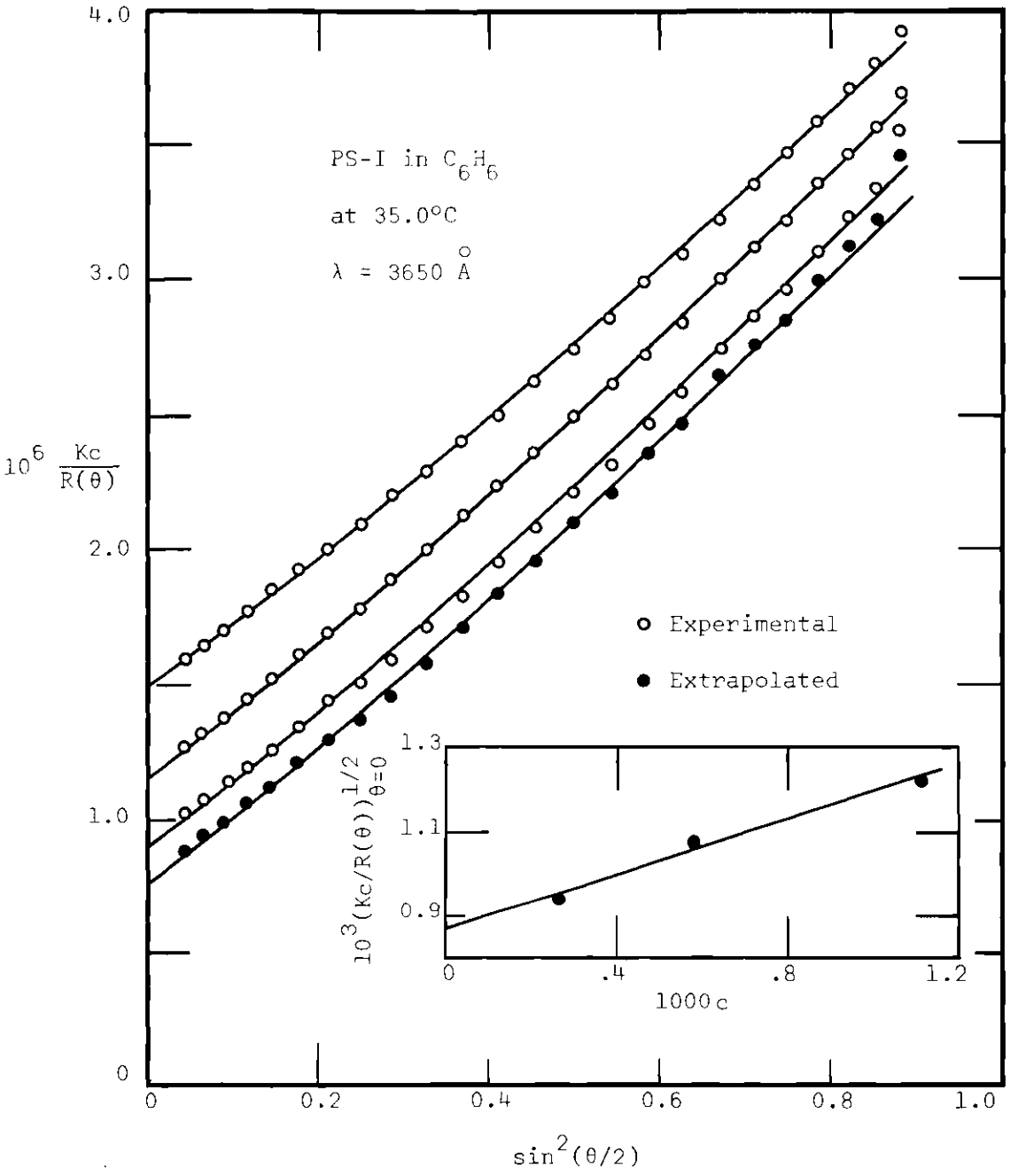

Figure 30. Scattering Data for PS-I in Benzene at 35.0°C. λ = 3650 Å

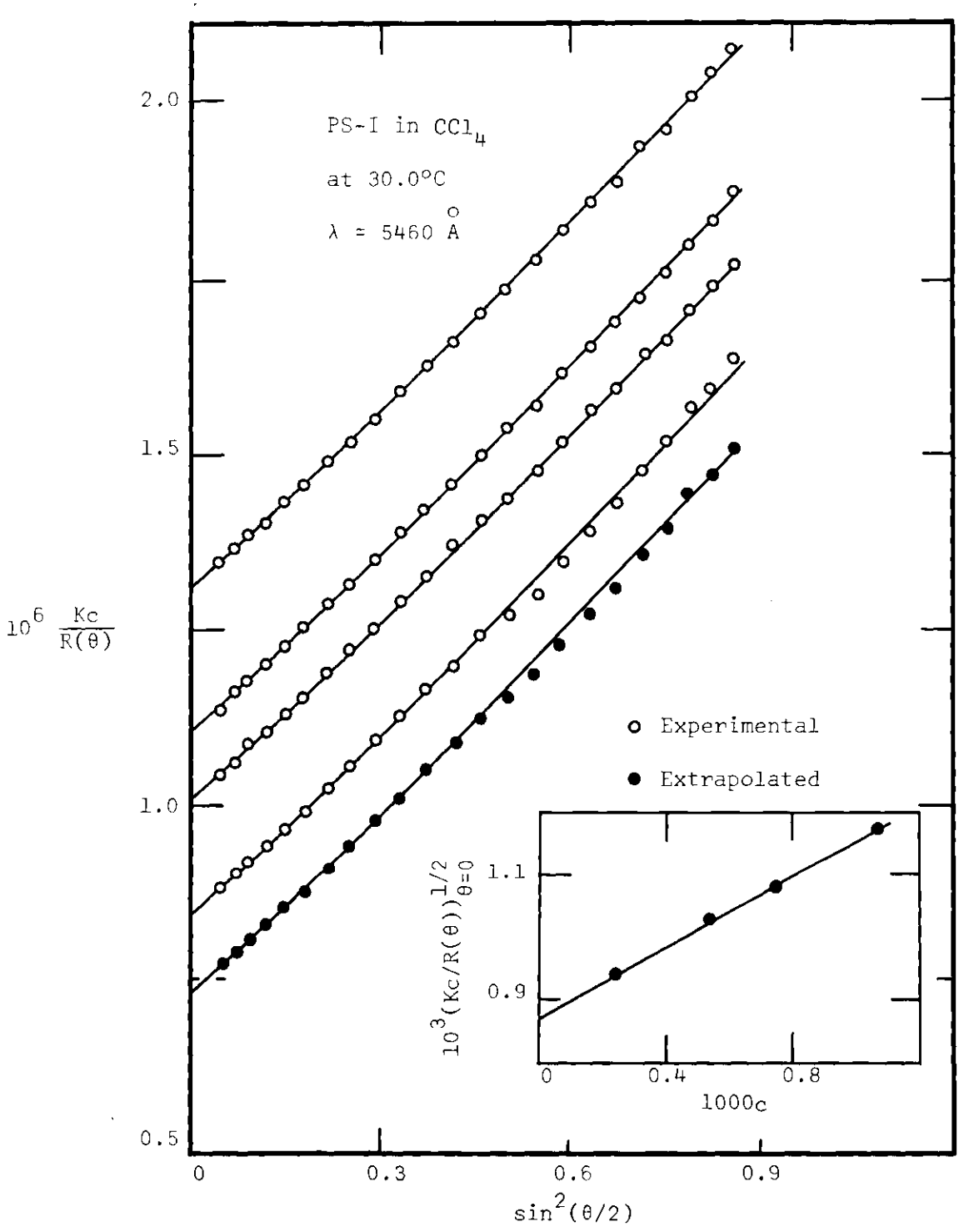

Figure 31. Scattering Data for PS-I in Carbon Tetrachloride at 30.0°C. λ = 5460 Å

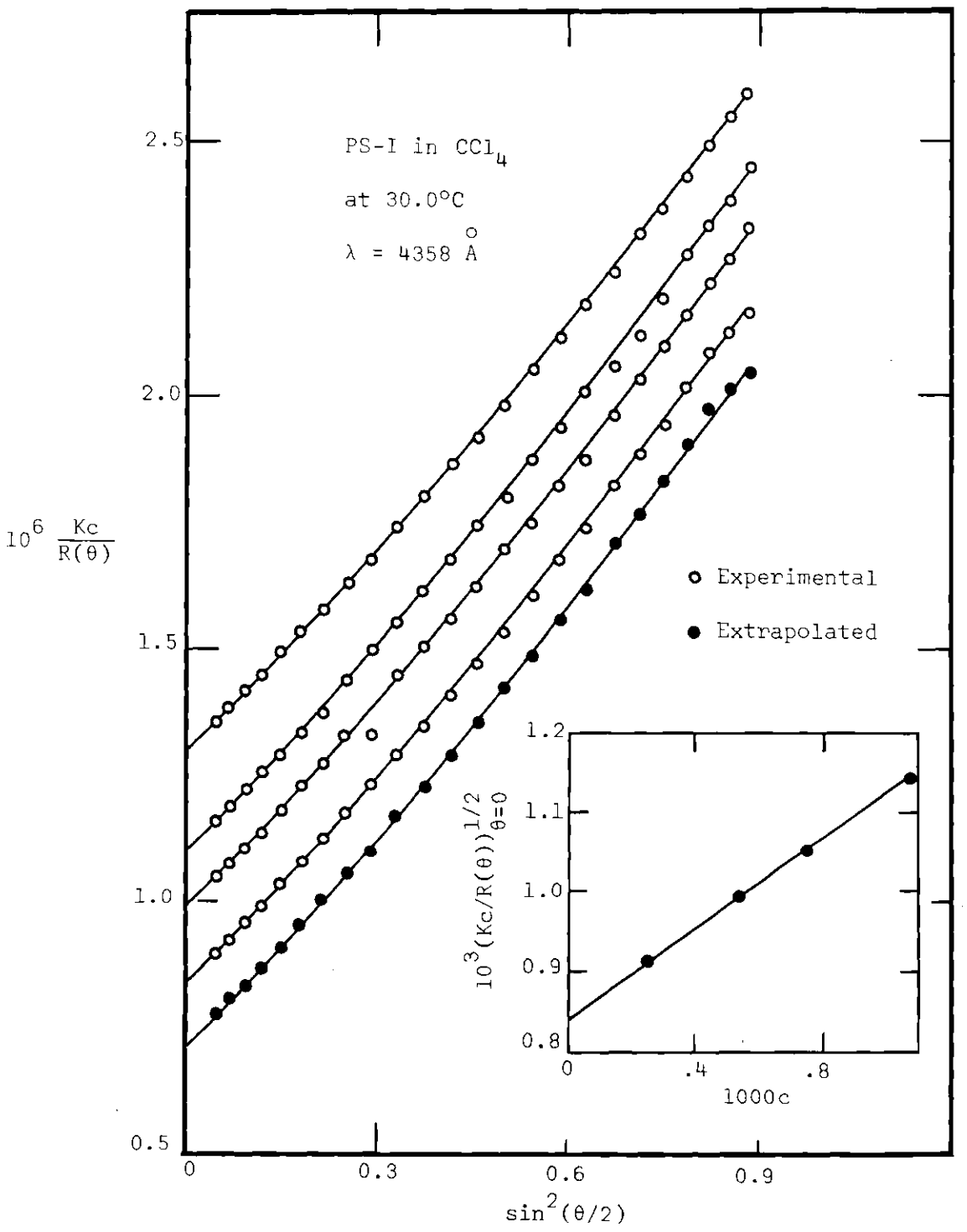

Figure 32. Scattering Data for PS-I in Carbon Tetrachloride at 30.0°C. λ = 4358 Å

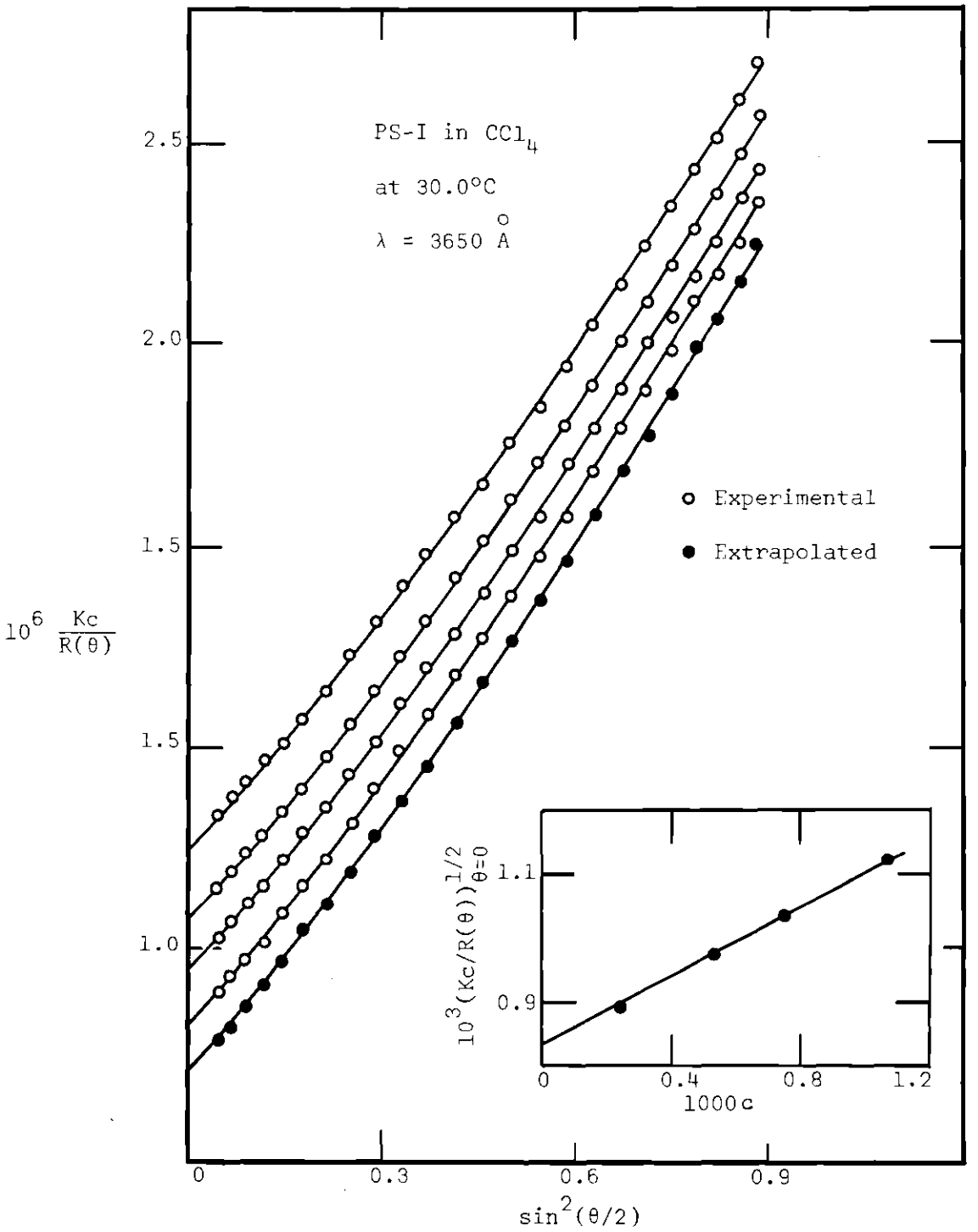

Figure 33. Scattering Data for PS-I in Carbon Tetrachloride at 30.0°C. λ = 3650 Å

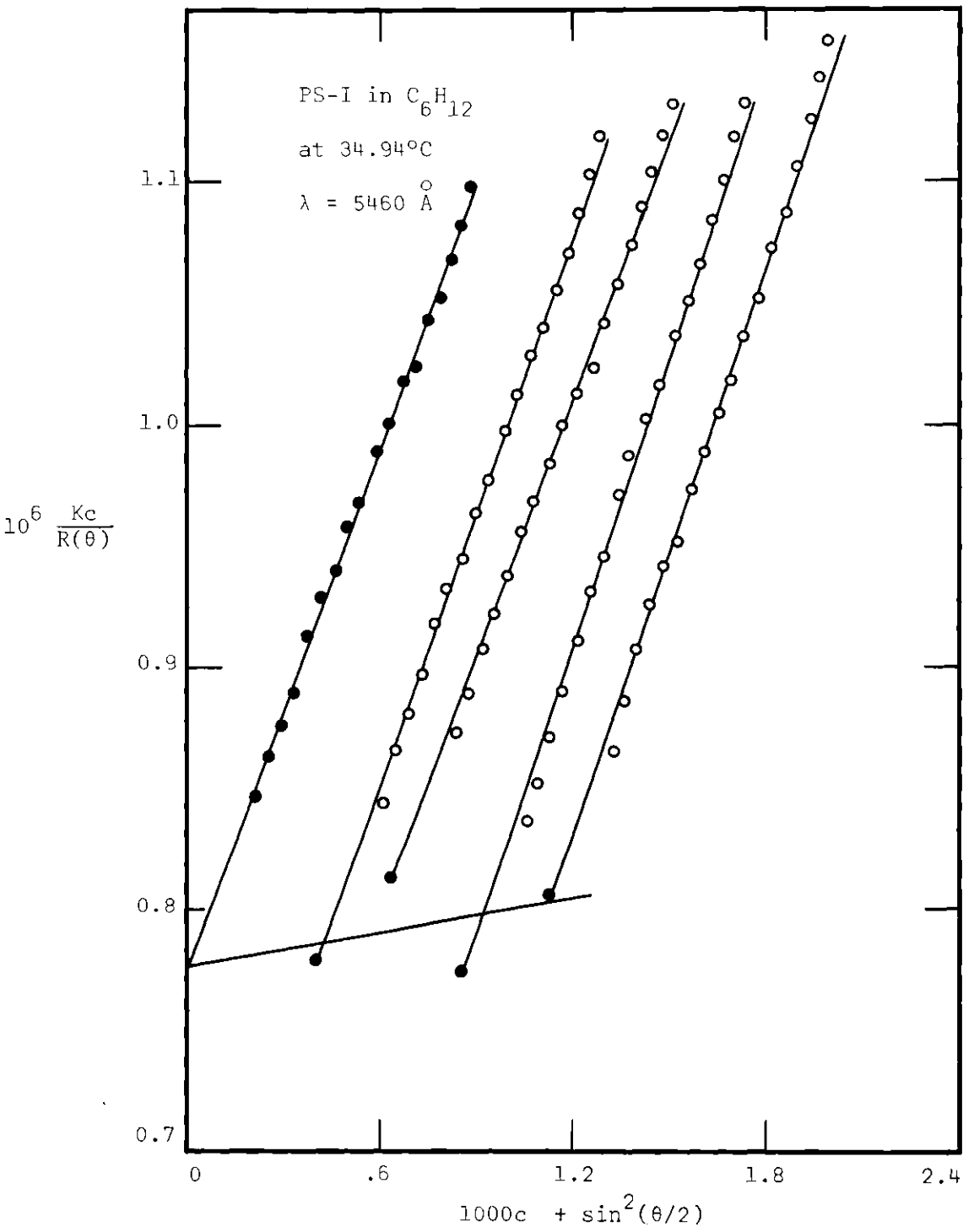

Figure 34. Scattering Data for PS-I in Cyclohexane at 34.94°C. λ = 5460 Å

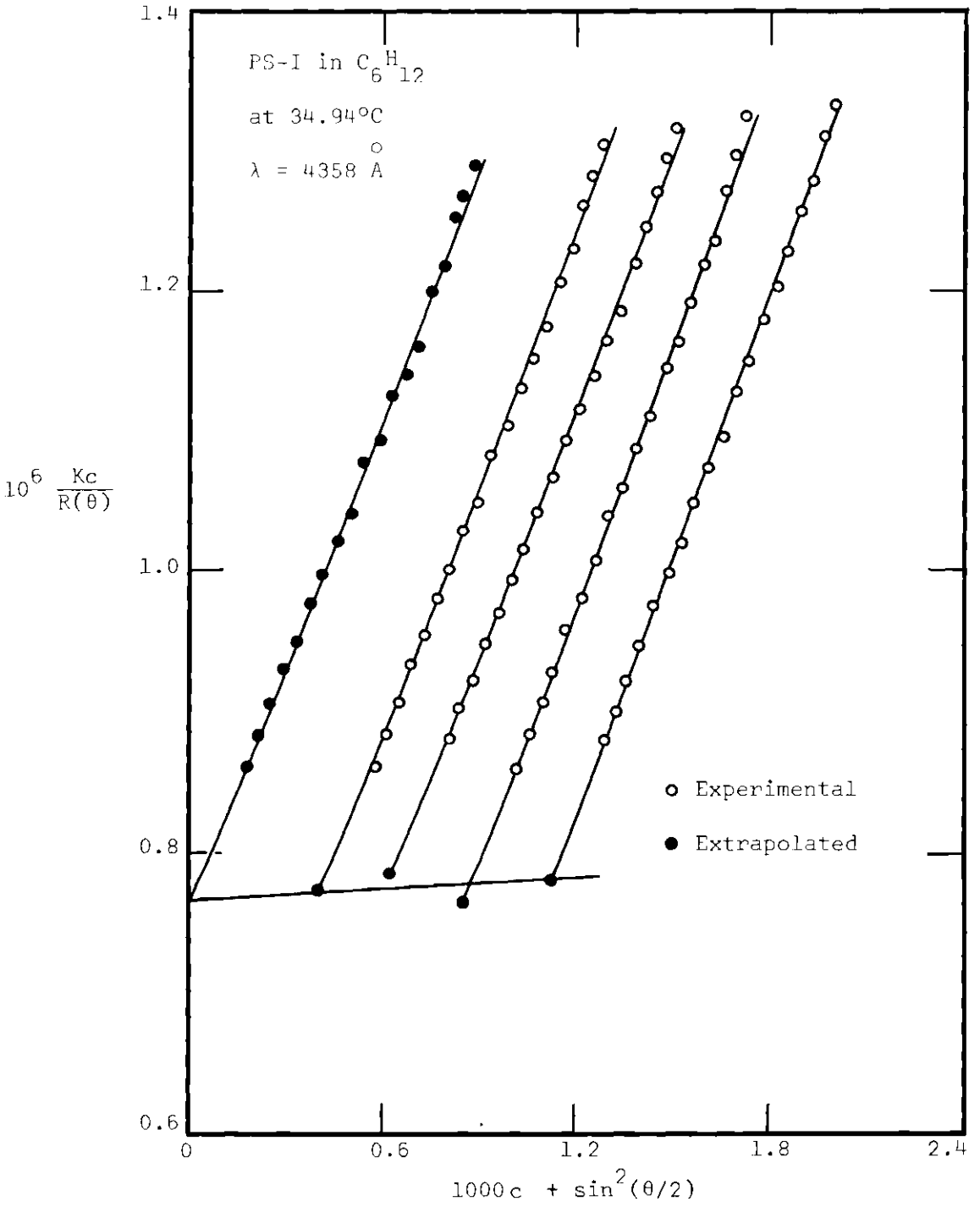

Figure 35. Scattering Data for PS-I in Cyclohexane at 34.94°C. λ = 4358 Å

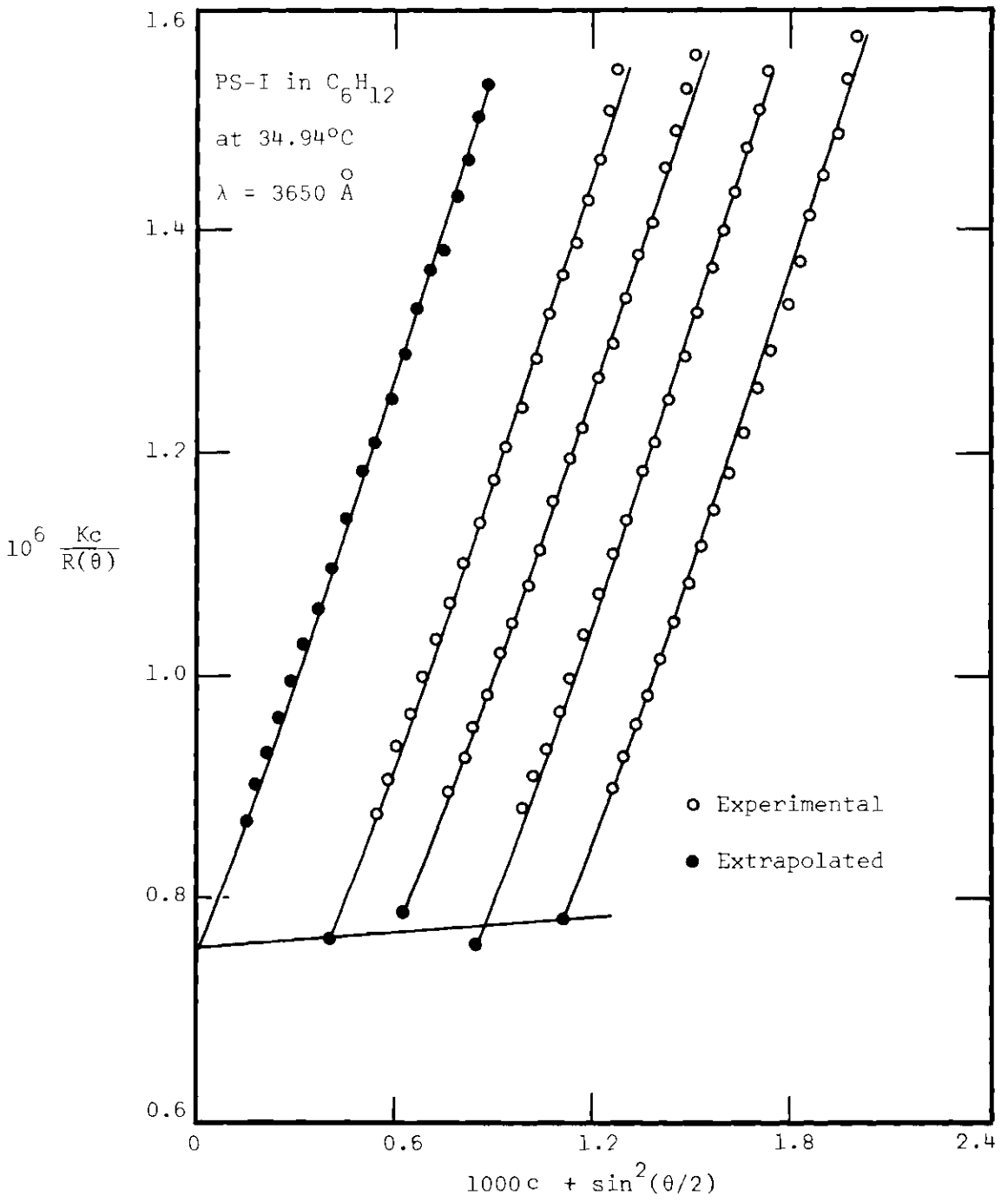

Figure 36. Scattering Data for PS-I in Cyclohexane at 34.94°C. λ = 3650 Å

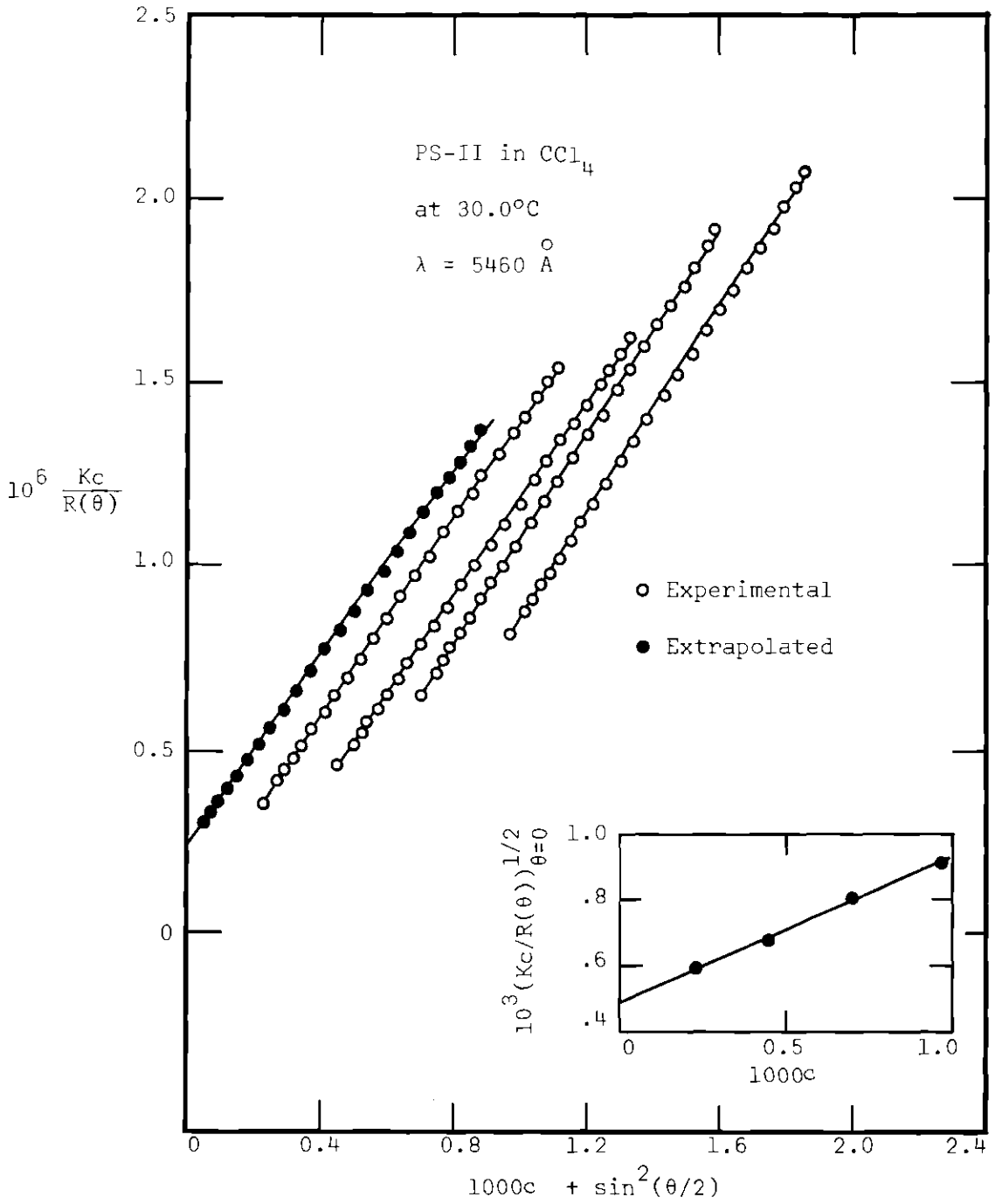

Figure 37. Scattering Data for PS-II in Carbon Tetrachloride at 30.0°C. λ = 5460 Å

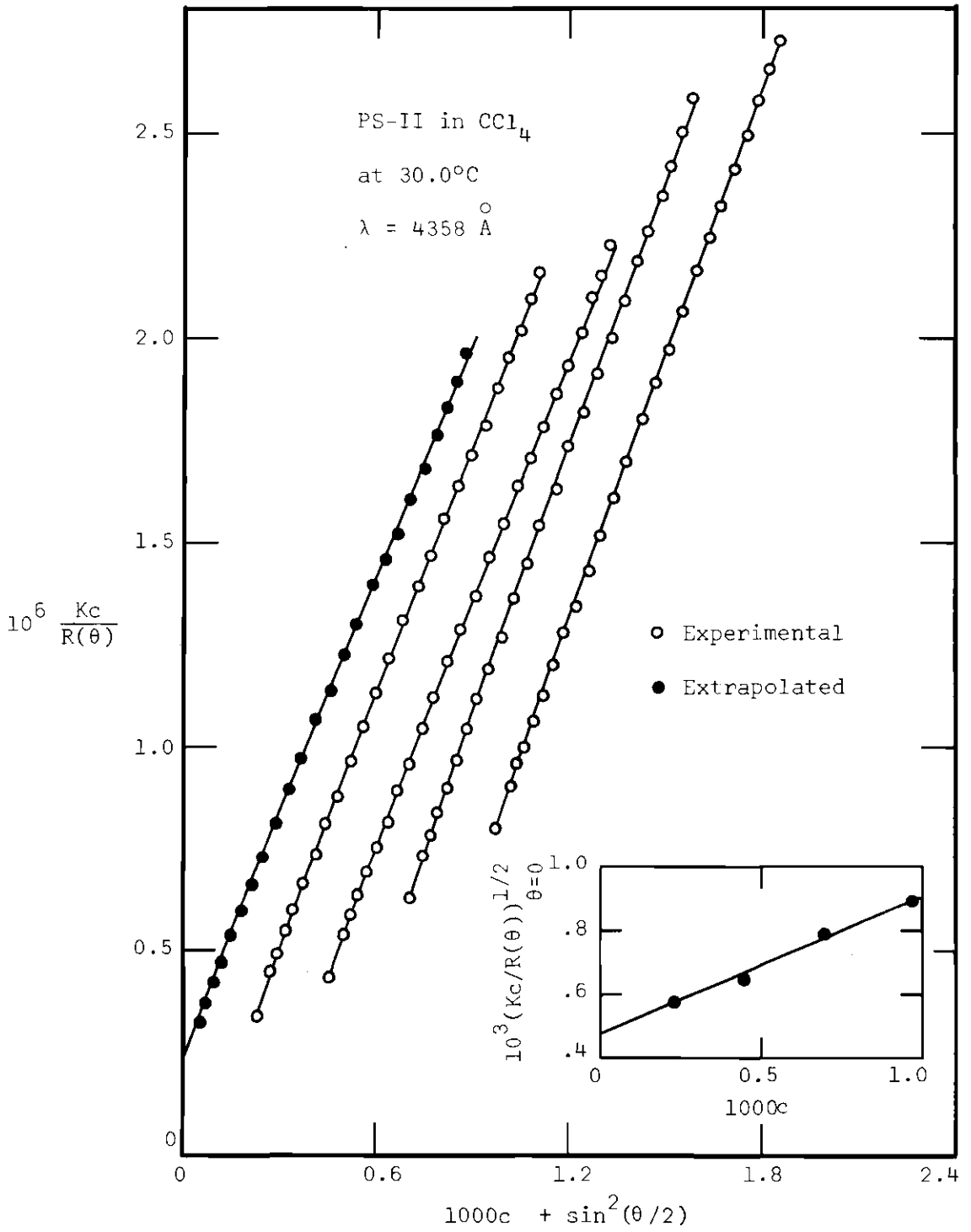

Figure 38. Scattering Data for PS-II in Carbon Tetrachloride at 30.0°C. λ = 4358 Å

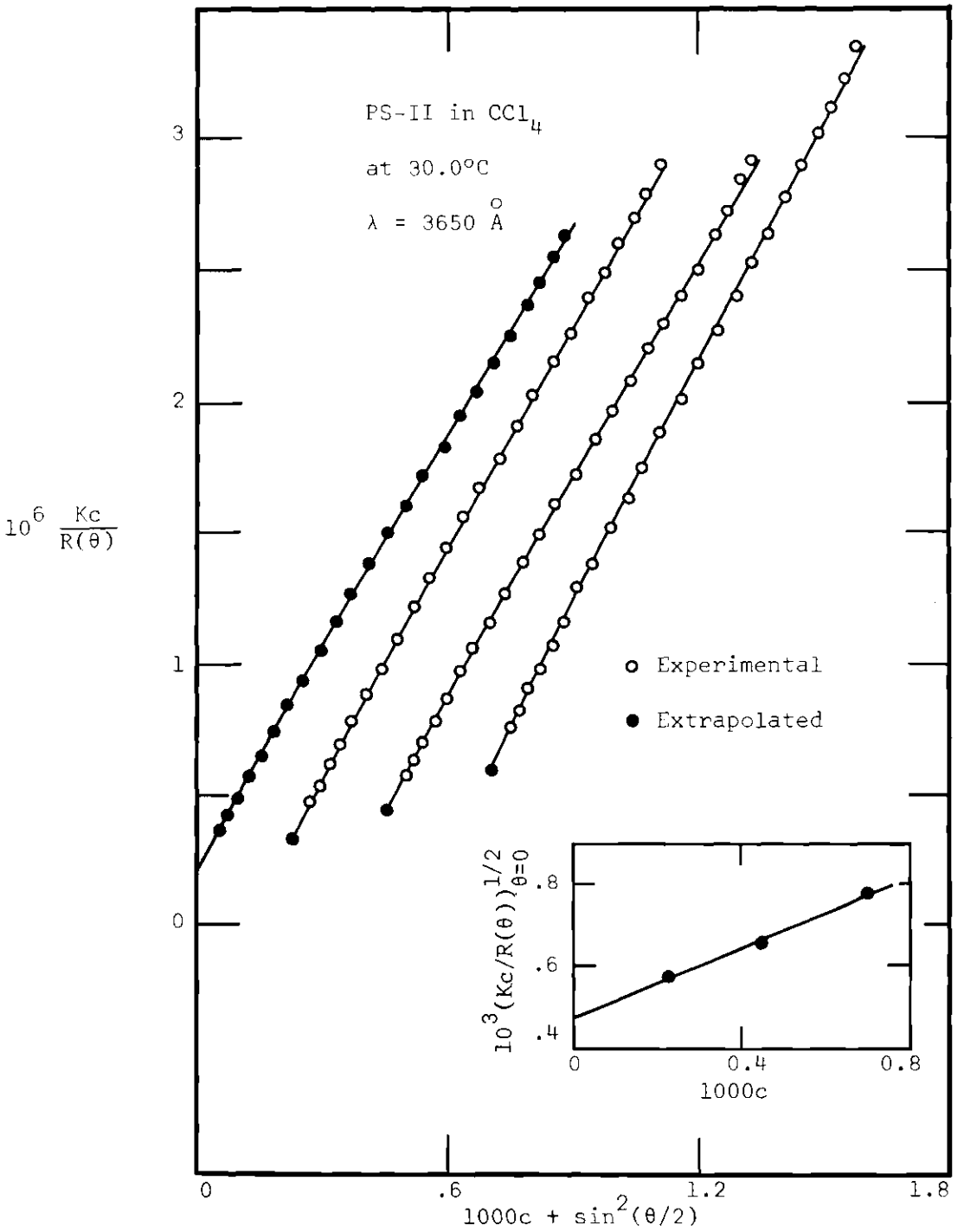

Figure 39. Scattering Data for PS-II in Carbon Tetrachloride at 30.0°C. λ = 3650 Å

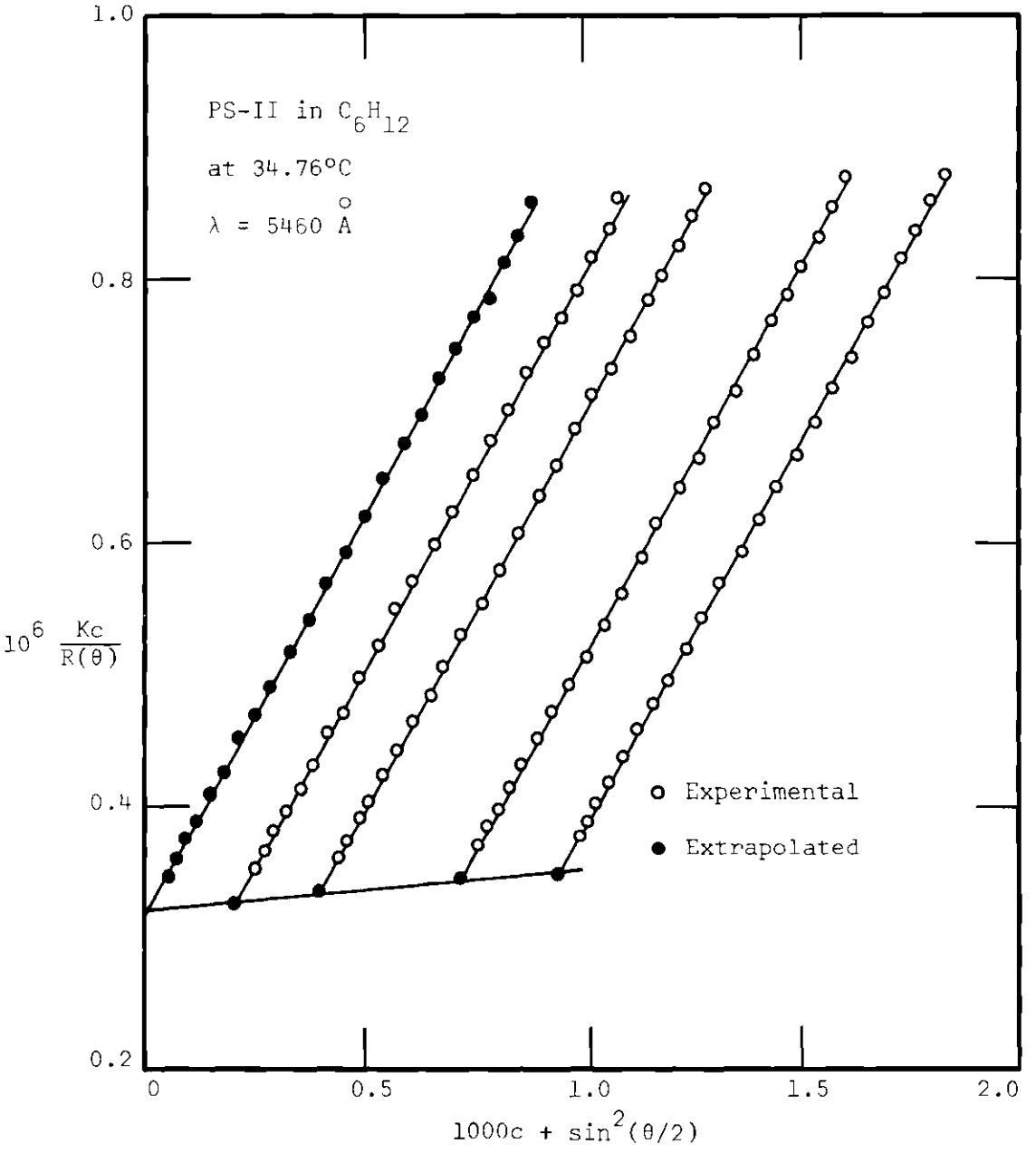

Figure 40. Scattering Data for PS-II in Cyclohexane at 34.76°C. λ = 5460 Å

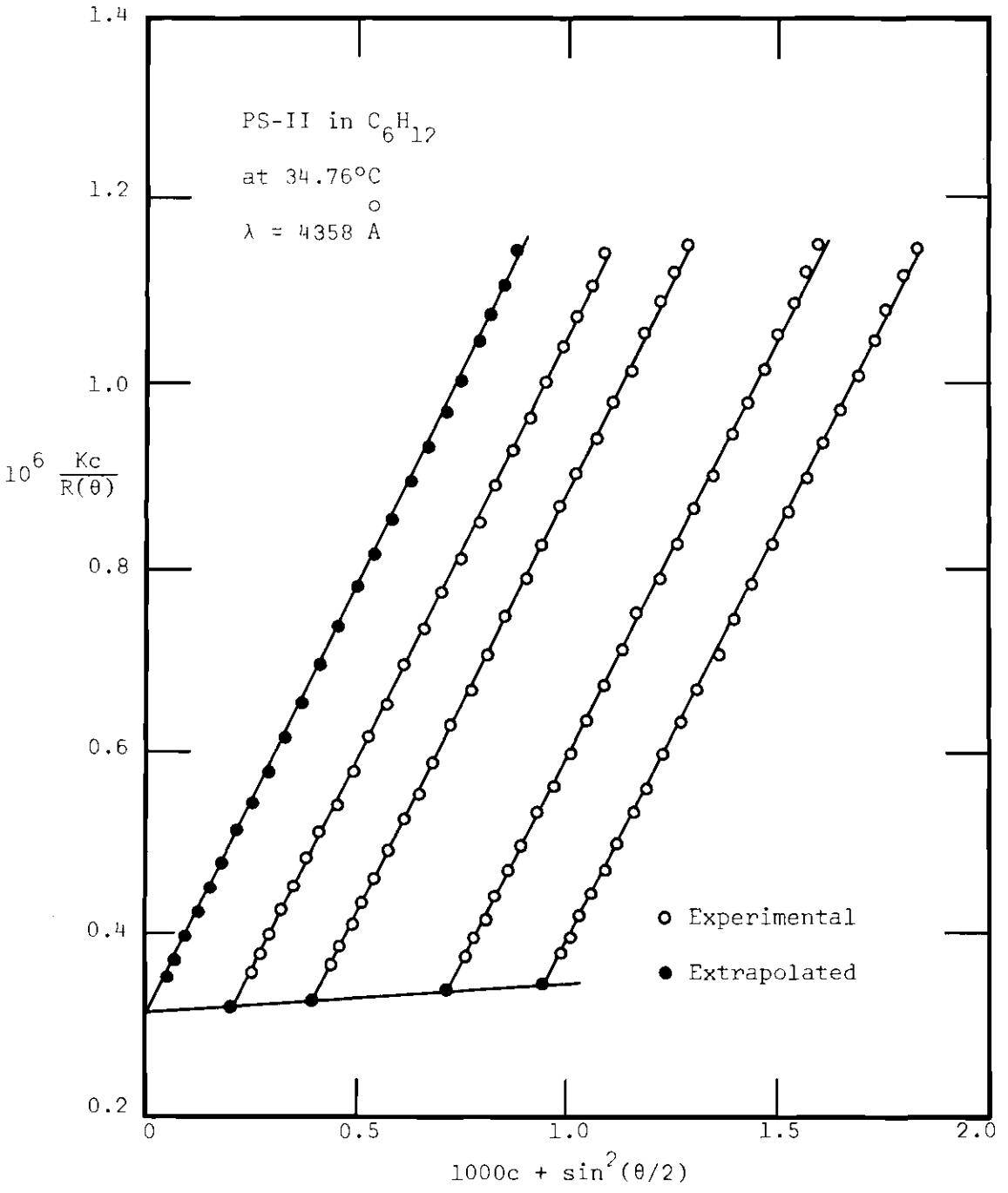

Figure 41. Scattering Data for PS-II in Cyclohexane at 34.76°C. λ = 4358 Å

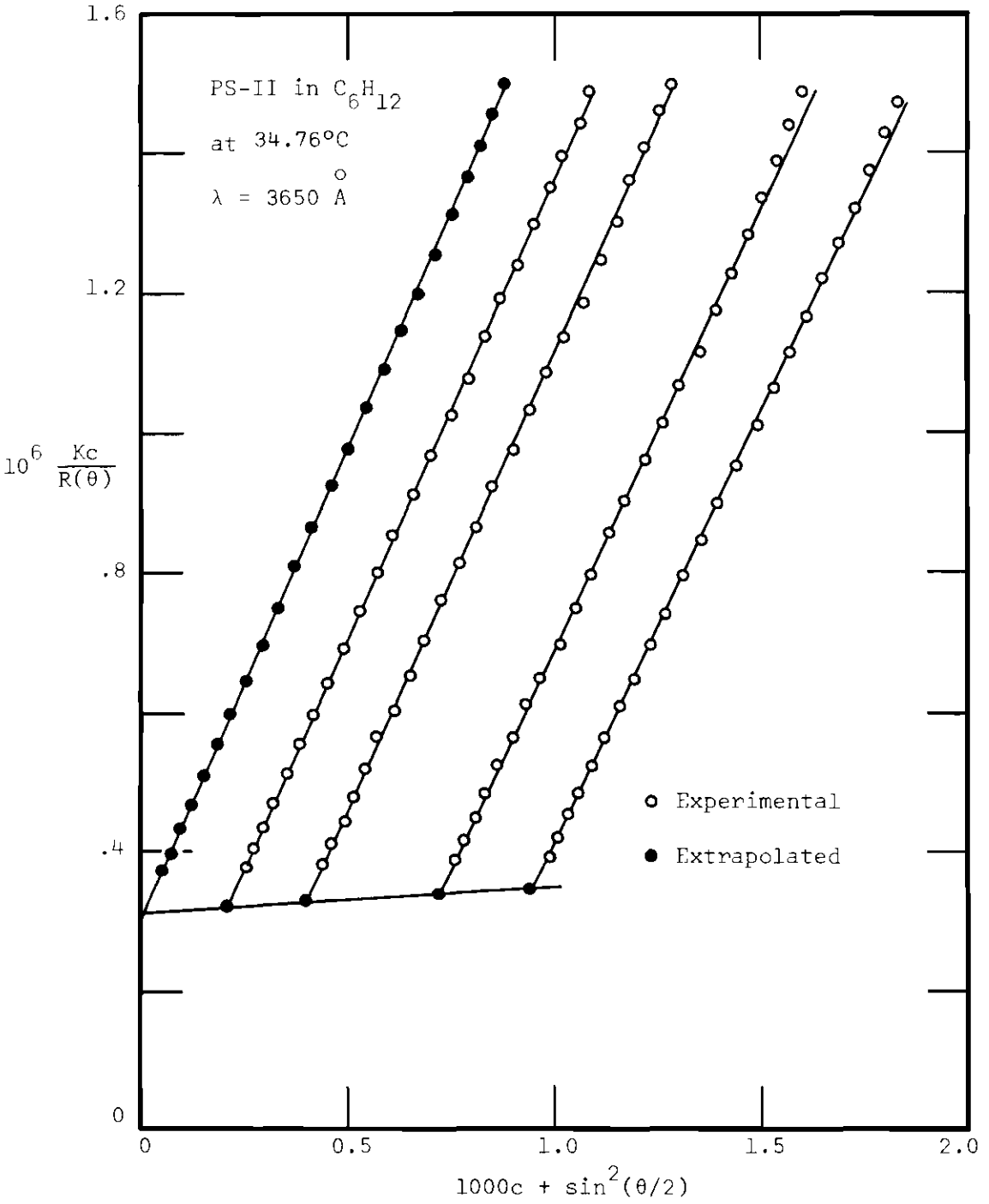

Figure 42. Scattering Data for PS-II in Cyclohexane at 34.76°C. λ = 3650 Å

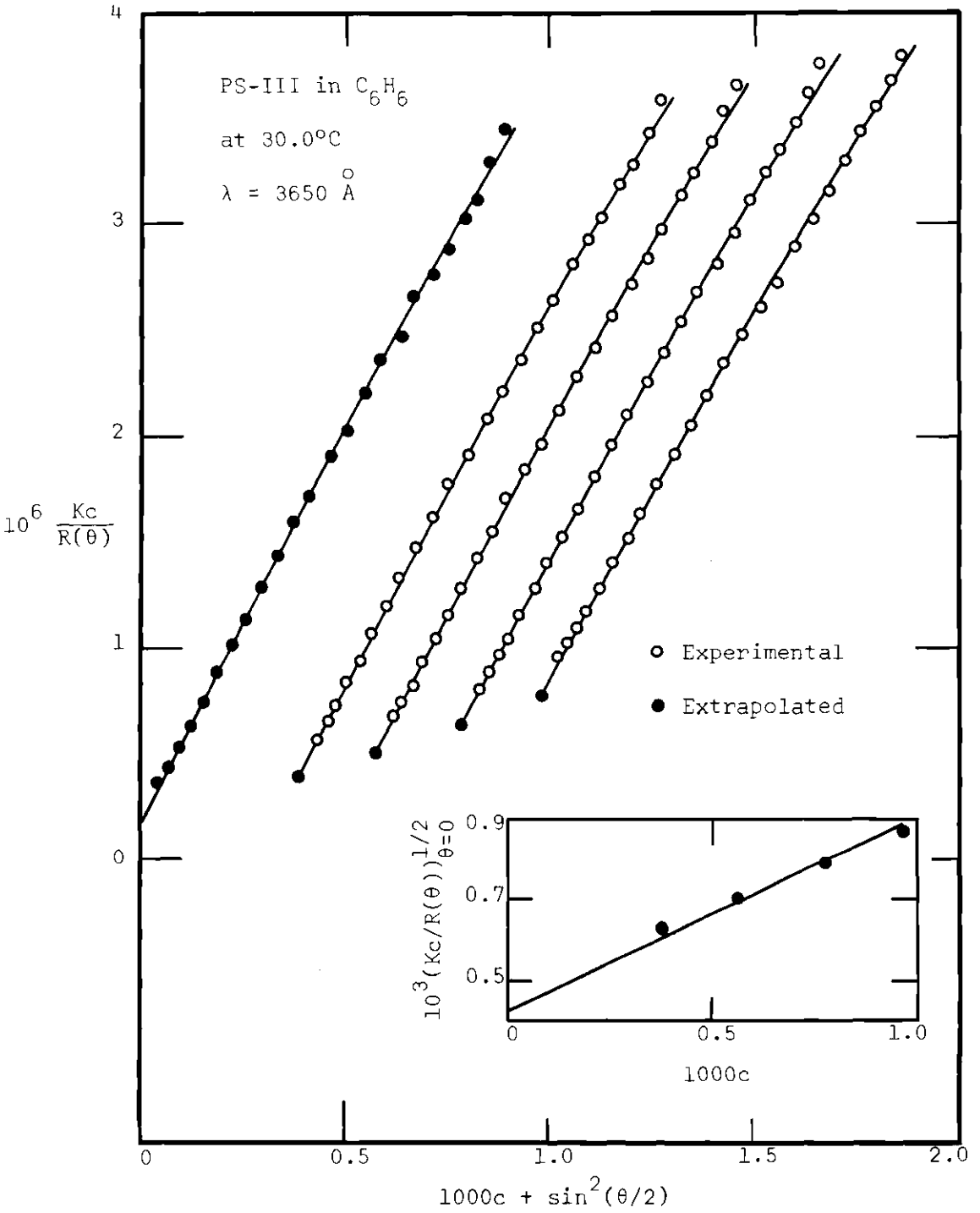

Figure 43. Scattering Data for PS-III in Benzene at 30.0°C.
λ = 3650 Å

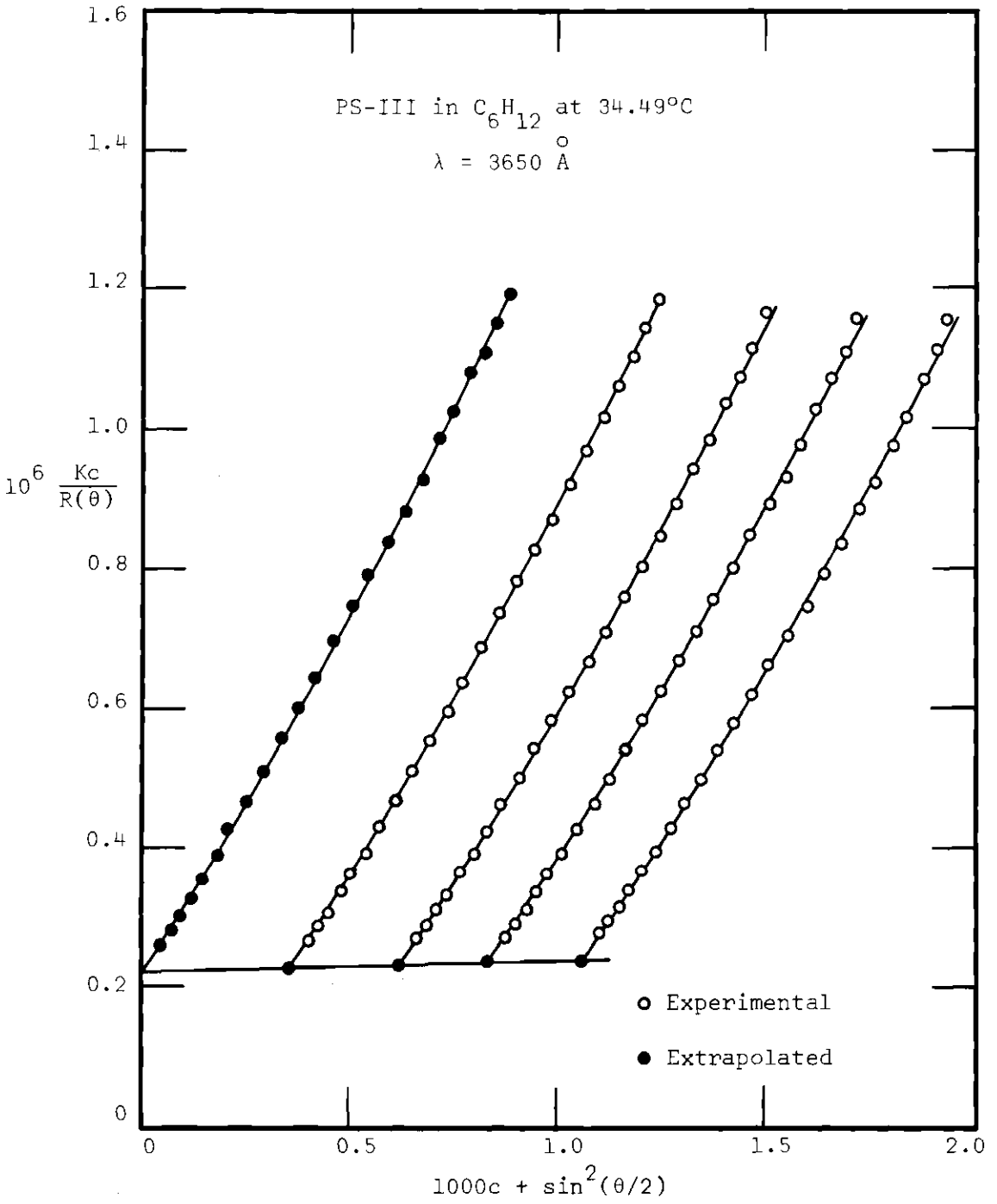

Figure 44. Scattering Data for PS-III in Cyclohexane at 34.49°C. λ = 3650 Å

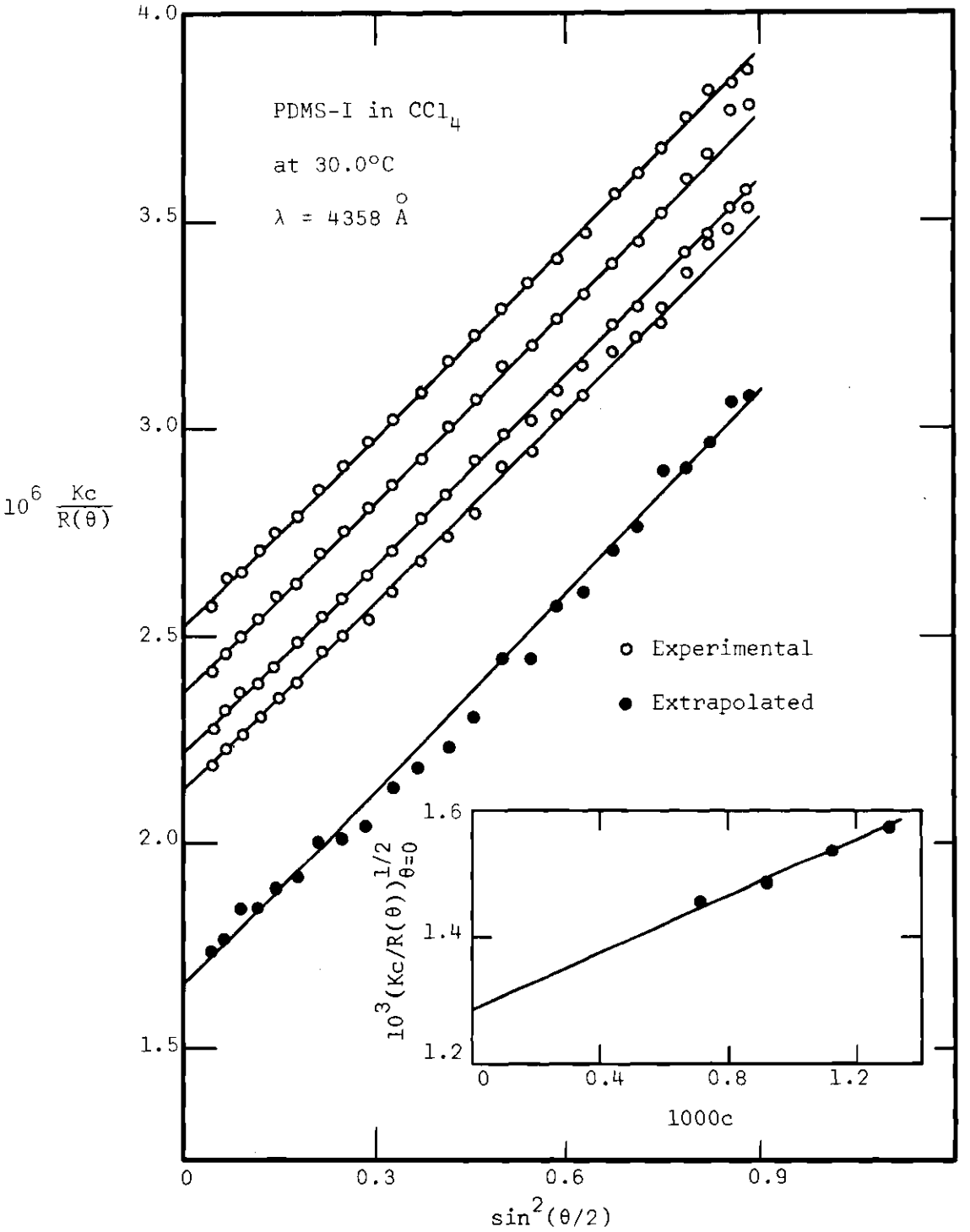

Figure 45. Scattering Data for PDMS-I in Carbon Tetrachloride at 30.0°C. λ = 4358 Å

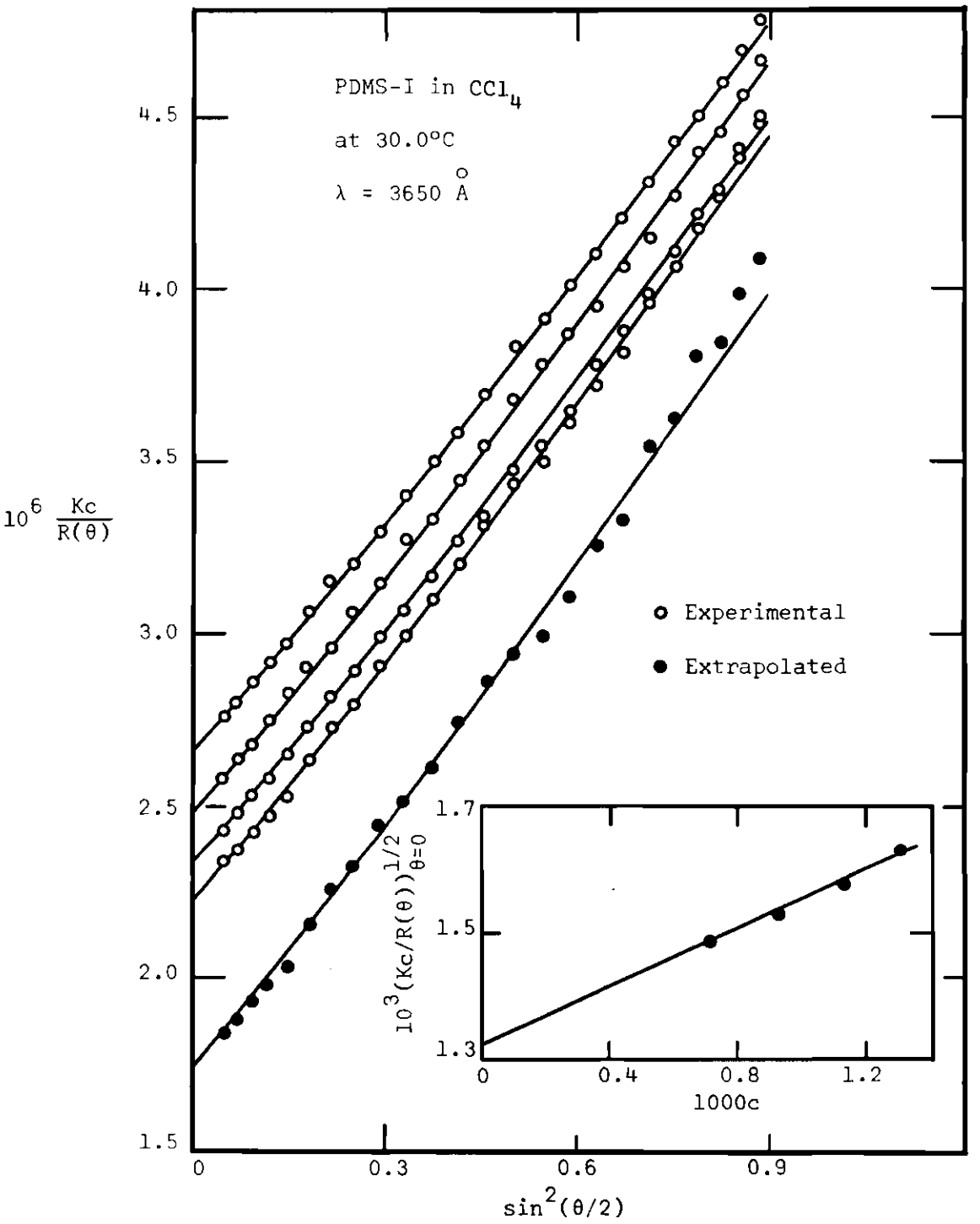

Figure 46. Scattering Data for PDMS-I in Carbon Tetrachloride at 30.0°C. λ = 3650 Å

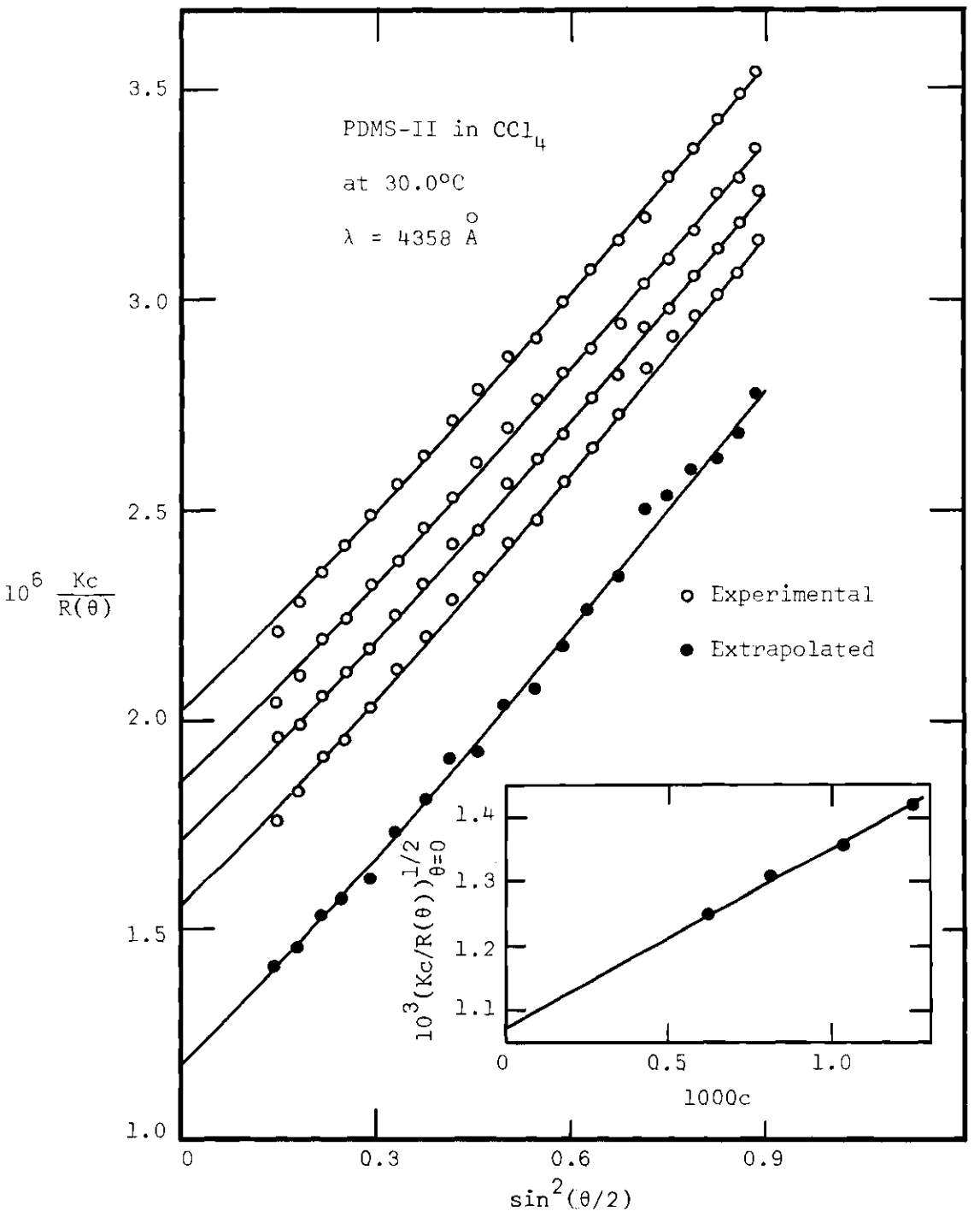

Figure 47. Scattering Data for PDMS-II in Carbon Tetrachloride at 30.0°C. λ = 4358 Å

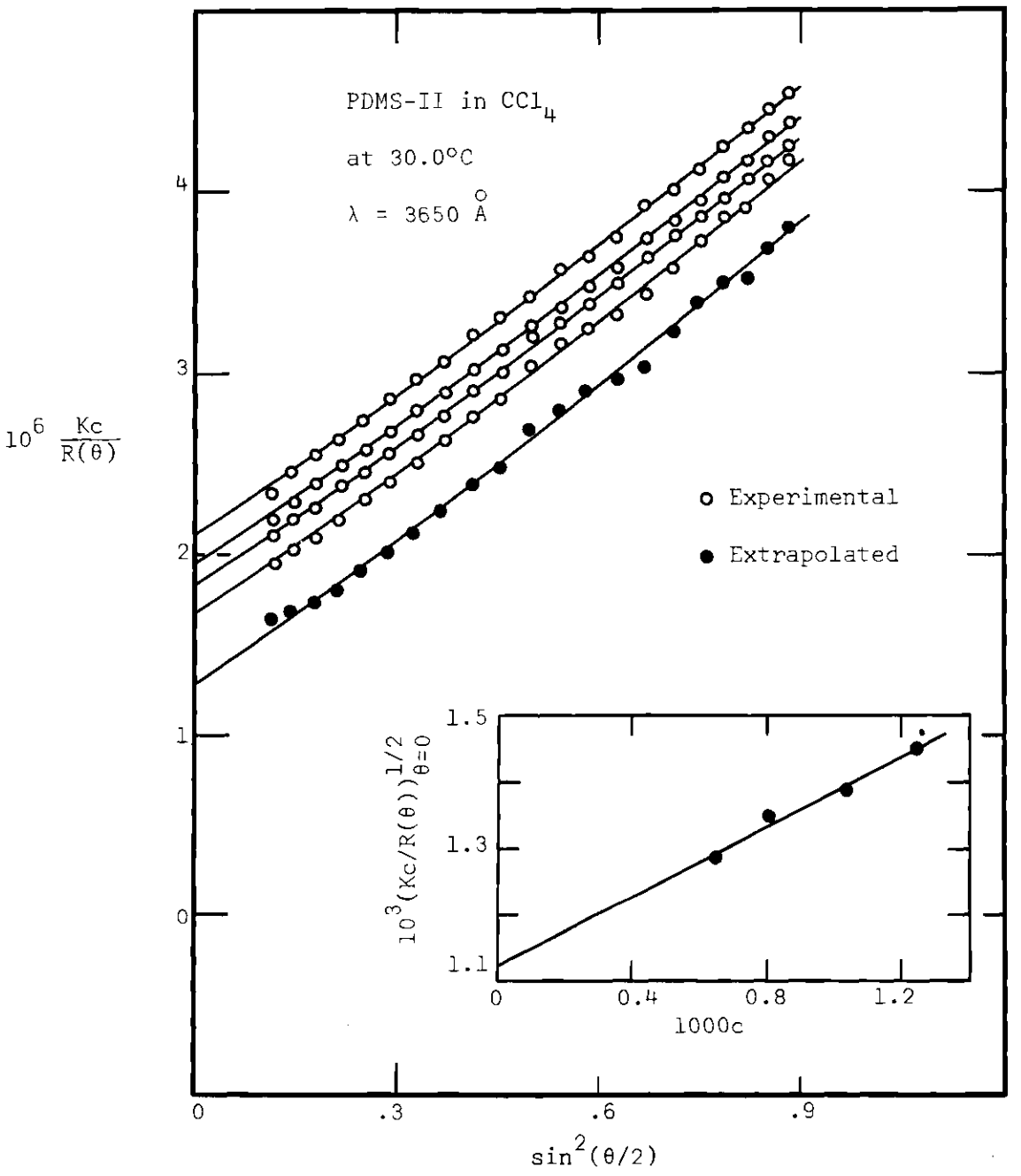

Figure 48. Scattering Data for PDMS-II in Carbon Tetrachloride at 30.0°C. λ = 3650 Å

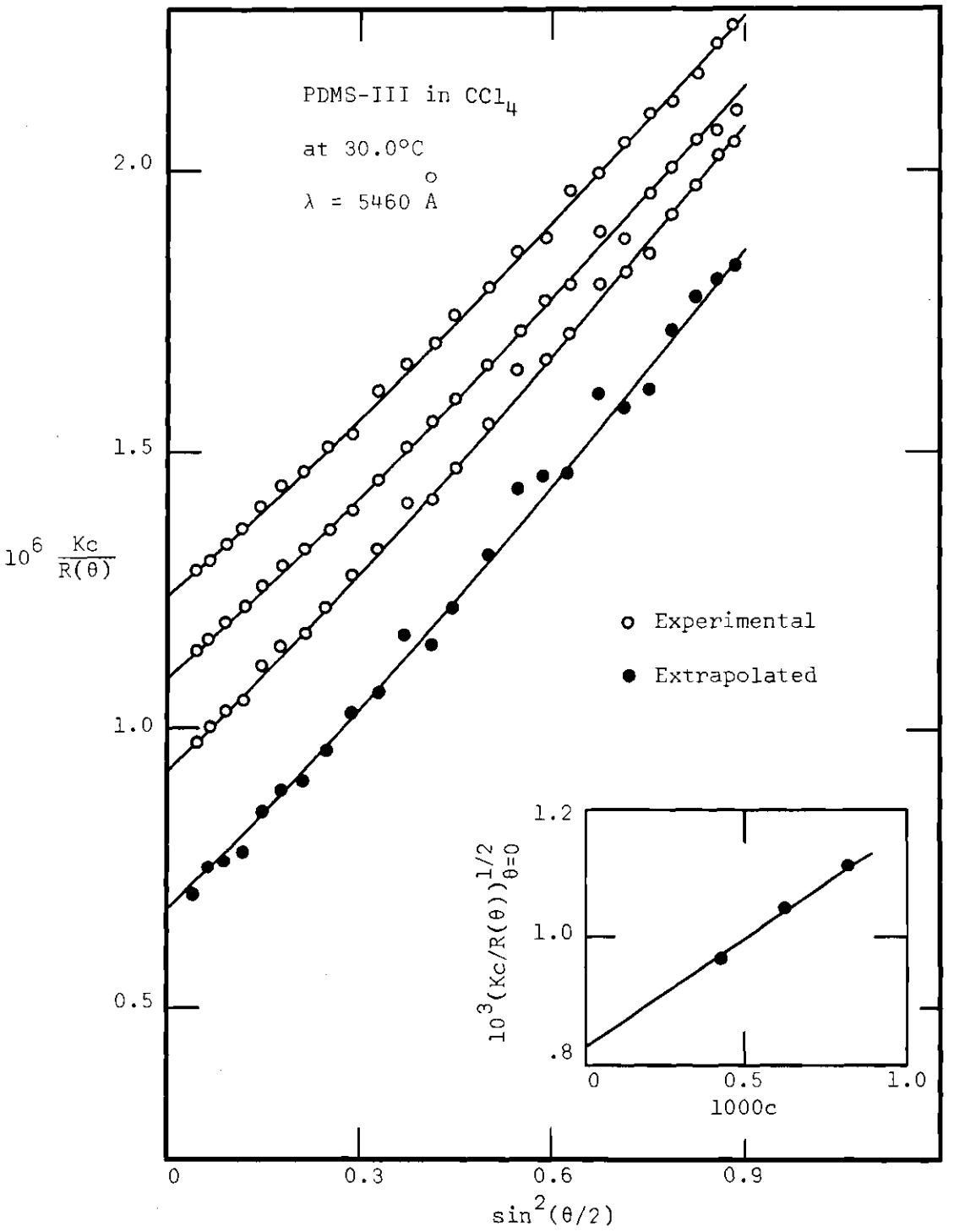

Figure 49. Scattering Data for PDMS-III in Carbon Tetrachloride at 30.0°C. λ = 5460 Å

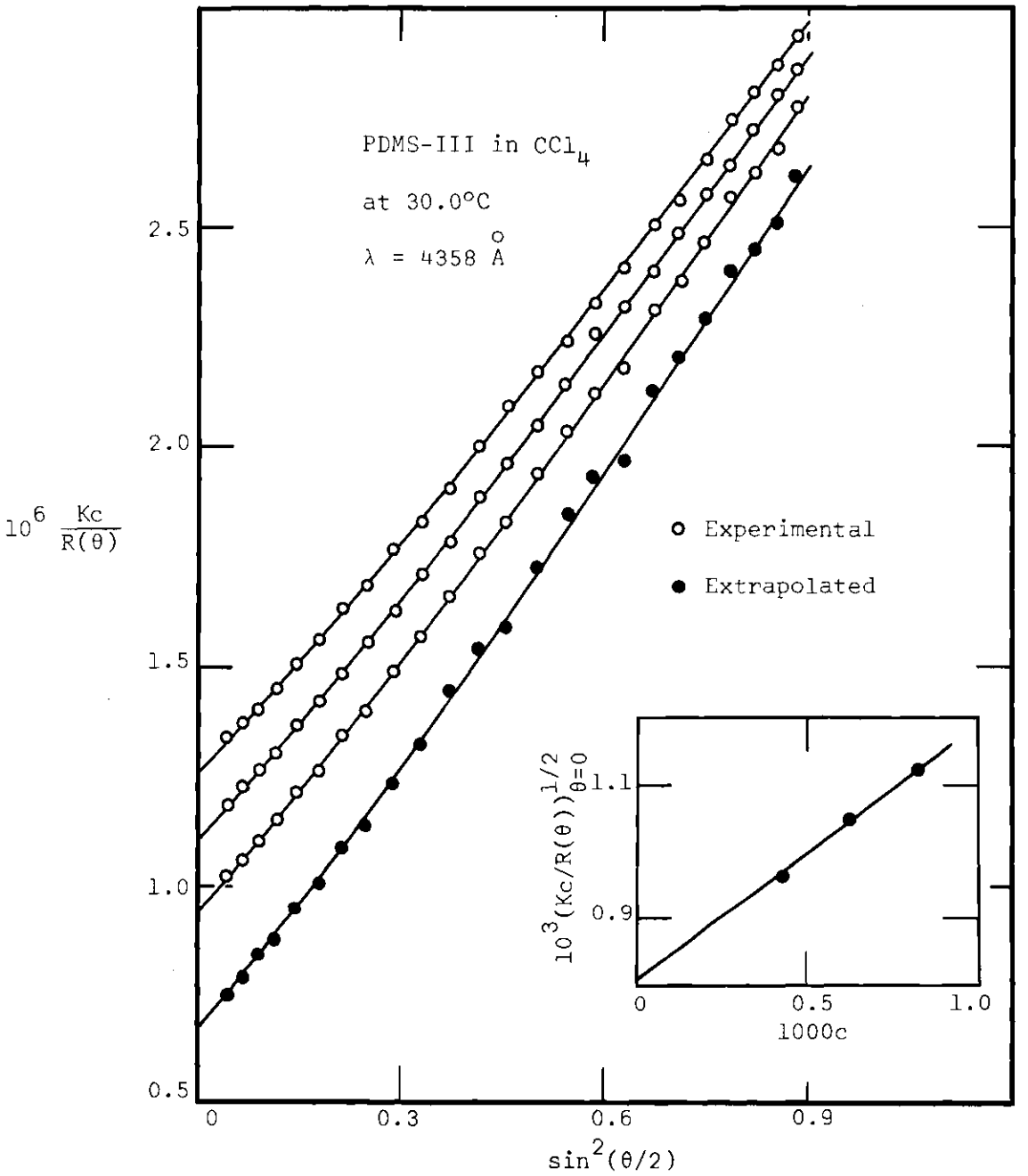

Figure 50. Scattering Data for PDMS-III in Carbon Tetrachloride at 30.0°C. λ = 4358 Å

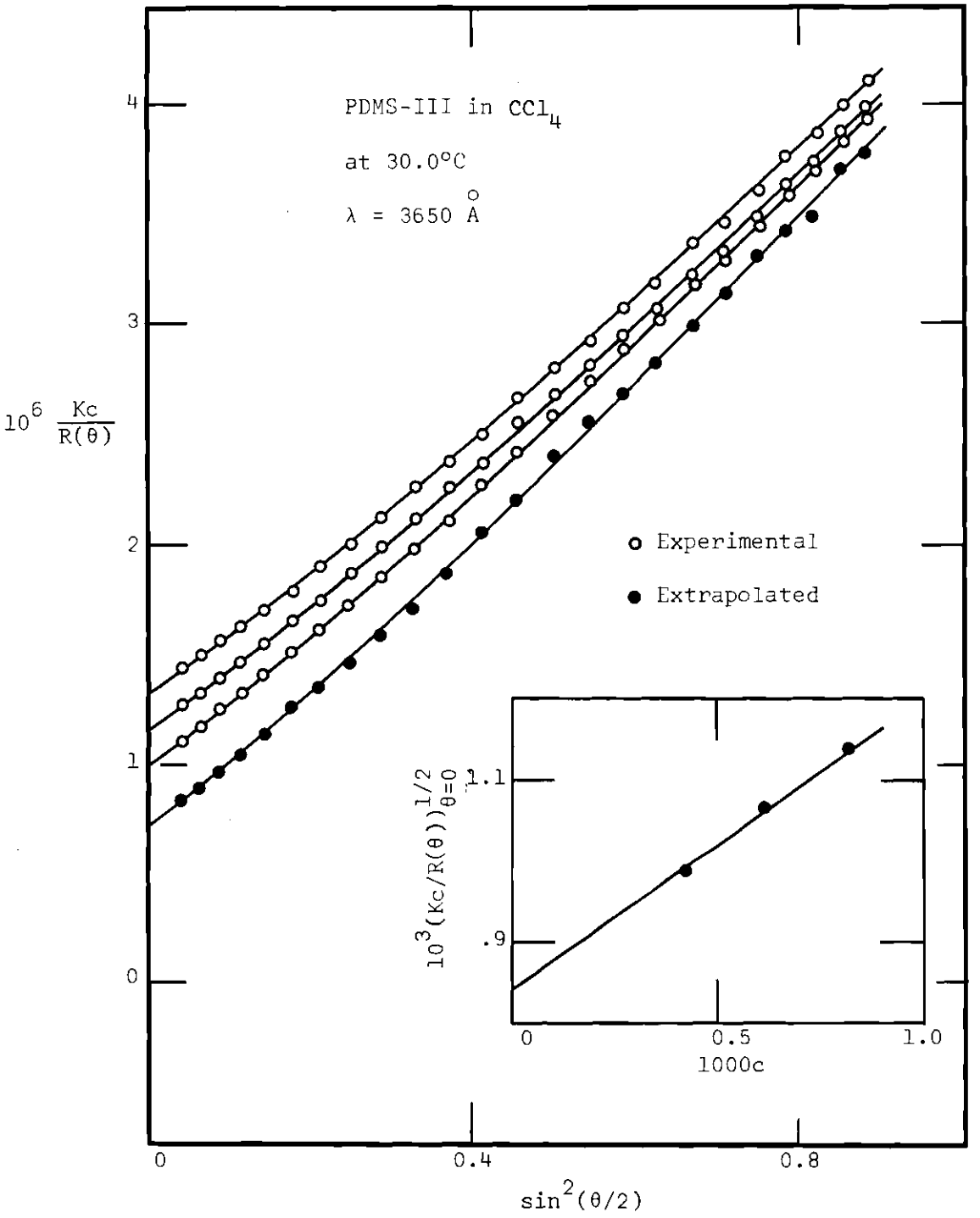

Figure 51. Scattering Data for PDMS-III in Carbon Tetrachloride at 30.0°C. λ = 3650 Å

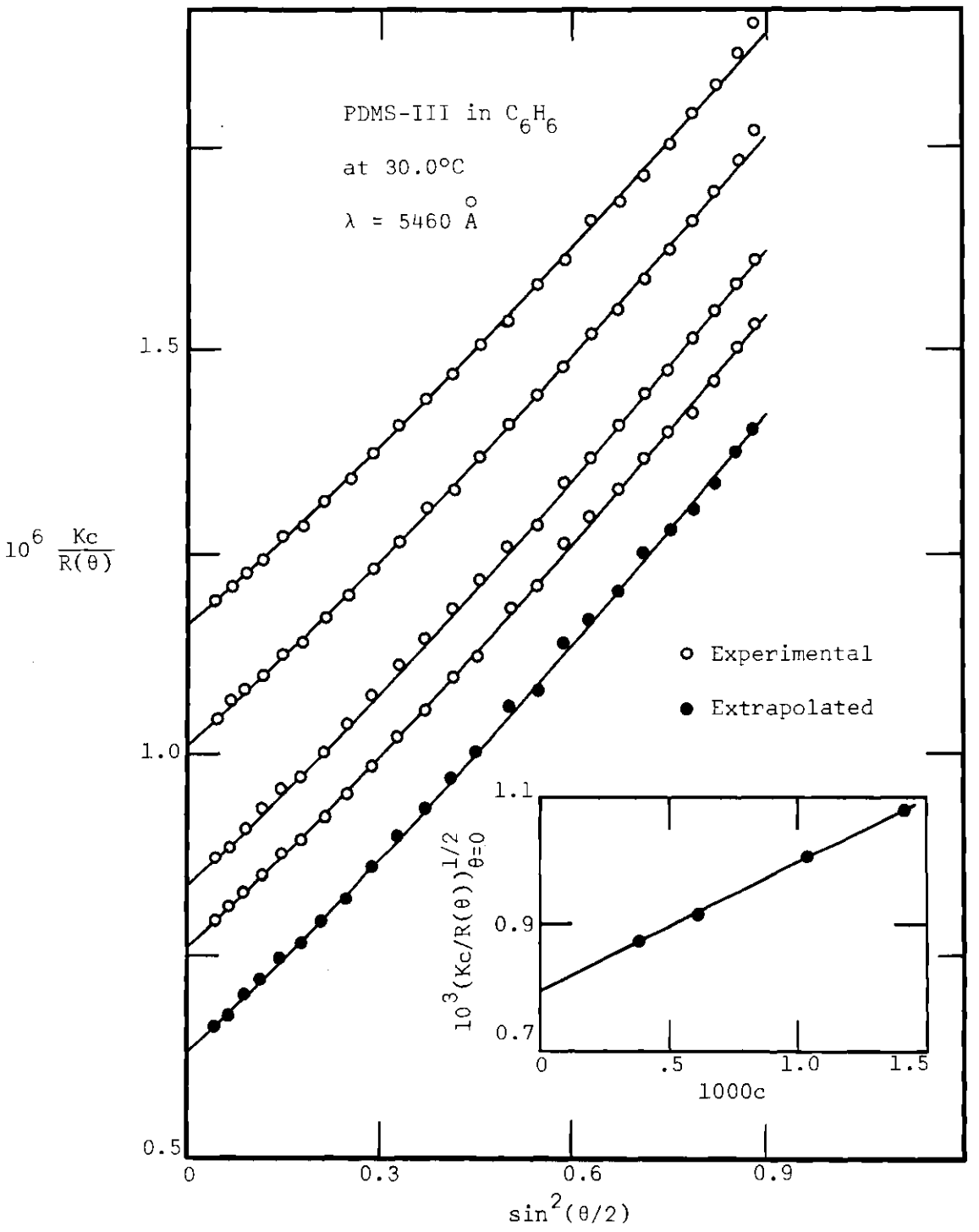

Figure 52. Scattering Data for PDMS-III in Benzene at 30.0°C. λ = 5460 Å

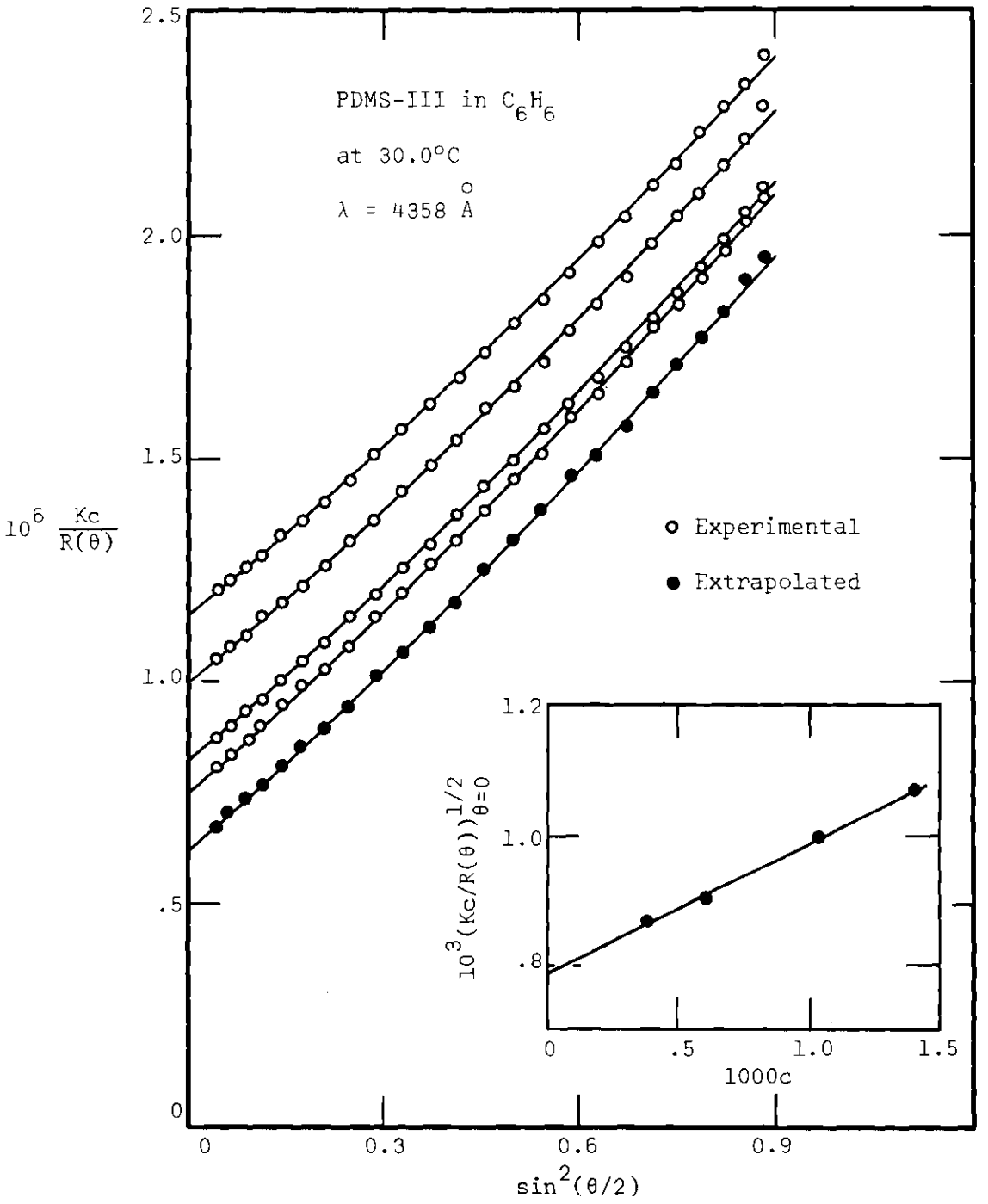

Figure 53. Scattering Data for PDMS-III in Benzene at 30.0°C.
λ = 4358 Å

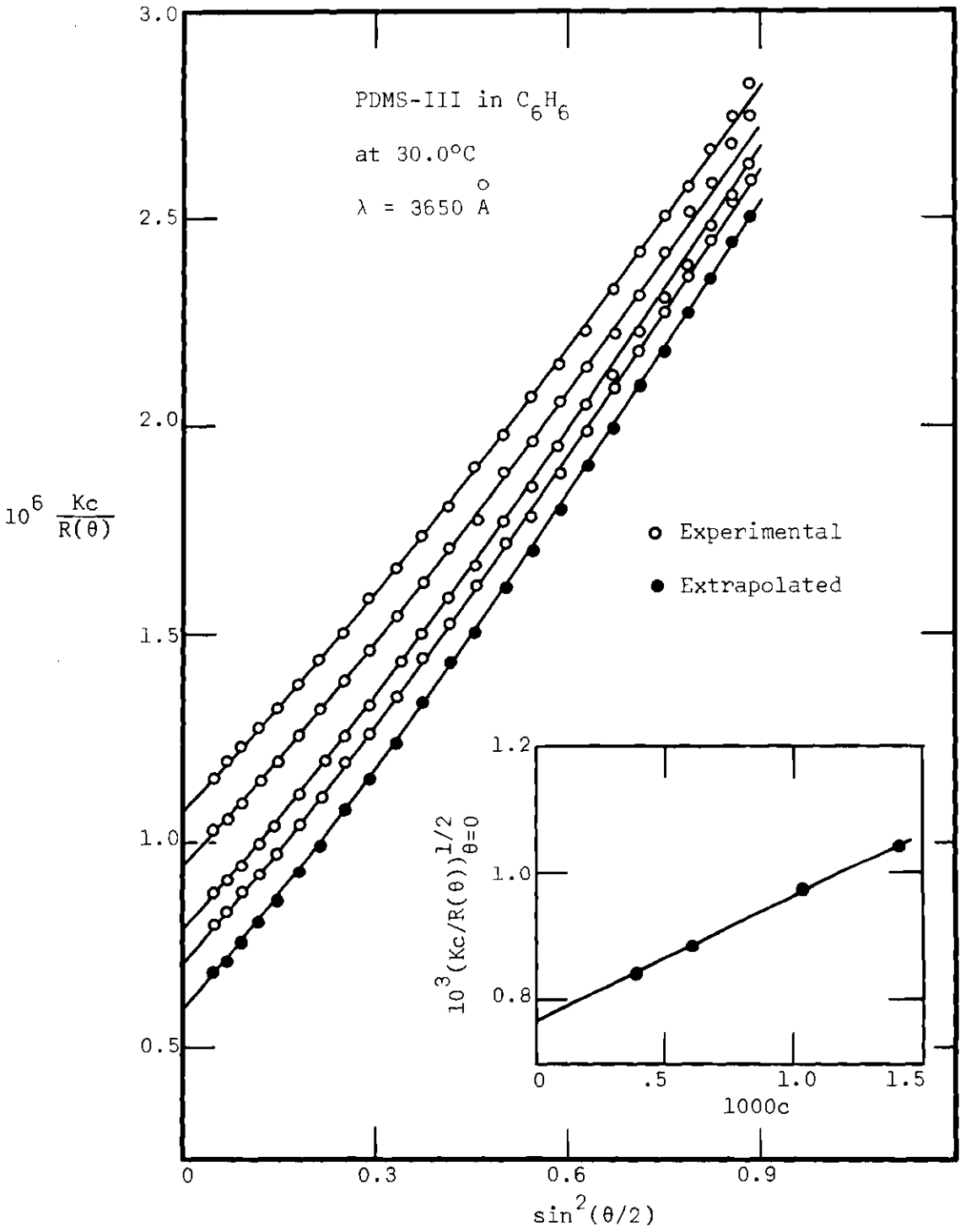

Figure 54. Scattering Data for PDMS-III in Benzene at 30.0°C.
λ = 3650 Å

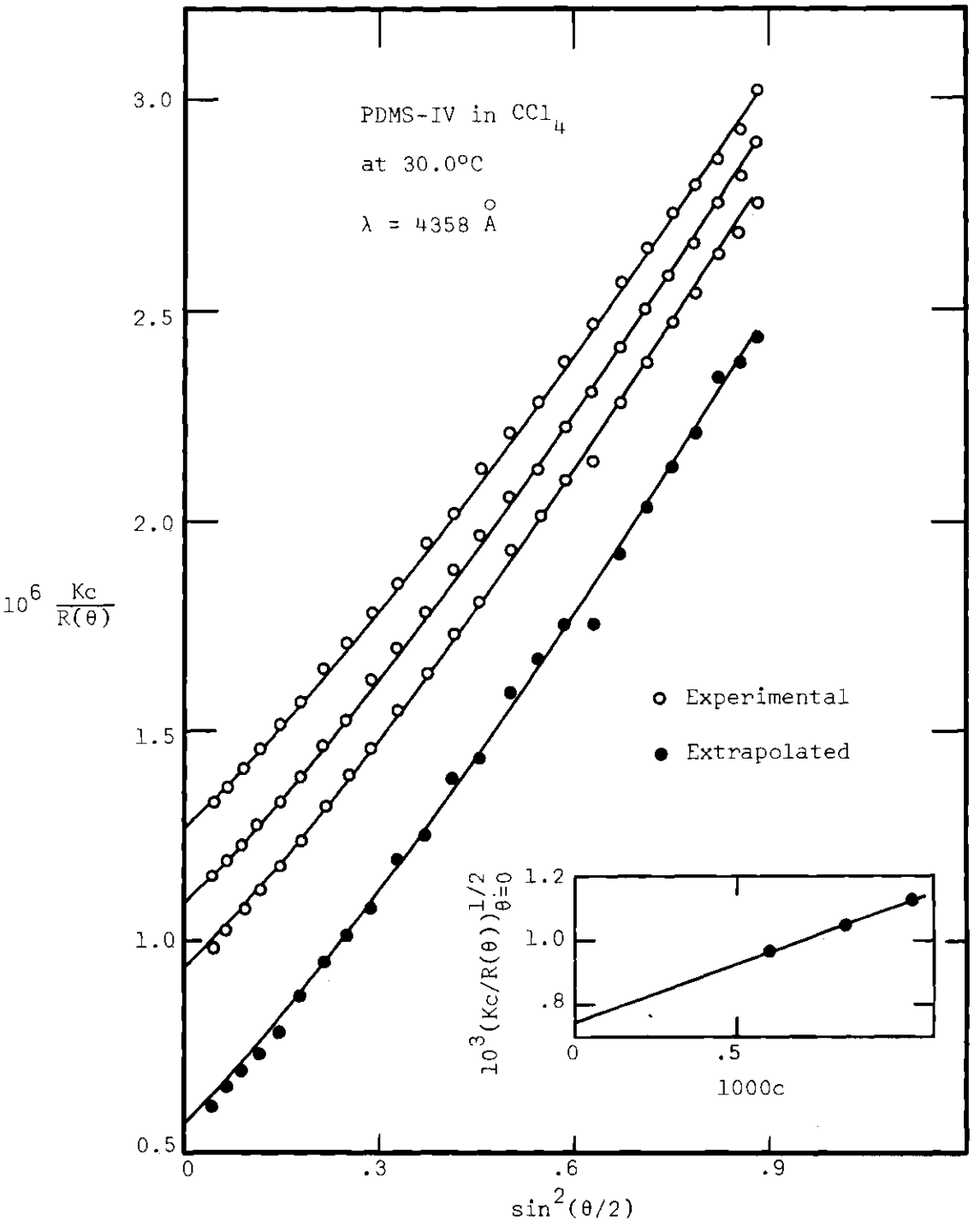

Figure 55. Scattering Data for PDMS-IV in Carbon Tetrachloride at 30.0°C. λ = 4358 Å

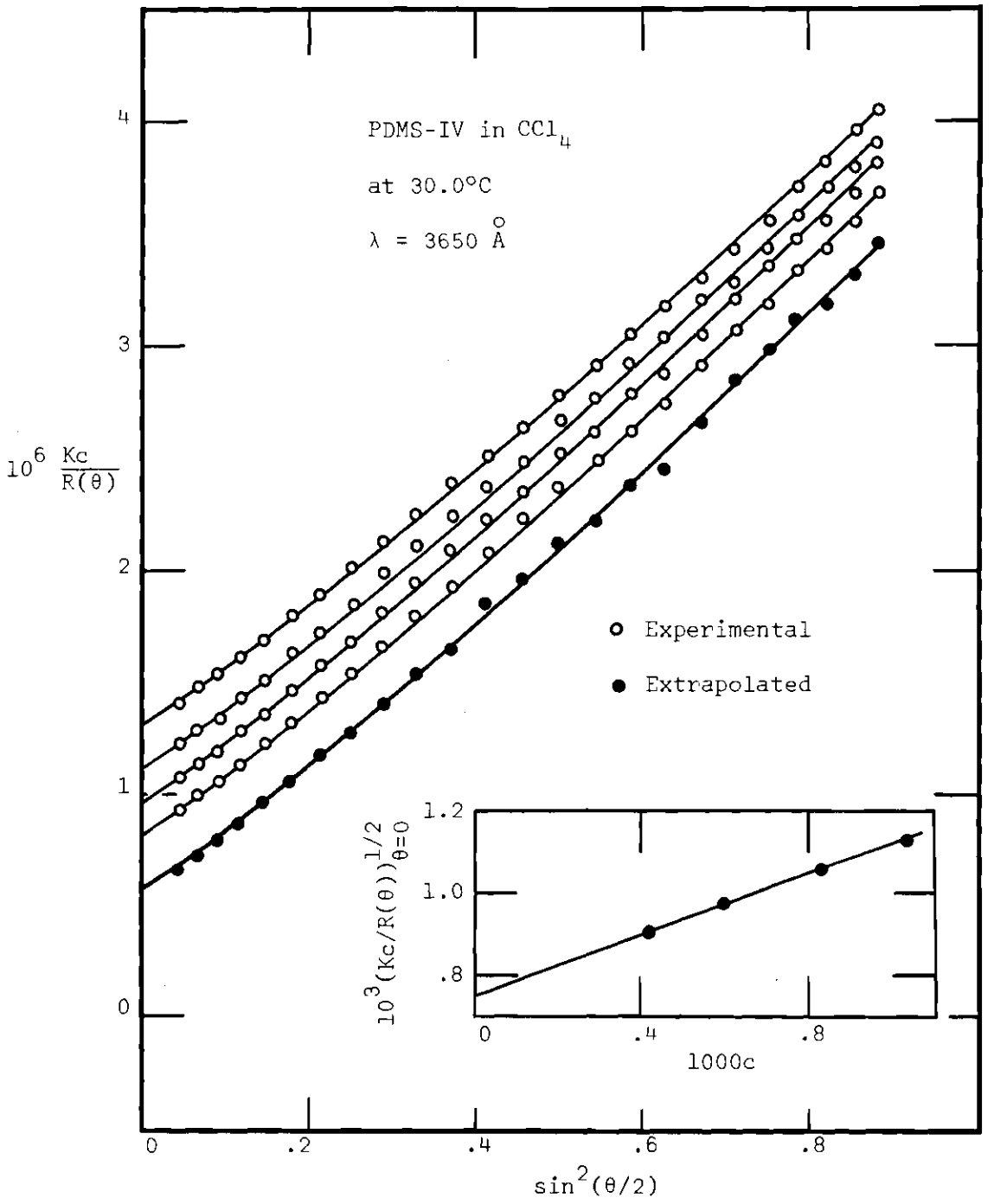

Figure 56. Scattering Data for PDMS-IV in Carbon Tetrachloride at 30.0°C. λ = 3650 Å

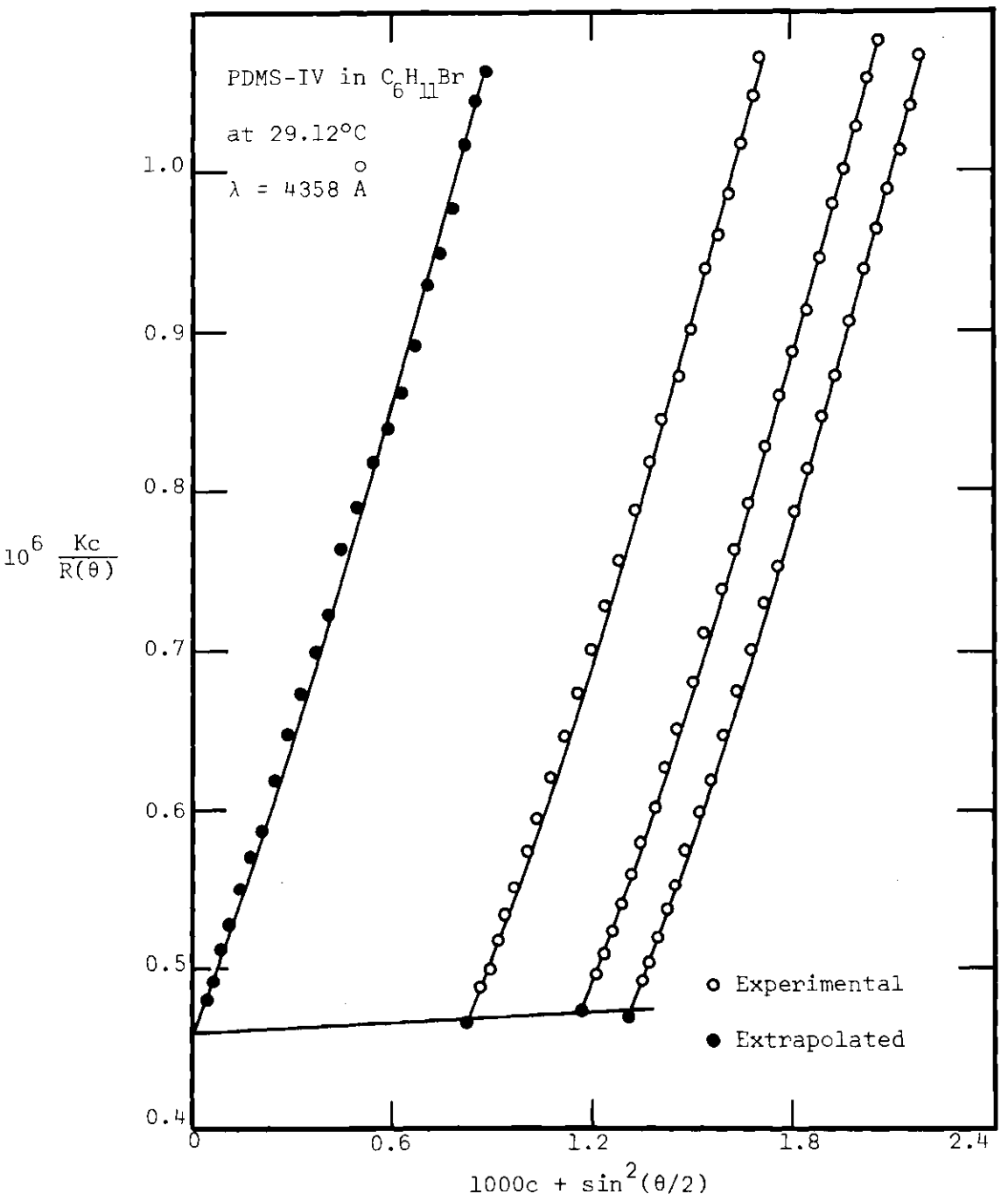

Figure 57. Scattering Data for PDMS-IV in Bromocyclohexane at 29.12°C. λ = 4358 Å

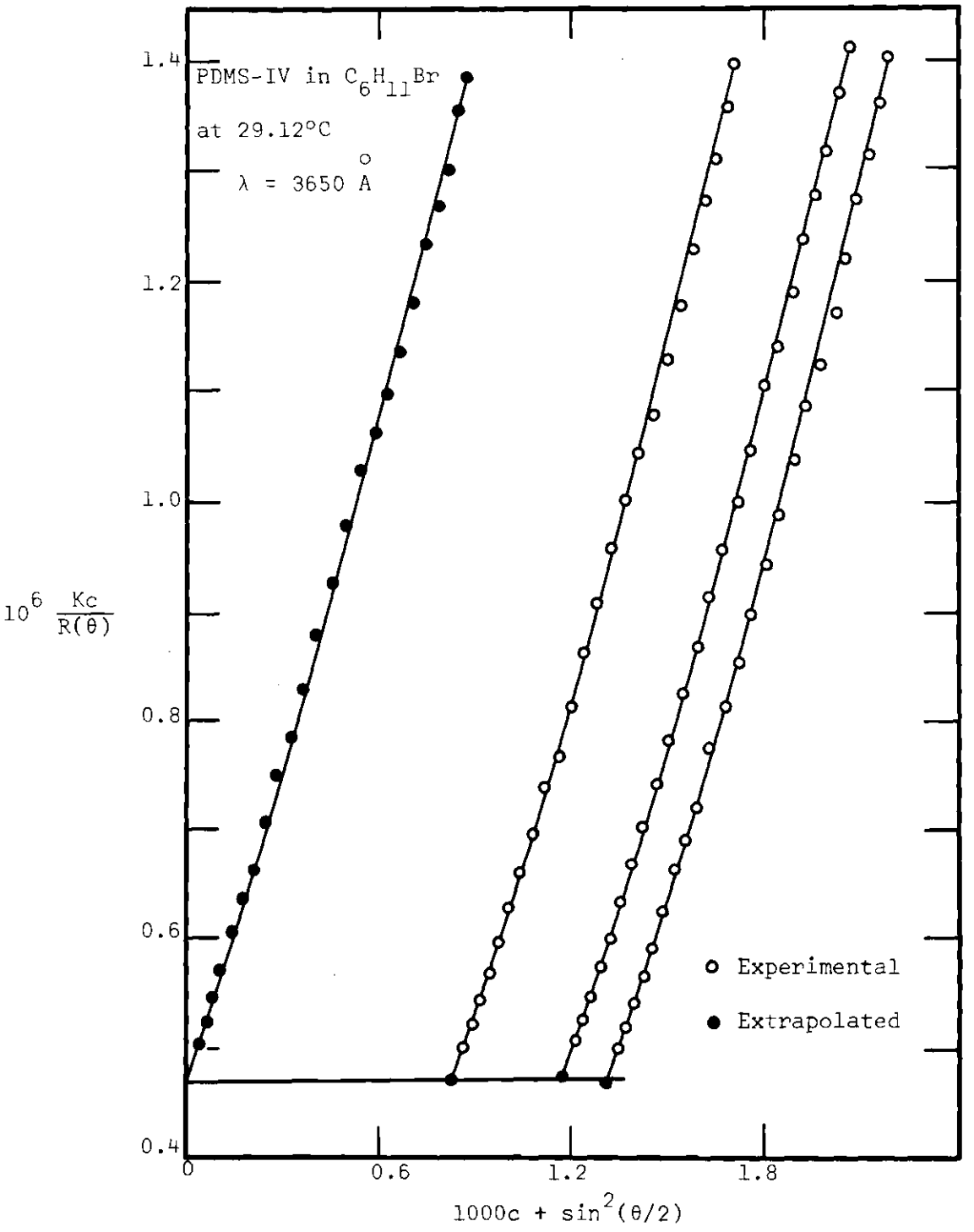

Figure 58. Scattering Data for PDMS-IV in Bromocyclohexane at 29.12°C. λ = 4358 Å

BIBLIOGRAPHY*

1. C. Tanford, *Physical Chemistry of Macromolecules*, John Wiley and Sons, Inc., New York, 1961, Chapter IV.

2. P. J. Flory, *Principles of Polymer Chemistry*, Cornell University Press, Ithica, New York, 1953, pp. 529, 607.

3. J. W. Strutt (Lord Rayleigh), *Phil. Mag. 41*, 107, 447 (1871).

4. P. Debye, *J. Appl. Phys. 15*, 338 (1944).

5. Tanford, Chapter V.

6. K. A. Stacey, *Light Scattering in Physical Chemistry*, Academic Press, New York, 1956, p. 14.

7. A. Einstein, *Ann. Physik 33*, 1275 (1910).

8. M. Smoluchowski, *Ann. Physik 25*, 205 (1908).

9. M. Fixman, *J. Chem. Phys. 23*, 2074 (1955).

10. P. Debye, *J. Phys. and Colloid Chem. 51*, 18 (1947).

11. P. Debye, *Ann. Physik 46*, 809 (1915).

12. G. Mie, *Ann. Physik 25*, 377 (1908).

13. Lord Rayleigh, *Proc. Roy. Soc. A84*, 25 (1910).

14. T. Neugebauer, *Ann. Physik 42*, 509 (1943).

15. Flory, Chapter X.

16. P. Debye, Technical Report CR-637, Private Communication to Reconstruction Finance Corporation, Office of Rubber Reserve (1945); found in D. McIntyre and F. Gornick, eds., *Light Scattering from Dilute Polymer Solutions*, Gordon and Breach, New York, 1964, p. 139.

17. Tanford, p. 167.

---

*Abbreviations used in this list follow the form employed by *Chemical Abstracts 55* (1961).

18. W. Kuhn, *Kolloid-Z. 76,* 258 (1936); *87,* 3 (1939).

19. A. Isihara, *J. Chem. Phys. 40,* 1137 (1964).

20. A. Peterlin, *J. Chem. Phys. 23,* 2464 (1955).

21. O. B. Ptitsyn, *Zh. Fiz. Khim. 31,* 1091 (1957); English translation found in D. McIntyre, *op. cit.,* p. 231.

22. H. Benoit, *Compt. Rend. 245,* 2244 (1957).

23. A. J. Hyde, J. H. Ryan, F. T. Wall, and T. F. Schatzki, *J. Polymer Sci. 33,* 129 (1958).

24. J. Mazur, *J. Res. Nat. Bur. Std. (US) 69A,* 355 (1965).

25. Flory, p. 600.

26. B. Zimm, W. Stockmayer, and M. Fixman, *J. Chem. Phys. 21,* 1716 (1953).

27. D. McIntyre, J. Mazur, and A. Wims, *Bull. Am. Phys. Soc. 11,* 165 (1966).

28. F. T. Wall, S. W. Windwer, and J. Gans, *J. Chem. Phys. 38,* 2220 (1963).

29. P. H. Verdier and W. H. Stockmayer, *J. Chem. Phys. 36,* 227 (1962).

30. A. K. Kron and O. B. Ptitsyn, *Vysokomolekul. Soedin. 6,* 862 (1964).

31. C. Domb, J. Gillis and G. Wilmers, *Proc. Phys. Soc. 85,* 625 (1965).

32. J. Oth and V. Desreux, *Bull. Soc. Chim. Belges 63,* 285 (1954).

33. P. Outer, C. Carr, and B. Zimm, *J. Chem. Phys. 18,* 830 (1950).

34. V. E. Eskin and T. I. Volkov, *Vysokomolekul. Soedin. 5,* 614 (1963).

35. M. Szwarc, M. Levy, and R. Milkovich, *J. Am. Chem. Soc. 78,* 2656 (1956).

36. B. H. Zimm, *J. Chem. Phys. 16,* 1099 (1948).

37. H. Benoit, *J. Polymer Sci. 11,* 507 (1953).

38. V. E. Eskin, *Vysokomol. Soed. 1,* 138 (1959).

39. C. Loucheux, G. Weill, and H. Benoit, *J. Chim. Phys. 55,* 540 (1958).

40. D. K. Carpenter, *J. Polymer Sci. 4A2,* 923 (1966).

41. A. J. Hyde, *Trans. Faraday Soc. 56,* 591 (1960).

42. J. Prud'homme and Y. Sicotte, *Can. J. Chem. 42,* 2078 (1964).

43. P. Debye, B. Chu, and H. Kaufmann, *J. Polymer Sci. 1A,* 2387 (1963).

44. F. W. Billmeyer, Jr., *Textbook of Polymer Chemistry,* Interscience Publishers, Inc., New York, 1957, pp. 120-123.

45. L. P. Witnauer and H. J. Scherr, *Rev. Sci. Instr. 23,* 99 (1952).

46. M. Gubler, C. Reiss, and H. Benoit, *J. Chim. Phys. 59,* 42 (1962).

47. B. A. Brice and M. Halwer, *J. Opt. Soc. Am. 41,* 1033 (1951).

48. R. Buch, Dow Corning Corporation, Private Communication.

49. National Bureau of Standards, Private Communication.

50. T. Orofino, Mellon Institute, Private Communication.

51. H. W. McCormick, Dow Chemical Company, Private Communication.

52. T. Orofino, Private Communication.

53. J. Timmermans, *Physico-chemical Constants of Pure Organic Compounds,* Elsevier, New York, 1950, p. 147.

54. Ibid., p. 196.

55. Ibid., p. 227.

56. R. R. Dreisbach, *Physical Properties of Chemical Substances,* Dow Chemical Company, Midland, Michigan, 1953.

57. Y. Tomimatsu and K. J. Palmer, *J. Polymer Sci. 35,* 549 (1959).

58. J. P. Kratohvil, Gj. Dezelic, M. Kerker, and E. Matijevic, *J. Polymer Sci. 57* (1962).

59. J. Ehl *et al., Makromol. Chem. 75,* 35 (1964).

60. H. J. Cantow, *Makromol. Chem. 18/19,* 367 (1956).

61. J. J. Hermans and S. Levinson, *J. Opt. Soc. Am. 41,* 460 (1951).

62. J. P. Kratohvil, *J. Coll. and Interface Sci. 21,* 498 (1966).

63. T. Lowry and C. Allsopp, *Proc. Roy. Soc. 133,* 26 (1931).

64. *Landolt-Bornstein Physikalisch-Chemische Tabellen,* Springer, Berlin, 1923.

65. B. A. Brice and M. Halwer, *J. Opt. Soc. Am. 41,* 1033 (1951).

66. C. A. Browne and F. W. Zerban, *Physical and Chemical Methods of Sugar Analysis,* Wiley, New York, 1941, p. 1206.

67. V. Crescenzi and P. J. Flory, *J. Am. Chem. Soc. 86,* 141 (1964).

68. G. V. Schulz and A. Haug, *Z. Physik. Chem. (Frankfurt) 34,* 328 (1962).

69. M. B. Huglin, *J. Appl. Polymer Sci. 9,* 4003 (1965).

70. G. M. Kline, *Analytical Chemistry of Polymers,* from *High Polymers,* volume XII, part 3, Interscience, New York, pp. 45-52.

71. *American Institute of Physics Handbook,* McGraw Hill, New York, 1957, p. 6-93.

72. J. Brandrup and E. H. Immergut, eds., *Polymer Handbook,* Interscience, New York, 1966, p. III-10.

73. M. L. Huggins, *J. Am. Chem. Soc. 64,* 2716 (1942).

74. P. F. Onyon, in P. W. Allen, *Techniques of Polymer Characterization,* Butterworth, London, 1959, p. 171.

75. Brandrup and Immergut, p. IV-1.

76. M. Kurata and W. H. Stockmayer, *Fortschr. Hochpolymer. Forsch. 3,* 196 (1963).

77. B. H. Zimm, *J. Chem. Phys. 16,* 1099 (1948).

78. Flory, pp. 297-303.

79. Flory, p. 535.

80. Brandrup and Immergut, p. IV-171.

81. K. Pearson, *Tables of the Incomplete Gamma Function,* Cambridge University Press, 1922.

82. Flory, p. 600.

83. Tanford, p. 305.

84. Q. A. Trementozzi and S. Newman, in *High Polymers*, vol. XX, part 1, Interscience, New York, 1965, p. 444.

85. W. R. Krigbaum and D. K. Carpenter, *J. Phys. Chem. 59*, 1166 (1955).

86. Flory, p. 616.

VITA

Terry Edward Smith, the elder son of Mr. and Mrs. Russell T. Smith, was born August 23, 1940, in Evansville, Indiana. There he lived with his parents and his brother, Paul, until 1958, when, following his graduation from high school, he entered David Lipscomb College in Nashville, Tennessee. After about four years, during which time he majored in chemistry, he received the Bachelor of Arts degree in June of 1962. The following September he began to pursue an advanced degree in physical chemistry at the Georgia Institute of Technology. He and his wife, formerly Linda Lee Newsom, were married in 1962 and now have two children, Jeffrey Russell and Virginia Lynn. Presently, he is employed by the American Cyanamid Company in Stamford, Connecticut.